Battelle
The Business of Innovation

PNWD-4368

Hydrologic Characterization Results and Recommendations for the Wallula Basalt Pilot Well

FA Spane
A Bonneville
BP McGrail
PD Thorne

Battelle
Pacific Northwest Division
Richland, Washington 99352

Prepared for
National Energy Technology Laboratory
Morgantown, WV 26507-0880
under Cooperative Agreement DE-FC26-05NT42587

August 2012

LEGAL NOTICE

This report was prepared by Battelle Memorial Institute (Battelle) as an account of sponsored research activities. Neither Client nor Battelle nor any person acting on behalf of either:

MAKES ANY WARRANTY OR REPRESENTATION, EXPRESS OR IMPLIED, with respect to the accuracy, completeness, or usefulness of the information contained in this report, or that the use of any information, apparatus, process, or composition disclosed in this report may not infringe privately owned rights; or

Assumes any liabilities with respect to the use of, or for damages resulting from the use of, any information, apparatus, process, or composition disclosed in this report.

Reference herein to any specific commercial product, process, or service by trade name, trademark, manufacturer, or otherwise, does not necessarily constitute or imply its endorsement, recommendation, or favoring by Battelle. The views and opinions of authors expressed herein do not necessarily state or reflect those of Battelle.

This document was printed on recycled paper.
(9/2003)

Battelle
The Business of Innovation

PNWD-4368

Hydrologic Characterization Results and Recommendations for the Wallula Basalt Pilot Well

FA Spane
A Bonneville
BP McGrail
PD Thorne

Battelle
Pacific Northwest Division
Richland, Washington 99352

Prepared for
National Energy Technology Laboratory
Morgantown, WV 26507-0880
under Cooperative Agreement DE-FC26-05NT42587

August 2012

Abstract

In 2009, the U.S. Department of Energy's Big Sky Regional Carbon Sequestration Partnership completed drilling the first carbon dioxide (CO_2) sequestration pilot borehole well with continental flood basalts, to a total depth of 4110 ft at the Boise Inc. mill property at Wallula, Washington. As part of the characterization program, hydrologic tests were conducted on selected basalt interflow reservoir zones and flow-interior/caprock intervals during, and at the completion of the borehole drilling activities, to support selection of a candidate injection reservoir for subsequent CO_2 sequestration studies. Based on the results obtained during the active borehole characterization program, an injection reservoir was identified between the depth interval of 2716 and 2910 ft that contained three individual Grande Ronde Basalt breccia interflow zones. The Wallula pilot well injection reservoir lies stratigraphically below the massive Umtanum Member of the Grande Ronde Basalt, whose flow-interior section possesses regionally recognized low-permeability characteristics.

Following well completion activities that occurred during May 2009, Wallula pilot well injection reservoir zone pressure was monitored for an extended period (i.e., between June 2009 and December 2010) for the purpose of evaluating seasonal and temporal reservoir pressure dynamics in response to natural and manmade-related stresses. Following completion of the baseline pressure monitoring phase, a series of hydrologic well tests were conducted to assess possible impacts to the injection reservoir due to previous well completion activities, and for determining large-scale hydraulic property and hydrologic boundary detection. Results for the characterization program conducted during the initial, active borehole drilling campaign were previously published in McGrail et al. (2009).[1] This report presents the hydrologic test results obtained following well completion, during the subsequent baseline monitoring period, and recent well testing phase of the characterization program. Recommendations are also provided to reduce the uncertainty concerning operative conceptual conditions within the candidate CO_2 injection horizon.

[1] McGrail, BP, EC Sullivan, FA Spane, DH Bacon, G Hund, PD Thorne, CJ Thompson, SP Reidel, and FS Colwell. 2009. *Preliminary Hydrogeologic Characterization Results from the Wallula Basalt Pilot Study*. PNWD-4129, Pacific Northwest National Laboratory, Richland, Washington.

Summary

Hydrologic characterization information for the Wallula pilot field site, located at the Boise Inc. mill facility at Wallula, Washington State, has been obtained during three, sequential characterization phases:

- Initial hydrogeologic reconnaissance-level characterization information obtained during the borehole drilling/advancement phase (January–May 2009)
- Baseline reservoir pressure monitoring for background formation dynamics assessment (June 2009–December 2010)
- Extended hydrologic well testing of the Wallula pilot well injection reservoir conducted for large-scale hydraulic property determination and hydrologic boundary detection (January–March 2011).

Preliminary results for the characterization program conducted during the initial, active borehole drilling campaign were previously published in McGrail et al. (2009).[1] Based on hydrogeologic information obtained during borehole drilling and advancement, a candidate injection reservoir zone was identified between the depth interval of 2716 and 2910 ft below ground surface. Specific criteria used in the reservoir zone selection included the following:

- In-situ, static formation fluid temperature and pressure conditions above supercritical carbon dioxide (CO_2) conditions
- Presence of nonpotable drinking water within the candidate injection zone (i.e., existing dissolved chemical constituents exceeding primary and secondary drinking water standards)
- Presence of sufficient reservoir formation injection capacity (i.e., hydraulic properties) and overlying caprock sealing characteristics to facilitate the subsequent injection and sequestration of CO_2 during a subsequent field pilot study phase.

Following well completion activities, baseline reservoir pressure monitoring of injection zone between June 2009 and December 2010 provided temporal and seasonal response dynamic information. Salient findings obtained from the baseline monitoring characterization phase indicated the following:

- Significant seasonal hydraulic head (pressure) cycle of approximately 2.15 m/year that appears casually coincident with agricultural pumpage within the basin
- Associated temporal response to natural external stresses (i.e., barometric and earth-tide fluctuations), but no apparent direct relationship to human-regulated, Columbia River/McNary reservoir elevation/loading fluctuations
- Detailed barometric response analysis that suggests the presence of formational leakage or presence of a communicative hydrologic boundary condition within the surrounding reservoir.

Following the baseline monitoring period, hydrologic well testing was conducted during late December 2010 and March 2011 with the objectives of identifying the operative aquifer model,

[1] McGrail, BP, EC Sullivan, FA Spane, DH Bacon, G Hund, PD Thorne, CJ Thompson, SP Reidel, and FS Colwell. 2009. *Preliminary Hydrogeologic Characterization Results from the Wallula Basalt Pilot Study*. PNWD-4129, Pacific Northwest National Laboratory, Richland, Washington.

determining large-scale hydraulic properties, and detecting the presence of surrounding hydrologic boundaries within the candidate injection reservoir. Diagnostic derivative analysis of the 7-day constant-rate pumping test and approximate 3-week recovery period response indicated establishment of nonradial, linear-flow regime to the well, and the existence of a hydrologic boundary condition. The lack of surrounding observation and monitoring well data within the test reservoir during the extended well test makes it difficult to identify the causative factors responsible for either the linear-flow regime condition or the observed hydrologic boundary.

Possible causative mechanisms and/or features that could produce the linear-flow regime response (i.e., one-half slope on diagnostic pressure and derivative log-log plot) during hydrologic testing include the following:

- Transmissive horizontal or vertical fracture intersected by the well
- Presence of a highly, horizontally anisotropic reservoir zone condition
- Presence of a linearly-shaped, higher permeability pathway or "embedded channel" within the interflow reservoir.

Characterization information currently available for the site cannot be used definitively to distinguish between the possible conceptual models that can produce the nonradial flow regime condition or the primary attributes (i.e., azimuth, width, length, thickness) of the feature producing the linear-flow behavior. The primary impact for the dominant linear-flow regime condition within the well/formation system would be the nonradial emplacement of any subsequent CO_2 injection into the surrounding test reservoir. Although some general directional CO_2 emplacement information may be realized from injection well geophysical surveys performed immediately after CO_2 injection, the level of characterization may not be sufficient to design the deployment of future re-entry and coring into the injection reservoir to retrieve geologic cores for CO_2 and basalt rock reaction assessment (see McGrail et al. 2009).[1] Earlier plans for this post-injection characterization activity assumed a homogeneous reservoir with essentially a nondirectional (i.e., radial) dependence for the injected CO_2. Given the heterogeneous characteristics of the feature producing the linear-flow regime, it is inherent these directionally dependent properties be known beforehand to assure a high probability of intersecting the CO_2 reactive reservoir areas for any future re-entry/coring activities.

The presence of the hydrologic boundary condition indicated by a distinctive diagnostic derivative plot pattern (i.e., declining pattern on diagnostic derivative log-log plot), can also be produced by a number of causative factors including the following:

- Pervasive caprock leakage
- Presence of a vertical, communicative hydrologic feature (i.e., linear constant-pressure boundary)
- An abrupt, significant lateral change in reservoir transmissivity conditions (i.e., a boundary increase in reservoir hydraulic properties with distance from the well)
- Spherical flow.

As in the case for flow-regime cause identification, the absence of observation/monitoring well reservoir response data during the extended hydrologic test also makes it difficult to definitively identify the cause of the observed hydrologic test boundary. However, subtle distinguishing differences in the

derivative response patterns for these identified boundary/formational conditions suggest the boundary condition exhibited during the hydrologic test was not likely produced by either establishment of spherical flow conditions or caused by pervasive caprock leakage. The most plausible explanation for the observed test boundary condition includes the following: an intersection of a ***vertical***, crosscutting, communicative hydrogeologic feature (e.g., tectonic fracture), or a significant ***lateral*** increase in reservoir hydraulic/storage properties (i.e., hydraulic diffusivity [T/S]) at a distance from the well. Of these two hydrologic boundary-producing scenarios, the vertical, crosscutting communicative feature has the most adverse or limiting impact for emplacement of any subsequent CO_2 injection into the surrounding test reservoir. This boundary condition would restrict or limit the volume/mass of CO_2 emplaced within the injection reservoir, if vertical CO_2 migration to overlying basalt reservoirs (i.e., via the communicative feature) is to be avoided. Theoretically, the distance to a hydrologic boundary can be approximated based solely on the test well response (and more precisely with multiple monitor well test data); however, this assumes radial reservoir flow conditions and knowing the effective well radius for the test well. Given the previously discussed linear-flow regime condition and unknown dimensional characteristics for the various possible causative mechanisms, boundary distance calculations are highly uncertain (e.g., ~50 to ≥300 ft).

To improve the design of the subsequent CO_2 injection and post-injection coring phases of the field pilot study, identifying the causative mechanism for the linear-flow regime and nature (type and distance) of the exhibited hydrologic boundary within the Wallula pilot well injection reservoir is of primary importance. Although this can be best resolved with drilling and completion of additional surrounding monitor wells within and in overlying reservoir horizons, less invasive techniques may be employed to reduce the uncertainty of these possible injection reservoir conditions. With this respect, the following test characterization recommendations are provided in lieu of constructing additional monitor wells and conducting multi-, inter-well hydrologic tests. The two primary test recommendations are to conduct the following:

- Dynamic fluid-logging survey of the open injection zone horizon
- Repeated, active surface gravity and land deformation surveys (interferometric synthetic aperture radar) during an extended, high-stress (drawdown), constant-rate pumping test.

The dynamic fluid-logging survey entails extracting groundwater from the test interval (e.g., pumping), and monitoring the influx of groundwater from the intersected open reservoir section to the wellbore. The measurement of fluid influx distribution to the well can be done directly using high precision flow metering (e.g., electromagnetic flow meter) and indirectly by fluid temperature logging, which indicates regions of groundwater influx by the distortion of the fluid-temperature profile from equilibrated, static, fluid-column temperature conditions. The primary objective of the dynamic fluid-logging survey is to establish the dimensional distribution of permeability within the open injection well section from which a refined conceptualization can be obtained for the mechanism responsible for linear-flow conditions within the reservoir.

The second recommended hydrologic test involves performing repeated high-precision surface gravity and land deformation surveys during the course of conducting an extended (e.g., 14-day), high-stress (~600 pounds per square inch [psi]), constant-rate pumping test. The main objective of this characterization test is to determine the lateral region impacted directly by groundwater extraction and formation pressure decline (i.e., the nonradial area of investigation) during the extended high-stress pumping test. The areal distortion pattern may provide direct evidence on the nature and characteristics

of the feature responsible for producing the hydrologic boundary condition exhibited during the earlier, shorter-duration (7-day) and lower stress (~190 psi) constant-rate pumping test. Physical measurement of the distortion of the land surface during pumping tests is a well-established technique involving compressible sedimentary formations. Basalt formations, however, exhibit considerably higher rigidity and associated formation dilation responses would be comparably smaller than for highly compressible formations. Nevertheless, success in applying these techniques for determining areal deformation associated with a large-scale aquifer storage and recovery project within basalts in nearby Pendleton, Oregon, has recently been demonstrated. Similar results would be expected for the recommended smaller-scale characterization test to be conducted at the Wallula pilot well site location.

Acknowledgments

Several Pacific Northwest National Laboratory (PNNL) staff provided contributions to this report's preparation and with the general performance of the field hydrologic tests. Technical peer review and editorial comments were provided by Darrell Newcomer and Hope Matthews, respectively. Bruce Bjornstad contributed graphics support for several of the report figures. Darrell Newcomer, Mickie Chamness, Jake Horner, and Robert Mackley provided field test support during performance of hydrologic well tests. Kyle Parker supported data acquisition of baseline monitoring activities.

In addition to PNNL staff, several individuals also provided significant field support for well test activities, including Larry Larson and Eric Steffensen from Boise Inc.; Marty Gardner and Dave Skoglie from Energy Solutions; and Jim Meisner, Arron Pope, and Alan Pearson from Stoller Corporation. Contributions by the Blue Star Drilling Company work crew who installed and removed the hydrologic test equipment at the Wallula pilot well are also recognized and appreciated.

Acronyms and Abbreviations

bgs	below ground surface
BRP	barometric response plot
DST	drill-stem test
gpm	gallons per minute
InSAR	interferometric synthetic aperture radar
KGS	Kansas Geological Survey
MCL	maximum concentration limits
P-InSAR	polarization-interferometric synthetic aperture radar
PNWD	Battelle Pacific Northwest Division
PST	Pacific Standard Time
STOMP	Subsurface Transport Over Multiple Phases
SW	slug withdrawal

Nomenclature

B	aquifer thickness; L
B	aquifer loss coefficient; dimensionless
C	well loss coefficient: dimensionless
E	well efficiency; dimensionless
H_D	dimensionless head (observed test response/initial test stress applied)
Δh_w	change in well water-level elevation due to atmospheric pressure change; L
K_{avg}	average horizontal hydraulic conductivity; L/T
K_D	vertical anisotropy (K_v/K_h); dimensionless
K_h	hydraulic conductivity in the horizontal direction; L/T
K_v	hydraulic conductivity in the vertical direction; L/T
L_f	vertical fracture length; L
mD	millidarcies
ΔP_a	change in atmospheric pressure; F/L^2
psia	pounds force per square inch absolute
psig	pound-force per square inch gauge
Q	pumping rate; L^3/T
r_c	radius of well casing; L
r_w	radius of well; L
R_f	horizontal fracture radius; L
s	drawdown; L
s/Q	specific drawdown; T/L^2
s_w	total well drawdown; L
S	storativity; dimensionless
S_s	specific storage; L^{-1}
T	transmissivity; L^2/T
T/S	hydraulic diffusivity; L^2/T
T	time; T
t’	elapsed recovery time following pumping test termination; T
t_p	elapsed pumping time; T
X_f	vertical fracture radial length; L
Z	aquifer depth below water table; L

Contents

Abstract iii
Summary v
Acknowledgments ix
Acronyms and Abbreviations xi
1.0 Introduction 1.1
2.0 Borehole Testing 2.1
3.0 Baseline Monitoring 3.1
3.1 Seasonal Characteristics 3.1
3.2 Temporal Stress Effects 3.4
4.0 Hydrologic Well Tests 4.1
4.1 Wireline Geophysical Surveys 4.1
4.2 Pneumatic Slug Tests 4.4
4.3 Step-Drawdown Test 4.7
4.4 Constant-Rate Test 4.12
4.4.1 Diagnostic Test Analysis 4.14
4.4.2 Linear-Flow/Boundary Conceptual Models 4.16
4.4.3 Linear Fracture-Flow Test Analysis 4.19
5.0 Conclusions 5.1
6.0 Recommendations 6.1
7.0 References 7.1
Appendix A - Hydrologic Test Methods A.1
Appendix B - Selected Hydrologic Test Analysis Figures B.1
Appendix C - Miscellaneous Wallula Well Test Equipment Pictures C.1

Figures

1.1. Aerial Photograph of Boise Mill Site and Wallula Pilot Well Location 1.2
1.2. As-Built Completion for the Wallula Pilot Well 1.3
2.1. Preliminary Transmissivity versus Depth Profile for the Wallula Pilot Borehole 2.2
3.1. Wallula Pilot Well Baseline Monitoring Response: June 2009 – December 2010 ..... 3.2
3.2. Baseline Response Comparison for Wallula Pilot Well and McNary Dam Reservoir 3.3
3.3. Baseline Response Comparison of Wallula Pilot Well and McNary Dam Tail-Water Elevation 3.4
3.4. Comparison of Wallula Pilot Well Water Level and Site Barometric Pressure 3.5
3.5. Wallula Pilot Well and Barometric Spectral Frequency Comparison 3.6
3.6. Wallula Pilot Well and Earth Tide Spectral Frequency Comparison 3.6
3.7. Wallula Pilot Well Barometric Response Plot Analysis 3.7
3.8. Comparison of Observed and Barometric-Corrected Well Response 3.8
3.9. Comparison of Barometric-Corrected Well Response and Earth Tide Potential 3.9
4.1. Comparison of Wallula Pilot Well Fluid Temperature Surveys 4.2
4.2. Fluid Temperature Profile Observations 4.3
4.3. Comparison of Wallula Pilot Well Pneumatic Slug Test Responses 4.4
4.4. Comparison of Wallula Pilot Well Pneumatic Slug and Earlier Borehole Slug/Drill Stem Test Responses 4.5
4.5. Pneumatic Slug Test Response Example 4.6
4.6. Pneumatic Slug Test SW-2 Analysis Plot: Homogeneous Formation Solution 4.7
4.7. Step-Drawdown Test: Baseline Pressure Response Characteristics 4.9
4.8. Step-Drawdown Test: Specific Drawdown/Head Loss Analysis 4.10
4.9. Step-Drawdown Test: Drawdown Component Analysis 4.11
4.10. Step-Drawdown Test: Well Efficiency Analysis 4.12
4.11. Fluoride Concentration Levels During Step-Drawdown and Constant-Rate Pumping Tests 4.13
4.12. Comparison of Normalized Drawdown and Recovery Responses 4.14
4.13. Diagnostic Composite Drawdown and Drawdown Derivative Plot 4.15
4.14. Diagnostic Composite Recovery and Recovery Derivative Plot 4.16
4.15. Areal Conceptualization of Developed Linear-flow Region Surrounding Well/Vertical Fracture 4.17
4.16. Map-View Comparison of Temporal, Test Flow-Regime Conditions for a Strip/Channel Aquifer 4.18
4.17. Constant-Rate Pumping Test: General Linear-Fracture Drawdown Analysis 4.20
4.18. Qualitative Assessment of Fracture Length Versus Test Zone Transmissivity 4.20
4.19. Surface Exposure Showing Two High Permeability, Horizontal Fracture Planes with Basalt Flow 4.22
4.20. Horizontal Fracture Type-Curve Analysis with Constant-Pressure Boundary 4.22
4.21. Vertical Fracture Type-Curve Analysis with Constant-Pressure Boundary 4.23

1.0 Introduction

In 2009, the U.S. Department of Energy's Big Sky Regional Carbon Sequestration Partnership drilled the first carbon dioxide (CO_2) sequestration pilot borehole within continental flood basalts, to a total depth of 4110 ft at the Boise Inc. mill at Wallula, Washington State (Figure 1.1). As part of the characterization program, reconnaissance-level hydrologic tests were conducted on selected basalt interflow reservoir zones and flow-interior/caprock intervals during, and at the completion of the borehole drilling activities, to support selection of a candidate injection reservoir for subsequent CO_2 sequestration studies. Based on the results obtained during the active borehole characterization program, an injection reservoir was identified within the Grand Ronde Basalt between the depth interval of 2716 and 2910 ft that appeared to meet established selection criteria discussed in Spane et al. (2008) and McGrail et al. (2009). Specific criteria used in the reservoir zone selection process included the following:

- In-situ, static formation fluid temperature and pressure conditions above supercritical CO_2 conditions
- Presence of nonpotable drinking water within the candidate injection zone (i.e., existing dissolved chemical constituents exceeding primary and secondary drinking water standards)
- Presence of sufficient reservoir formation injection capacity (i.e., hydraulic properties) and overlying caprock sealing characteristics to facilitate the subsequent injection and sequestration of CO_2 during a subsequent field pilot study phase.

Following well completion activities that occurred during May 2009, Wallula pilot well injection reservoir zone pressure (i.e., hydraulic head) was monitored for an extended period (i.e., between June 2009 and December 2010) for the purpose of evaluating long-term seasonal and short-term, temporal reservoir response dynamics to natural and artificially induced stresses. Following completion of the baseline pressure monitoring, a series of hydrologic well tests were conducted to assess possible impacts to the injection reservoir as a result of well completion activities, and for determining large-scale hydraulic properties and hydrologic boundary conditions. Figure 1.2 shows the as-built completion details for the Wallula pilot well during the baseline monitoring and extended hydrologic testing phases of the candidate injection reservoir.

Preliminary results for the reconnaissance-level characterization program conducted during the initial, active borehole drilling campaign were previously published in McGrail et al. (2009). These results are summarized in Section 2.0. The remainder of this report presents the hydrologic characterization results obtained following well completion during the subsequent baseline monitoring period (Section 3.0), and recent extended hydraulic test phase of the characterization program (Section 4.0). Hydrologic characterization conclusions are provided in Section 5.0, and test characterization recommendations are presented in Section 6.0 to reduce the uncertainty concerning conceptual conditions within the candidate CO_2 injection horizon. References cited in this report are provided in Section 7.0.

Figure 1.1. Aerial Photograph of Boise Mill Site and Wallula Pilot Well Location (view to the northeast)

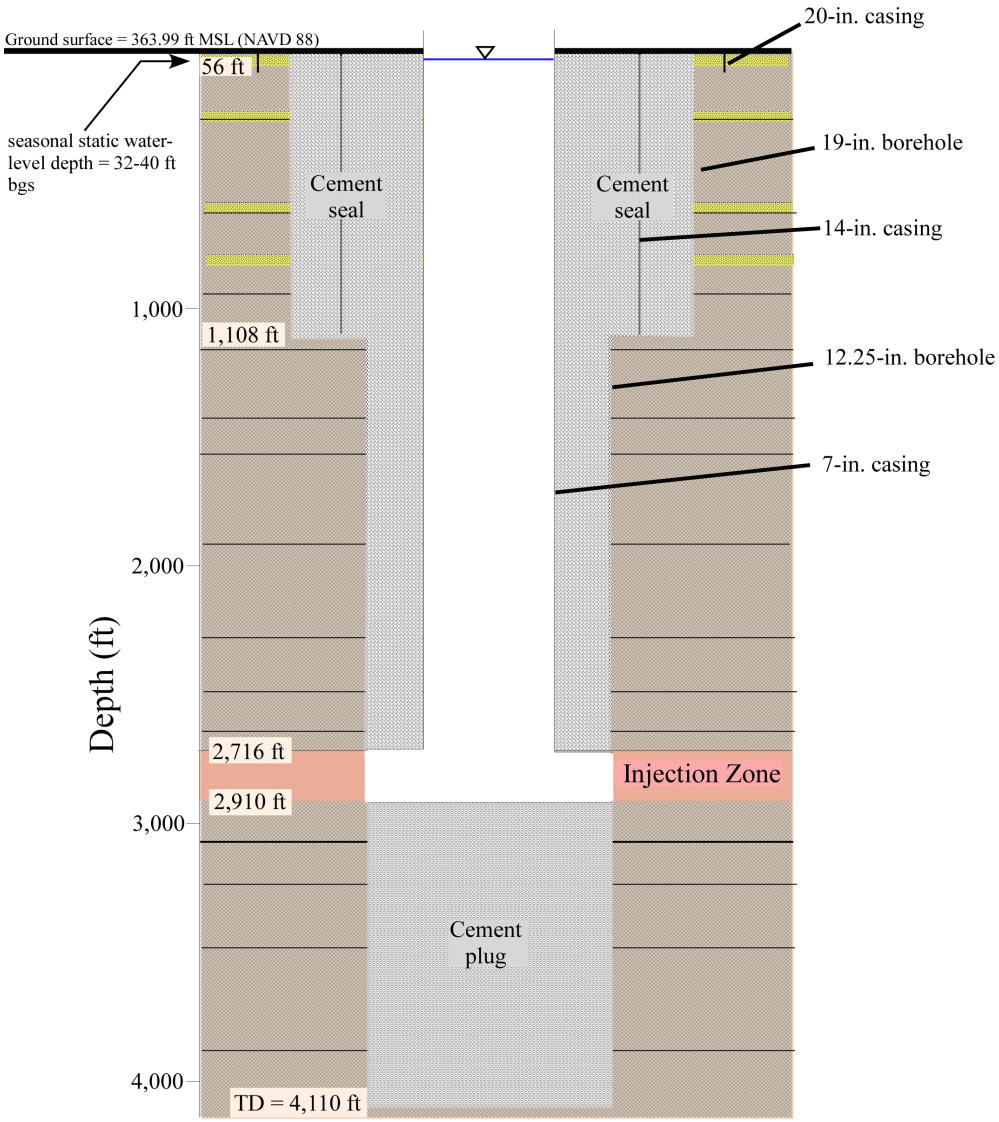

Figure 1.2. As-Built Completion for the Wallula Pilot Well

2.0 Borehole Testing

Preliminary results for the characterization program conducted during the initial, active borehole drilling campaign were published in McGrail et al. (2009). As discussed in McGrail et al. (2009), hydrogeologic information was obtained primarily during borehole drilling/advancement using the progressive drill-and-test characterization strategy. This strategy involved the use of a downhole packer testing assembly to isolate the underlying test zone from the overlying open borehole section. Following test zone isolation, a series of reconnaissance-level hydrologic tests were performed to provide initial hydraulic property information of the isolated zone and to obtain representative hydrochemical samples. A detailed description of the packer test system and hydrologic testing methods used is provided in McGrail et al. (2009).

Based on hydrogeologic information obtained during borehole drilling/advancement, a candidate injection reservoir zone was identified between the depth interval of 2716 and 2910 ft below ground surface (bgs). As noted in Section 1.0, specific criteria used in the reservoir zone selection included the following: in-situ, static formation fluid temperature and pressure conditions above supercritical CO_2 levels; the presence of nonpotable drinking water within the candidate injection zone (i.e., existing dissolved chemical constituents exceeding primary and secondary drinking water standards); and the presence of sufficient reservoir formation injectivity (i.e., hydraulic properties) and overlying caprock sealing characteristics to facilitate the subsequent injection and sequestration of CO_2 during a subsequent field pilot study phase.

In all, 10 basalt interflow reservoir zones were characterized within the Wallula pilot borehole during drilling or immediately before final well completion. In addition to the 10 basalt interflow zone tests, 3 low-permeability caprock test intervals were also characterized above the selected candidate Wallula pilot well injection reservoir. Figure 2.1 shows the preliminary transmissivity versus depth profile for the Wallula pilot borehole, as determined for the 10 interflow zone tests during the active borehole testing campaign. As indicated, a general decrease in test zone transmissivity with depth was exhibited for the site. As discussed in McGrail et al. (2009), this general decreasing transmissivity trend with depth pattern is consistent with results exhibited for Columbia River basalt interflow zones at a number of other (but not all) deep, intensively characterized Hanford Site basalt boreholes, as reported in Gephart et al. (1979), Spane (1982), DOE (1988), and Reidel et al. (2002). This apparent permeability-depth dependence is attributed to compaction (i.e., increasing effective stress), increased secondary mineral formation with depth, and in some basinal geologic settings, increasing horizontal to vertical stress-field conditions (Reidel et al. 2005). Of particular note is the significant decrease in reservoir interflow zone transmissivity below a depth of ~2600 ft within the Wallula pilot borehole. Below this depth, interflow zone transmissivity decreased significantly and ranged between 10^{-2} and 10^{1} ft^2/day.

The candidate injection zone selected during the borehole characterization program contains three Grande Ronde flowtop/interflow zones separated by dense flow interiors. These flowtop/interflow zones have a composite thickness of 91 ft within the 194-ft long open-borehole section, from 2716 to 2910 ft. Based on depth-isolated, packer-test zone characterization tests performed during the borehole testing program, most of the injection zone transmissivity (i.e., ~90%) is contained within the uppermost flowtop, occurring between the depth of ~2721 and 2769 ft. As discussed in McGrail et al. (2009), a series of hydrologic tests were performed for the candidate injection zone over a 5-day period in 2009. Tests included a cyclic constant-rate pumping test and a series of slug and drill-stem tests (DST).

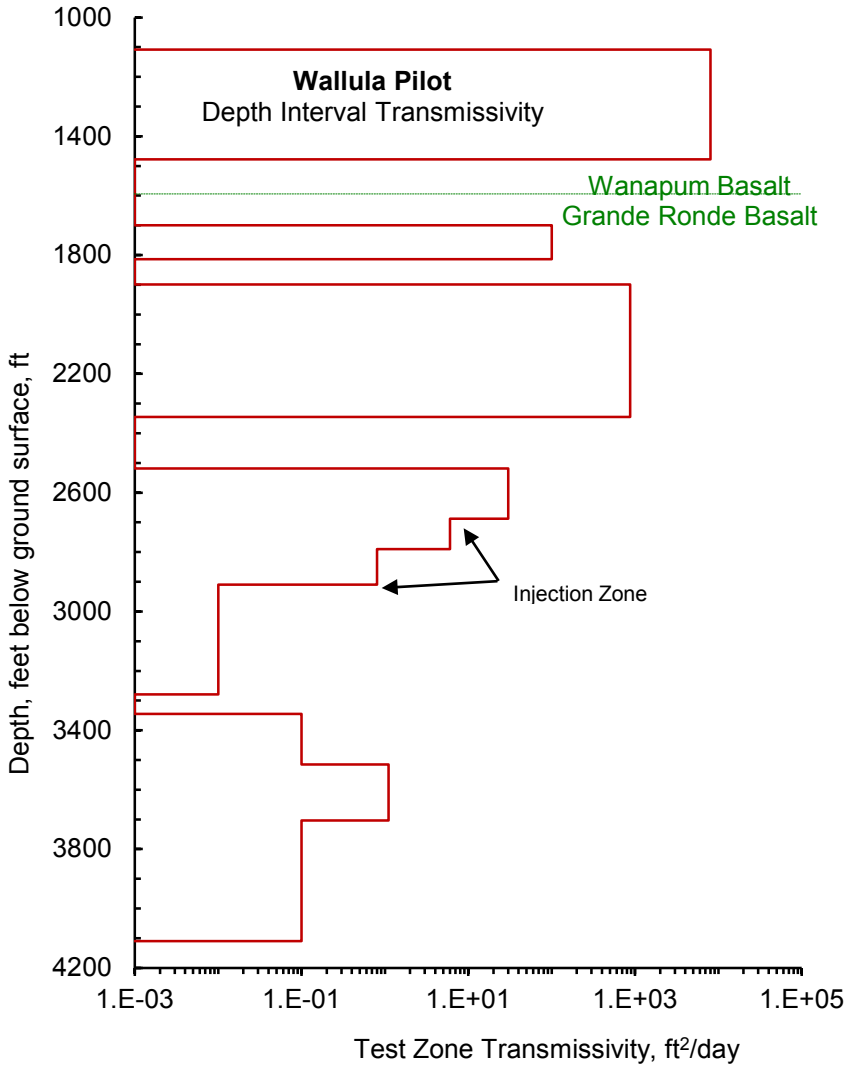

Figure 2.1. Preliminary Transmissivity versus Depth Profile for the Wallula Pilot Borehole (adapted from McGrail et al. 2009)

Preliminary analytical results for individual hydraulic characterization tests provided a transmissivity range for the composite, candidate injection reservoir of T = 9.8 to 19.8 ft^2/day (k = 4005 to 8190 mD-ft), based on homogeneous formation/radial flow model assumptions.

Three low-permeability flow interior/caprock test intervals were also characterized above the candidate injection zone, with borehole test interval lengths ranging between 35 and 99 ft. As discussed in McGrail et al. (2009), multi-step, constant-head injection pressure tests were conducted for all three caprock horizons, with surface injection pressures ranging between 0 and a maximum 150 psi. The multi-step injection tests were completed over test periods ranging between 4.5 and 5.5 hours, with individual injection steps generally ≥ 1 hour in duration. Injection pressure was provided by high-pressure gas cylinders and adjusted appropriately using a high-precision pressure regulator. Average hydraulic conductivity estimates, K, were reported in McGrail et al. (2009) to range between ~$1.0E^{-12}$ to $1.0E^{-13}$

m/sec (i.e., k ~0.01 to ~0.1 microdarcies) for the 3 caprock test intervals. These caprock estimates are consistent with low-permeability, Hanford Site basalt flow interior tests reported in Eslinger (1986).

The low-permeability caprock test values obtained from the borehole tests suggest that overlying thick basalt flow interior sections may represent an effective seal for isolating CO_2 injected into underlying Wallula pilot borehole well completion zone. As noted in McGrail et al. (2009), this assumption concerning sequestration potential assumes that the overlying caprock flow interiors are laterally extensive, and assumes the absence of nearby localized, crosscutting, geologic features; e.g., faults, tectonic fractures, and joints.

Groundwater samples were collected from 6 of the 10 interflow test zones prior to final well completion. The samples were collected at the end of long-duration, constant-rate pumping or cyclical pumping characterization periods primarily using a downhole submersible pump. Collection of the samples at the end of the pumping periods provided for maximum test zone development and removal or minimization of potential antecedent drilling or open borehole conditions. A discussion of sampling procedures, protocols, analyses and interpretation is provided in McGrail et al. (2009). Of particular relevance to the Wallula CO_2 pilot borehole injection study is the requirement of nonpotable groundwater within the candidate injection reservoir. Accordingly, exceeding maximum concentration limits (MCLs) listed in 40 CFR 141.62 is the standard adopted in Washington State for permitting geologic sequestration projects under WAC 173-218-115.

Relatively high fluoride concentrations (3.2 to 11.9 mg/L) were observed within the six interflow zones sampled within the borehole characterization program, which generally increased with increasing test zone depth. A uniform fluoride concentration level of 4.98 mg/L was determined from groundwater samples collected from an extended cyclical pumping cycle used to characterize the candidate injection zone interval. This fluoride concentration level exceeds both the secondary and primary drinking water standards of 2.0 and 4.0 mg/L, respectively.

Note that because of programmatic limitations, no extended hydrologic characterization tests were performed on the injection zone immediately following well completion activities. These extended well tests were designed primarily for determining large-scale hydrologic properties that are important for assessing the suitability of an injection reservoir for CO_2 injection; i.e., detection of lateral hydrologic boundaries and presence of reservoir leakage. As a result of these programmatic issues, a protracted baseline monitoring phase followed the initial borehole test characterization, with extended hydrologic well test characterization occurring after completion of the baseline monitoring. Results from baseline monitoring and hydrologic well testing are discussed in subsequent report sections, respectively.

3.0 Baseline Monitoring

Following Wallula pilot well completion activities, baseline reservoir pressure monitoring of injection zone between June 2009 and December 2010 provided temporal and seasonal response dynamic information. Long-term water level changes within the Wallula pilot well were monitored using two AquiStar® PT2X vented pressure/temperature sensors, with integrated data loggers made by Instrumentation Northwest, Inc. The pressure range of the well water-level sensor was 0 to 5 psi, and after some minor, infrequent pressure shifts were observed during December 2009 (possibly due to freezing of the desiccant within the vent tube), a second 0 to 5 psi pressure probe was installed to serve as a backup system. The sensors were placed in the well at a depth below the well water level (i.e., $\leq$ 3 m), that maintained the probe pressures within the 0.5 to 5 psi range. The use of low-range pressure transducers greatly increases the accuracy and resolution characteristics for monitoring temporal and long-term reservoir pressure patterns, in comparison to high-range pressure probes installed at formation depths. In addition, shallow-based pressure sensors do not exhibit excessive trend (either linear or nonlinear) characteristics, which commonly occur for long-term formation-depth pressure probe installations. For these reasons, shallow-based pressure monitoring systems are preferable to high-range pressure probes installed at formation depths provided that relatively stable environmental conditions are exhibited during the monitoring period (i.e., no significant well fluid-column temperature or pressure changes). These observations are consistent with findings presented in Spane and Mercer (1985) and Spane and Thorne (1986) that compare pressure response results obtained with shallow and deep monitoring well systems.

Pressures from the well sensors were recorded every 15 minutes. Barometric pressure was recorded at the field site every 15 minutes simultaneously with the well water-level measurements, using a BaroTROLL® pressure transducer (made by In-Situ, Inc). The range for this instrument was 0 to 16.5 psi, with a manufacturer-stated accuracy 0.02% of full scale (0.0033 psi).

Salient findings concerning long-term or seasonal and temporal injection reservoir pressure characteristics obtained from the baseline monitoring characterization phase are discussed in Section 3.1.

3.1 Seasonal Characteristics

For long-term season pattern assessment, a simple, visual direct comparison procedure was adopted. Figure 3.1 shows the long-term hourly hydraulic head (well water-level elevation) response pattern exhibited for the Wallula pilot well injection reservoir during the continuous baseline monitoring period of June 2009 to December 2010. As indicated in Figure 3.1, a significant seasonal hydraulic head (pressure) cycle of approximately 2.15 m/year is evident over the ~1.5-year baseline monitoring period. Long-term seasonal aquifer response characteristics are normally reflective of areal and point-source recharge/discharge components and proximity to flow-system boundaries (e.g., Columbia River). For the Wallula pilot well site, possible recharge/discharge mechanisms include both natural processes and human-related activities (e.g., seasonal agricultural pumping).

The strong seasonality component of the well water-level response appears to be casually coincident with expected agricultural groundwater withdrawal patterns within the basin, which normally start in late March/April and continue through September. River stage and/or dam reservoir fluctuations may also impose associated well water-level response effects due to formation loading and communicative

mechanisms. River-stage imposed effects on aquifer response have been discussed and documented in numerous hydrologic papers (e.g., Ferris 1963; Pinder et al. 1969), and a study of Columbia River fluctuation effects on deep basalt formations at the Hanford Site was presented by Nevulis et al. (1989). As summarized in Spane and Mackley (2010), the magnitude of the associated response within a communicative aquifer due to river-stage fluctuations is a function of several physical factors, including well conditions (wellbore storage and well-skin effects), aquifer characteristics (hydraulic diffusivity), boundary conditions (well and river distance, aquifer penetration, river-bed resistance), and characteristics of river-stage fluctuations (magnitude and period/frequency of the fluctuation).

Figure 3.1. Wallula Pilot Well Baseline Monitoring Response: June 2009 – December 2010 (hourly measurements)

Figure 3.2 shows a visual comparison between hourly Wallula pilot well water levels and the corresponding Columbia River and McNary Reservoir (i.e., Lake Wallula) hourly elevations over the entire baseline monitoring period. As shown in Figure 3.2, no significant visual association was evident during the baseline monitoring period (note the Wallula pilot well is located ~ 520 m (1706 ft) east of the McNary Reservoir). However, the McNary Reservoir elevation is highly controlled and limited as are other dam reservoir impoundments on the Columbia River and neighboring Snake River systems. These regulatory controls limited the elevation fluctuations of McNary Reservoir to only 0.89 m (2.9 ft) over the ~1.5 year baseline monitoring period. Similarly, small reservoir elevation fluctuations were also observed for other neighboring dam reservoirs (not shown) on the lower Columbia River and neighboring Snake River systems.

Because tail-water reaches, immediately downstream from lower Columbia River dams are generally free-flowing and have smaller surface-water storage areas, significantly greater seasonal surface-water elevation height fluctuations are exhibited for varying seasonal dam release discharges. Figure 3.3 shows the surface-water elevation fluctuation pattern for the Columbia River elevation immediately downstream from McNary Dam (i.e., tail-water elevation), which varied 2.45 m (8 ft) over the baseline monitoring period. The lateral distance between these Wallula pilot well and McNary Dam tail-water measurement location is ~32 km (~20 mi). To facilitate the visual comparison, a 48-hour backward moving average scheme was used to remove short-term (i.e., higher frequency) fluctuations for the river data. As shown, some visual correspondence is suggested between the McNary Dam tail-water elevation and the Wallula pilot well water-level response, particularly over the spring to early fall seasonal period. However, this partial seasonal correspondence may be coincidental, particularly due to the lack of a predominant river-stage elevation increase that could be responsible for the significant recovery well response exhibited between late summer and early spring months. Nevertheless, some secondary river-induced impacts may be present that are masked by larger seasonal and temporal processes. Note that due to common seasonal discharge patterns, the seasonal McNary Dam tail-water elevation pattern is very similar to that exhibited at other downstream river reach sections below the lower Columbia River (not shown), particularly to the neighboring Snake River Ice Harbor Dam, which is located ~16 km (~10 mi) from the Wallula pilot well.

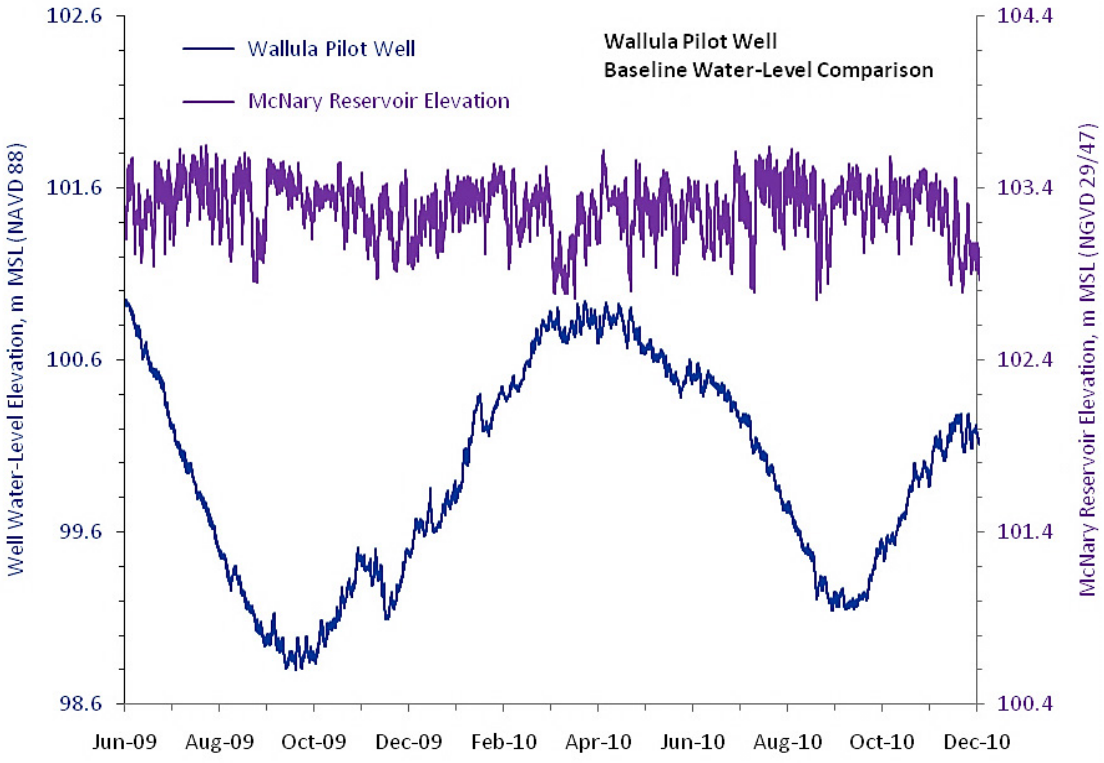

Figure 3.2. Baseline Response Comparison for Wallula Pilot Well and McNary Dam Reservoir

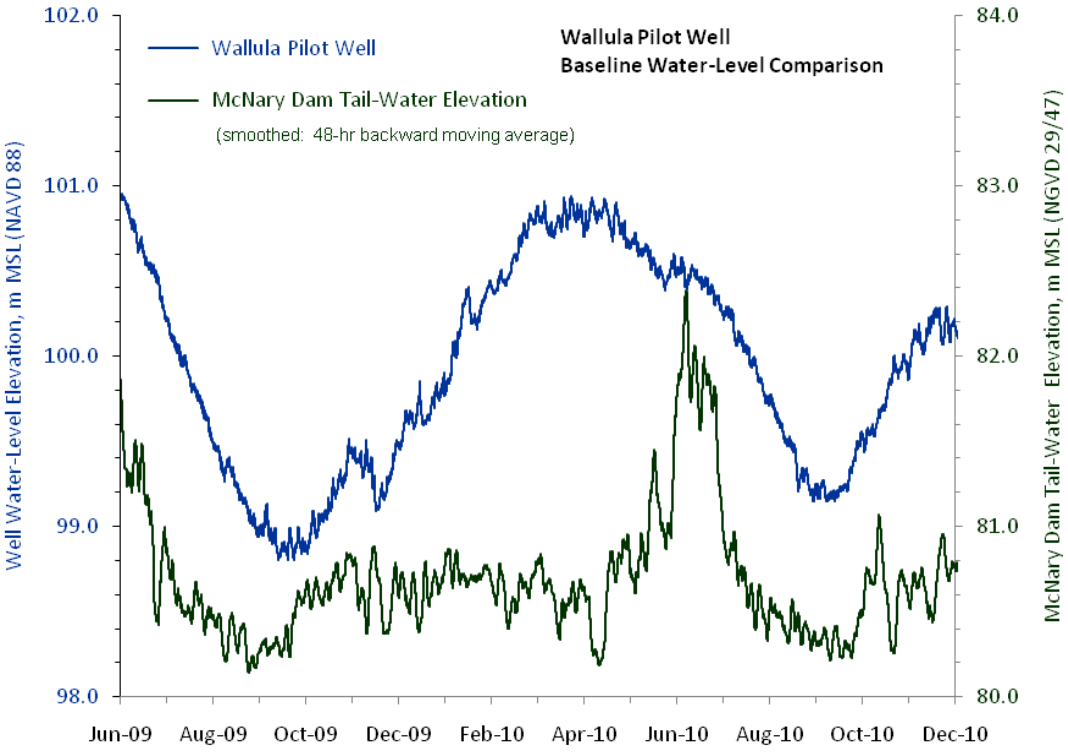

Figure 3.3. Baseline Response Comparison of Wallula Pilot Well and McNary Dam Tail-Water Elevation

3.2 Temporal Stress Effects

In addition to long-term seasonal stress processes, temporal natural external stresses (e.g., barometric effects, earth tides) can also produce observable associated reservoir pressure and well water-level responses. A number of earlier investigations have addressed these natural stress effects on aquifer response and well water-level measurements. Examples of such investigations pertaining to confined aquifer systems are provided in Jacob (1940); Ferris (1963); Bredehoeft (1967); Bower and Heaton (1978); and Hsieh et al. (1988).

To assess the temporal impact of barometric and earth tide stress fluctuations on the Wallula pilot well water levels, hourly water levels and atmospheric pressure measurements were examined from the baseline monitoring dataset described in Section 3.0. Hourly earth tide stress potentials for the Wallula pilot well site (not shown) were generated using the ETIDE program described in Hydrotechnique (1984). Because barometric effects are generally greater than associated earth-tide responses, barometric analysis was applied first to the available Wallula baseline dataset. This is the approach used successfully by Spane and Thorne (2000) for similar baseline well datasets exhibiting observable barometric and earth tide effects.

Although barometric response analysis can be applied in the presence of other extraneous background stress effects, it is best performed when these overlapping background impacts are at a minimum. In examining the total baseline well response shown in Figure 3.1, the longest continuous period not significantly impacted by background seasonal effects appears to occur during the spring season from

March to early May. Based on this visual assessment, hourly barometric and well water-level responses were examined over a 60-day period from March 6 through May 5, 2010 (2010 calendar days 65–125). Figure 3.4 shows a direct comparison between well and barometric response over this 60-day period.

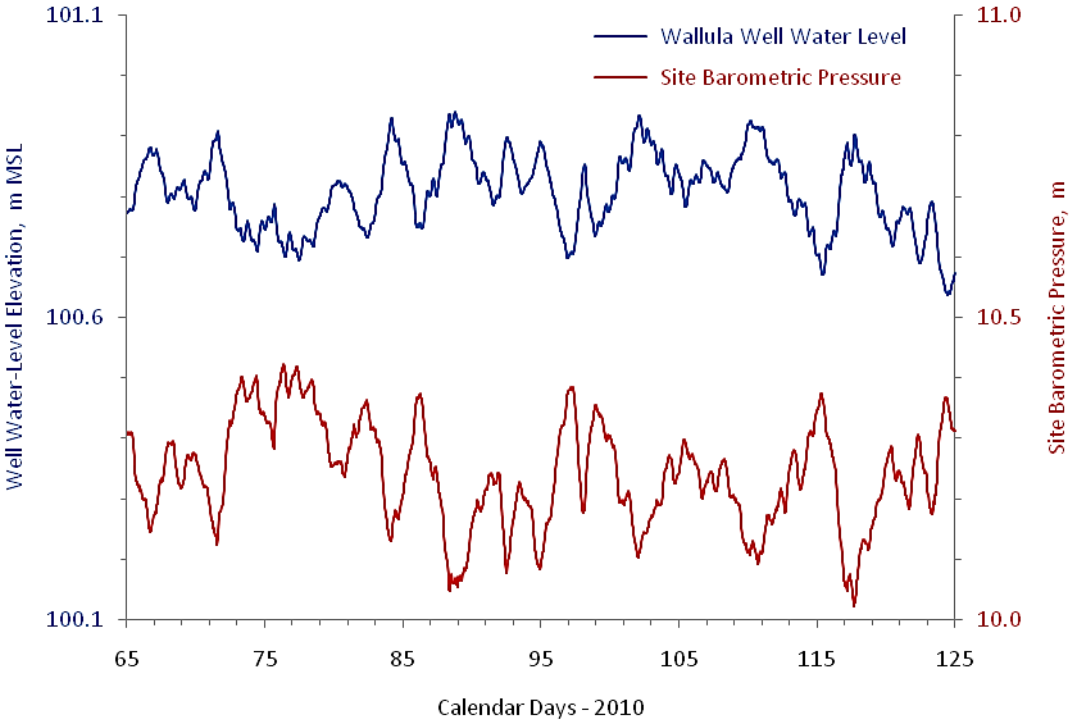

Figure 3.4. Comparison of Wallula Pilot Well Water Level and Site Barometric Pressure

As indicated, a high-inverse correspondence between well response and barometric pressure is exhibited. This high level of visual correspondence between well and barometric response can be examined statistically in the frequency domain using spectral analysis methods as discussed in Spane (2002). Figure 3.5 shows a continuous spectral-frequency plot comparison for the two responses over this 60-day period. The spectral-frequency plot was developed using the procedure presented in Hydrotechnique (1984) and summarized in Chien et al. (1986). Visual examination of the plots indicates a nearly identical spectral pattern, both in frequency and amplitude. The spectral patterns exhibit distinctive diurnal (~0.042 cycles/hr) and semi-diurnal (~0.083 cycles/hr) frequency peaks that are commonly associated with atmospheric heating and cooling. Most of the spectral response energy, however, is expressed in the low-frequency range of ≤ 0.045 cycles/hour (i.e., periods ≥ 22 hr), which is characteristic of longer period climatic patterns (i.e., storm events). Diurnal and semi-diurnal stress responses associated with earth tide fluctuations are also relevant as indicated in a similar spectral-frequency comparison shown in Figure 3.6. No obvious correlation was exhibited between spectral-frequency comparisons of Wallula pilot well responses to McNary Dam reservoir or tailwater elevations during this 60-day baseline comparison (see Appendix B, Figures B.1 and B.2).

To quantitatively examine the dependence of the well response to barometric pressure in the time-domain, a barometric response plot (BRP) was developed following the procedures initially described in Rasmussen and Crawford (1997), and expanded upon by Spane (1999, 2002).

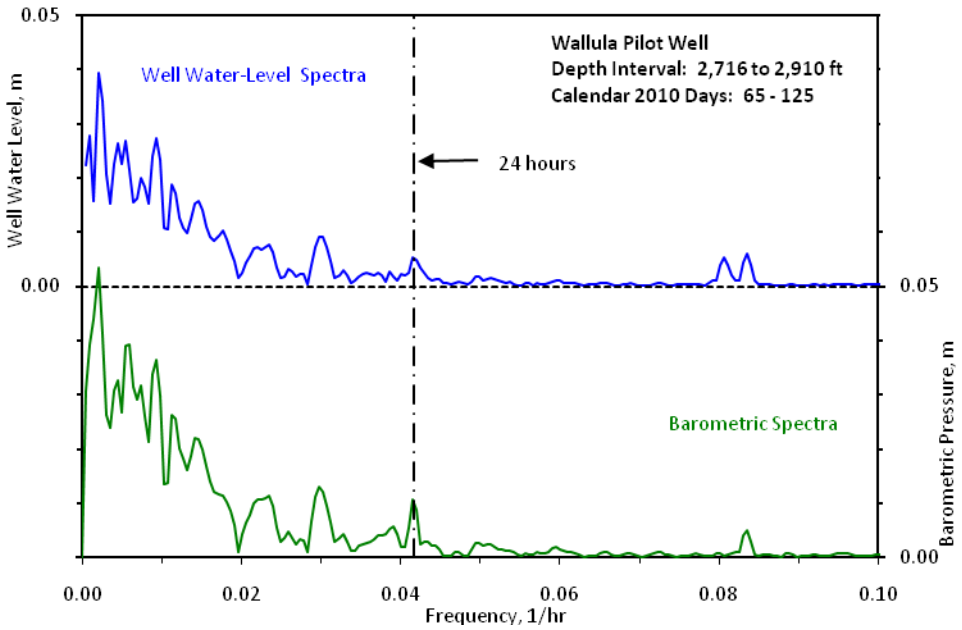

Figure 3.5. Wallula Pilot Well and Barometric Spectral Frequency Comparison

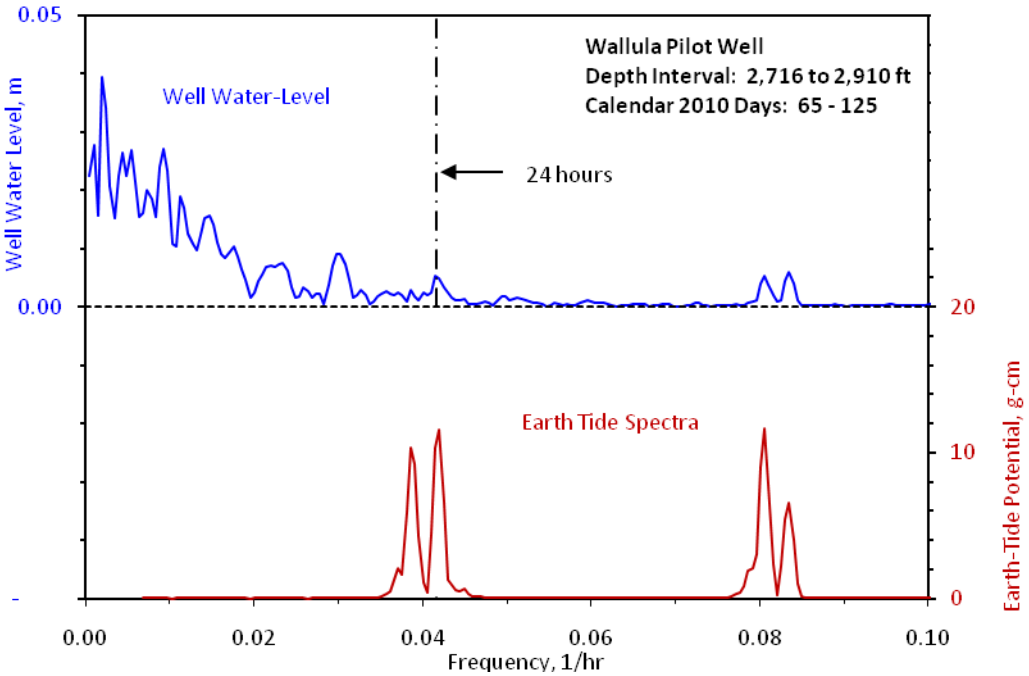

Figure 3.6. Wallula Pilot Well and Earth Tide Spectral Frequency Comparison

Development of a BRP provides a diagnostic method for identifying operative aquifer model conditions (i.e., unconfined versus confined) and the presence of aquifer leakage or existence of hydrologic boundaries, as proposed in Spane and Didricksen (2005). The plots are developed by performing multiple linear regression convolution analysis of the water-level response to the barometric pressure change over the time-lag period with a constant observation period. For the Wallula pilot well baseline dataset, a 1-hour frequency was used. The BRP is constructed by summing the calculated, time-

lag regression coefficients over time-lag intervals that indicates relevance. For the Wallula pilot well response analysis, the continuous time-lag sequence used in constructing the BRP was expanded up to 400 hourly time lags. Results of multiple-regression time-lag analyses in this report were calculated using Minitab 15 Statistical Software (Minitab, Inc. 2007). Detailed discussion and examples of BRP development are provided in Spane (1999), Toll and Rasmussen (2007), and Spane and Mackley (2010).

Figure 3.7 shows the BRP developed for the Wallula pilot well reservoir zone. As indicated in the figure, a number of diagnostic hydrologic features are exhibited.

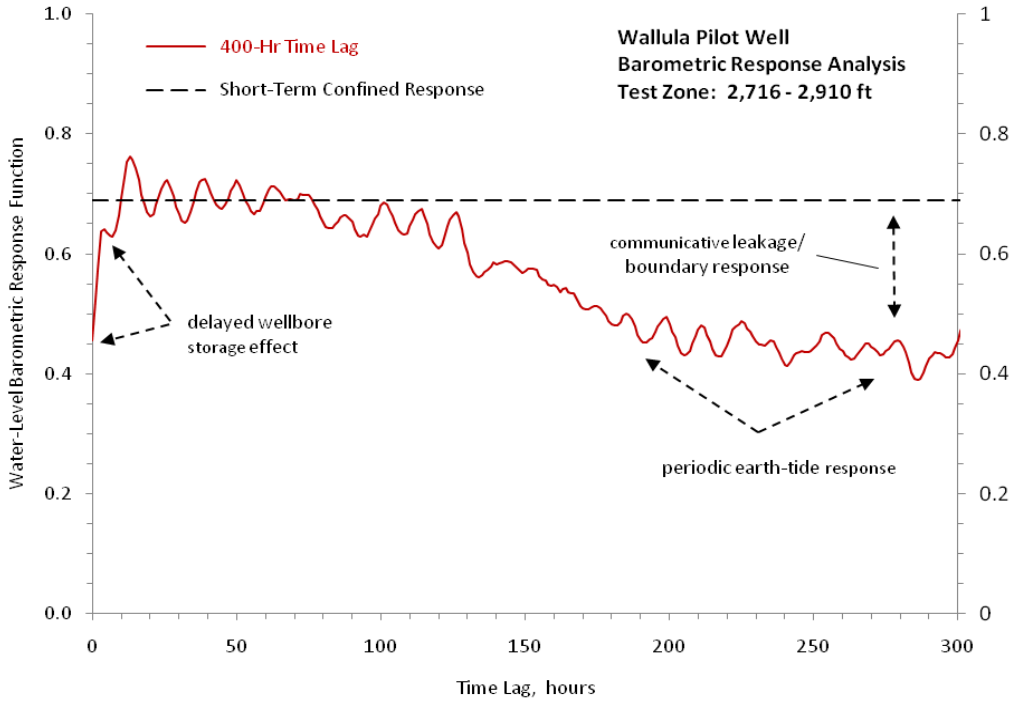

Figure 3.7. Wallula Pilot Well Barometric Response Plot Analysis

For early time lags (i.e., <4 hours), an attenuated response is indicated that is characteristic of wellbore storage effects. This is expected for a well or aquifer system possessing a relatively large well-casing and exhibiting low-formation transmissivity conditions. A background uniform barometric response function value of ~0.69 is exhibited following wellbore storage effects for time-lag values up to ~75 hours. This response is characteristic of nonleaky, confined aquifer conditions over this time period. Small, characteristic 12-hour and 24-hour time-lag, earth-tide induced signatures are exhibited over the majority of the time-lag period. Of particular hydrologic significance is the barometric response decline pattern that occurs after a time lag of 75 hours and then stabilizes at a barometric response value of ~0.45 for time lag values greater than ~230 hours. Although barometric response analysis techniques have not been developed to definitively characterize this response condition, the declining pattern is consistent with a number of theoretical formation conditions, including a leaky (pervasive) confined aquifer system (see Spane and Didricksen 2005); a confined aquifer system in hydraulic connection with a vertically communicative hydrologic feature at a distance from the well (constant pressure boundary); or an abrupt, significant increase in reservoir hydraulic/storage properties at a distance from the well. At this time, it is not possible to distinguish between the various causative factors that may be responsible for this barometric response pattern.

The construction of a well BRP, with developed time-lag dependent regression coefficients, provides the opportunity to remove the barometric pressure stress effects from the Wallula pilot well response for other possible characterization applications. The removal process follows the multiple-regression deconvolution process described in Spane (1999, 2002) and Spane and Mackley (2010). Figure 3.8 shows the observed and barometric-corrected well response over a 15-day period using a 68-hour multiple-regression time-lag deconvolution.

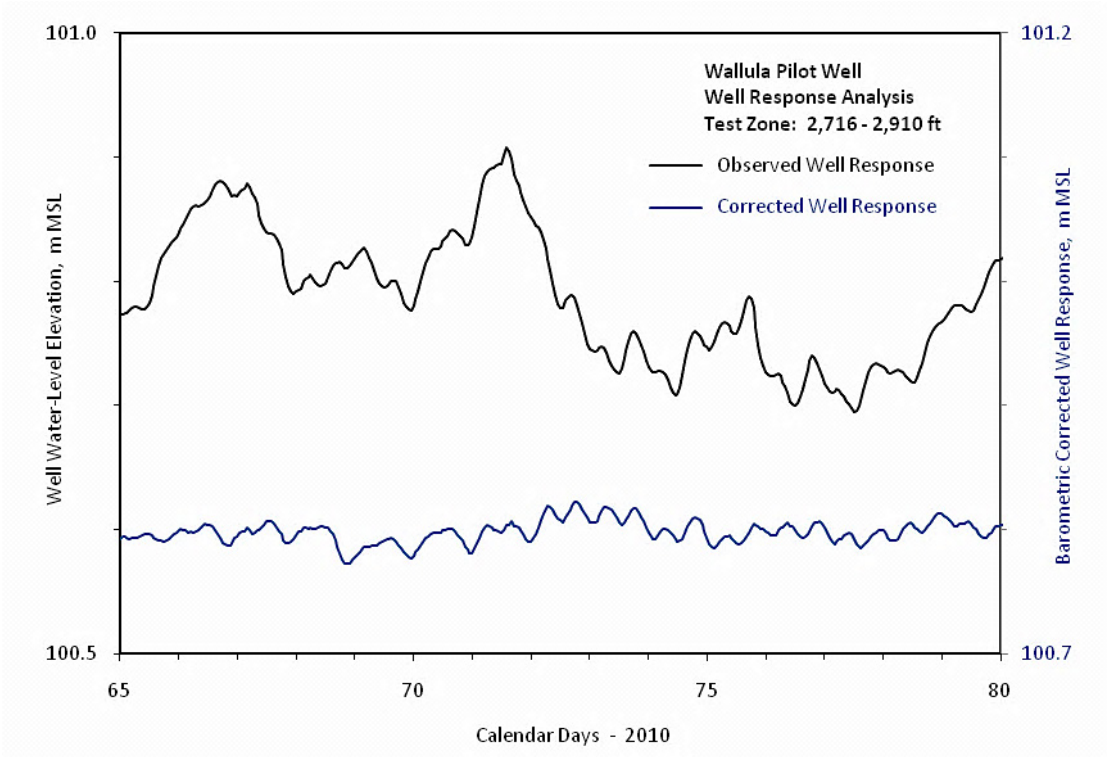

Figure 3.8. Comparison of Observed and Barometric-Corrected Well Response

The 68-hour time-lag regression used exhibits the highest level of statistical correspondence during the BRP development. As indicated, the ~0.2 m (7.8 in.) of barometric fluctuation evident during this 15-day example period was effectively removed by the deconvolution process, leaving a residual well pattern that is responding primarily to earth-tide stress effects. The high level of correspondence between the barometric corrected well response and earth-tide potential is shown in an expanded well response plot shown in Figure 3.9. As noted previously, the earth-tide potential for the Wallula pilot well site was developed using the ETIDE program described in Hydrotechnique (1984).

The ability to correct the well response for barometric pressure fluctuations provides a basis for additional analysis of other temporal stress effects for reservoir characterization applications (e.g., earth tides, reservoir loading). However, these types of hydrologic analyses were not initiated at the time of report preparation. Of particular interest is a recently reported method by Cutillo and Bredehoeft (2011) of combining barometric and earth tide analysis. This composite approach is reported to be particularly applicable in characterization of storage properties within highly rigid formations (such as basalt). Knowing the reservoir storage properties of the Wallula pilot well injection zone more precisely would improve the accuracy for modeling estimates of the impacted area following CO_2 injection.

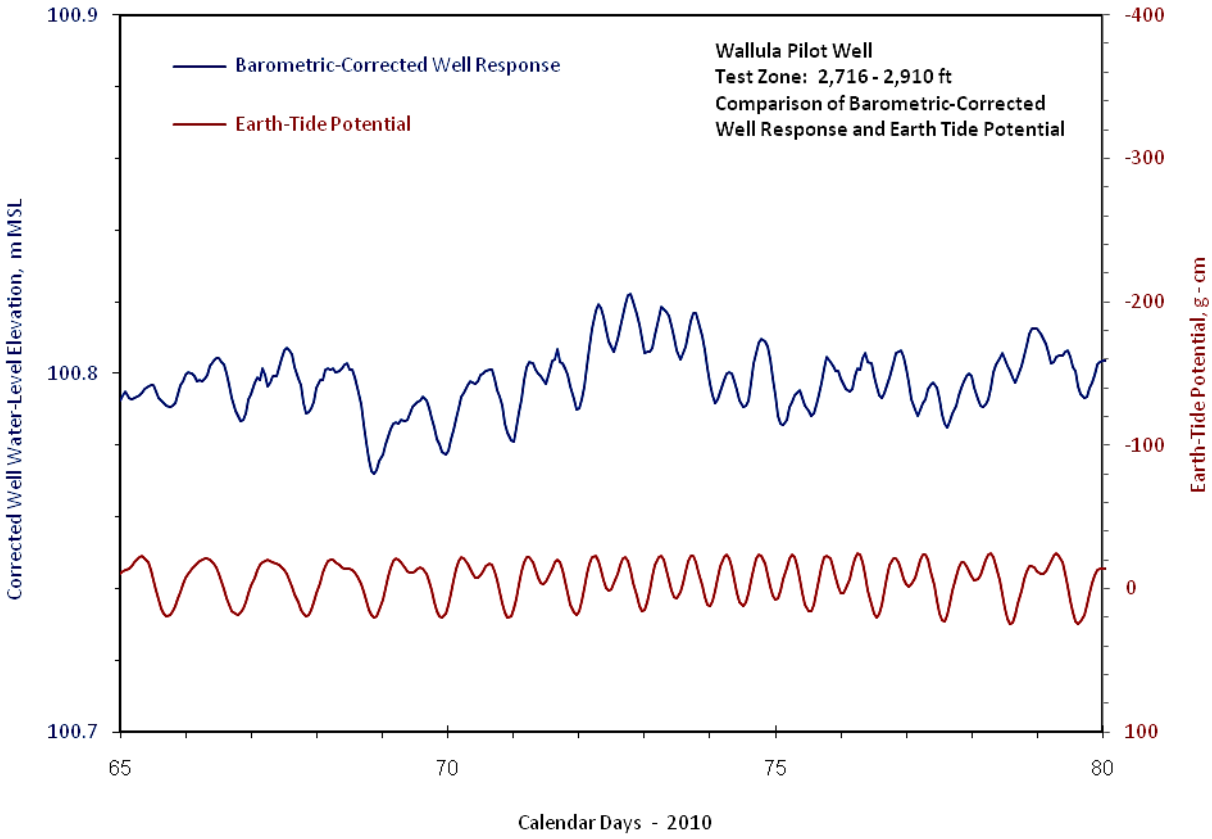

Figure 3.9. Comparison of Barometric-Corrected Well Response and Earth Tide Potential

4.0 Hydrologic Well Tests

Following the baseline monitoring period, hydrologic testing was conducted between late December 2010 and March 2011 with the following objectives:

- Establish current well and test zone conditions
- Identify the operative aquifer flow model
- Determine large-scale hydraulic properties
- Detect the presence of surrounding hydrologic boundaries within the candidate injection reservoir.

To accomplish these objectives, an initial, limited wireline logging survey was performed, followed by three sequential hydrologic testing activities: pneumatic slug testing; a step-drawdown test, and a 7-day, constant-rate discharge test. Pneumatic slug tests were designed to assess whether formational hydraulic property conditions near the well had changed following the completion of well construction activities. A step-drawdown pumping test was conducted following pneumatic slug testing to assess well-loss conditions (i.e., nonformational head loss) and to select an optimum pumping rate for the subsequent constant-rate pumping test. A 7-day constant-rate pumping test was performed following a 4-day, step-drawdown test recovery period. The objectives of the constant-rate pumping test were to support aquifer flow model identification, determine large-scale hydraulic properties, and to detect the presence of nearby hydrologic boundaries.

Of particular importance was the diagnostic analysis of the 7-day constant-rate pumping test and ~3-week recovery period response that indicated a nonradial, linear-flow regime within the formation immediately surrounding the well, and the existence of a nearby hydrologic boundary condition. A number of hydrogeologic conditions can produce the observed hydrologic test conditions, and the lack of surrounding observation and monitor well data within the test reservoir during testing makes it difficult to identify the causative factor(s). Recommendations to help identify the causative hydrogeologic conditions are presented in Section 7.0. Results obtained from the various detailed well tests and activities are provided in the following report subsection discussions. A general discussion of the various hydrologic tests and the analysis methods employed for the Wallula hydrologic test characterization program is in Appendix A.

4.1 Wireline Geophysical Surveys

Stoller Corporation conducted a limited suite of wireline geophysical surveys on December 29, 2010, to assess the general condition of the Wallula pilot well over the protracted 1.5 year period since well completion. Of particular interest was the assessment of well depth and diameter of the open borehole section of the well, and determination of the stabilized fluid temperature profile within the well. Three geophysical surveys were utilized: caliper, sonic and fluid temperature. These same surveys were conducted previously by Stoller Corporation during the active Wallula pilot borehole drilling phase and results are provided in McGrail et al. (2009). A comparison of the caliper and sonic log information with prior Stoller Corporation survey results (not shown) indicated no significant change in borehole conditions (i.e., borehole diameter and near-well formation physical properties). However, more recent survey results did indicate a small amount of bottom borehole infill had occurred (i.e., ≤3 ft), with a current bottom borehole depth determination of ~886 m (2907 ft) bgs.

Fluid temperature surveys can be significantly impacted by prior drilling activities and ambient, in-borehole, cross-flow conditions. As a result, fluid temperature surveys obtained after a significant time following well completion activities are preferred for establishing representative, in-situ depth and profile conditions. Figure 4.1 shows a comparison between a fluid temperature survey profile obtained by Schlumberger Wireline Services immediately prior to well completion (April 19, 2009), and the recent Stoller Corporation survey conducted on December 29, 2010. Figure 4.1 also shows the open borehole section of the well and location of the overlying Umtanum basalt flow interior caprock. As indicated in Figure 4.1, the most recent fluid temperature profile appears to "mimic" but is offset ~ +3°F over the earlier survey that was conducted shortly after cessation of borehole drilling. As noted in McGrail et al. (2009), the borehole was drilled with make-up water that was stored at land surface, which due to the time of the year, had a major impact in lowering the injection zone formation temperature over in-situ conditions at the time of the 2009 survey. The more recent fluid temperature survey indicates the stabilized, in-situ injection reservoir temperature ranges from 94.7°F to 97.7°F from the top to the bottom of the injection zone, respectively.

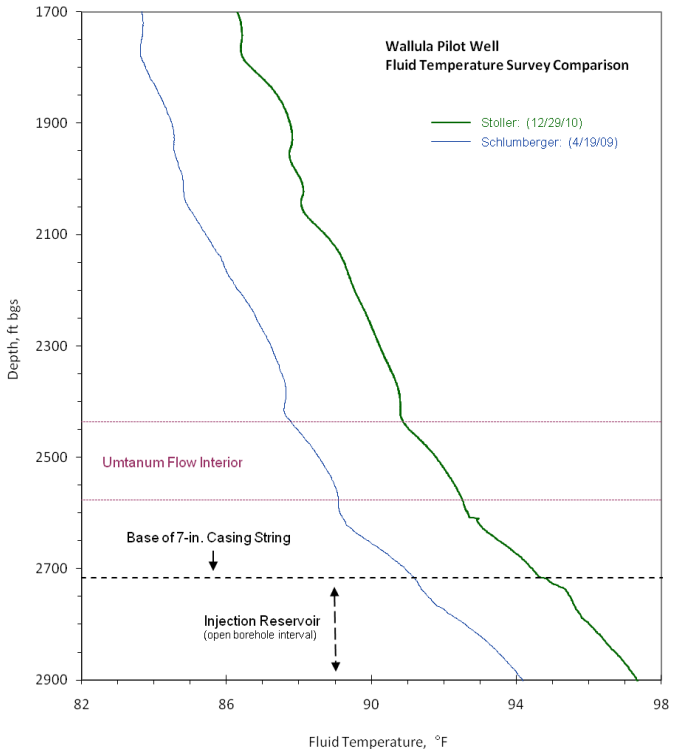

Figure 4.1. Comparison of Wallula Pilot Well Fluid Temperature Surveys

Observations based on the recently acquired, stabilized fluid temperature survey are shown in Figure 4.2 and include the inference of permeable basalt interflow zones at depths of ~533, 592, 620, and 731 m (~1750, 1945, 2035, and 2400 ft, respectively) and two contrasting, well-defined, fluid temperature gradients for the upper Grande Ronde (between 485 and 739 m [1594 and 2425 ft, respectively]) and the Grande Ronde Basalt below the top of the Umtanum basalt flow interior to the bottom of the borehole (between 742 and 886 m [2436 and 2910 ft, respectively]). The presence of permeable basalt interflow zones at these general depths is supported by hydrologic test results obtained during the active borehole test characterization program (Test Zones 2 and 3), as reported in McGrail et al. (2009).

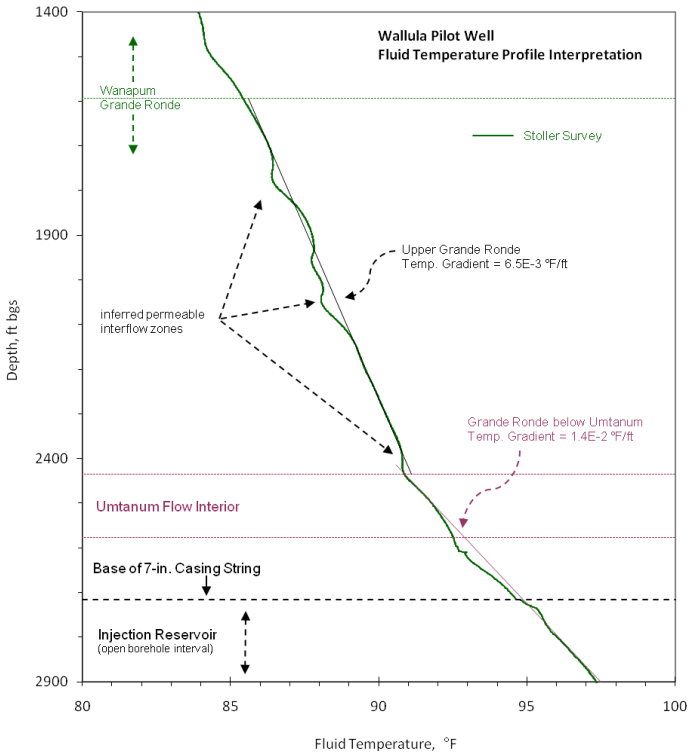

Figure 4.2. Fluid Temperature Profile Observations

The observed fluid temperature profile exhibits a significant change in fluid temperature gradient for the Grande Ronde Basalt well section below the top of the Umtanum basalt. As indicated in Figure 4.1, the upper Grande Ronde basalt section above the Umtanum basalt exhibits a fluid-temperature gradient of 6.5E-3°F/ft, while the gradient below the Umtanum is over twice as high, at 1.4E-2°F/ft. However, the significantly lower fluid-temperature gradient exhibited for the upper Grande Ronde section at Wallula appears to be due to greater advective groundwater flow within the surrounding basalt formations. This lower temperature gradient condition (i.e., in comparison to the lower Wallula pilot well section) can be produced by several hydrologic conditions including higher lateral groundwater and/or active vertical groundwater mixing.

The observed Wallula pilot well fluid temperatures versus depth are significantly lower than that observed for deep basalt wells/boreholes at the neighboring Hanford Site, as reported in DOE (1988). Appendix B, Figure B.3 shows a comparison of fluid temperature versus depth profiles for the Wallula pilot well and the Hanford Site well DC-15 (699-S16-E14), as reported in Schroder and Strait (1987). It should be noted that well DC-15 is located at a similar distance west of the Columbia River, as the Wallula pilot well is positioned to the east of the river. As indicated, the temperature gradient for the lower section of the Wallula pilot well is similar to that exhibited at well DC-15, although the temperatures are significantly lower (i.e., ~20°F). The causative factor(s) responsible for the lower basalt temperatures observed at the Wallula pilot well in comparison to Hanford Site conditions is not currently known. However, note that Hanford Site and Wallula site temperature versus depth relationships may be reflective of being within different groundwater flow systems, with different contributing basin sizes, and depth of groundwater circulation.

4.2 Pneumatic Slug Tests

A series of five, multi-stress level pneumatic slug tests were performed between December 30, 2010, and January 6, 2011, to determine near-well, reservoir hydraulic property conditions and assess any dependence to applied stress levels. The test well condition during testing is indicated in Figure 1.2. To facilitate the performance of the pneumatic tests, a sealed surface wellhead constructed of polyvinyl chloride pipe was fabricated and attached with a surface flange/seal to the top of the 17 cm (7-in.) well casing as shown in Appendix C, Figure C.1. The fluid column within the well was depressed pneumatically using regulated compressed air cylinders, and in-well fluid levels were monitored using a surface-based 50-pound-force per square inch gauge (psig) vented strain-gauge pressure transducer (Druck, model PDCR 1830-8388), that was installed a short distance below the projected fluid-column depression. After the depressed fluid column pressure stabilized, the compressed air inside the sealed well column was released by opening two opposing wellhead ball valves (see Appendix C, Figure C.1), thereby initiating a slug withdrawal test caused by the depressed water column. The cross-sectional area of the surface wellhead ball valves was ~1.5 times the cross-sectional area of the well-casing column, and is consistent with test recommendations specified in Spane et al. (1996) for the performance of pneumatic slug tests. Test pressure responses were recorded using a surface datalogger (Campbell Scientific, Inc., model CR10X).

Applied stress levels used for the five individual pneumatic slug withdrawal tests ranged from 9.7 to 30.1 psi. Figure 4.3 shows a comparison of the normalized slug test responses (expressed as dimensionless head, H_D) versus test time.

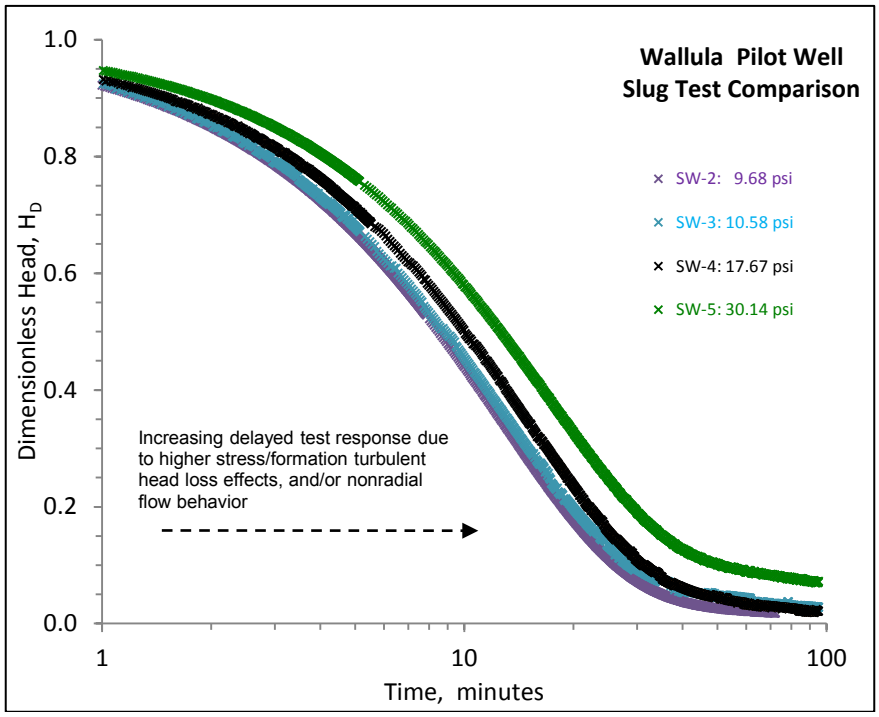

Figure 4.3. Comparison of Wallula Pilot Well Pneumatic Slug Test Responses

Note that the first slug withdrawal test (SW-1) is not included in the comparison because of a premature release of the compressed-air and well column prior to achieving fluid-column pressure

stability. As indicated, the four pneumatic slug tests exhibited a distinct, delayed-test response pattern with correspondingly higher applied stress levels. This type of stress dependence in tests has been commonly attributed to turbulent well losses, particularly prevalent in high-permeability formations, or due to test length (e.g., Butler 1997). In these situations, the lower applied stress tests are expected to provide more representative analytical results. The Wallula pilot well injection zone does not exhibit high-permeability characteristics, and the associated observed stress dependence is believed attributable to intersection of thin higher permeability feature by the open borehole (e.g., fracture) that acts as an extension of the wellbore. Given this proposed test scenario, higher slug stress applications encompass progressively larger formation areas of the reservoir (via the communicative feature), thereby creating an associated stress dependence with increasing test area/length.

To examine if this stress-dependence condition was exhibited during the earlier 2009 borehole testing of this test interval (McGrail et al. 2009; Test Zone 8B), the free flowing phases (i.e., slug test response period) of DSTs that were performed for the Wallula pilot well injection reservoir were plotted (Figure 4.4) with the recent slug test responses (Figure 4.3). Stress levels for the three earlier slug/DST tests were significantly higher than the recent pneumatic slug tests, and ranged between 48 and 108 psi. Coincidently, the slug DST responses during the earlier borehole testing campaign occurred within a 17.7-cm (7-in.) casing cross-over (used to house the submersible pump), which was connected to the underlying 7.3-cm (2-7/8 in.) diameter packer test-tubing string. The common dimensional test conditions indicate no significant response corrections for these earlier tests were necessary for the test comparisons in Figure 4.4. Figure 4.4 shows that the stress dependence exhibited for the lower stress pneumatic slug tests is also consistently expressed as well for the higher pressure slug/DST tests.

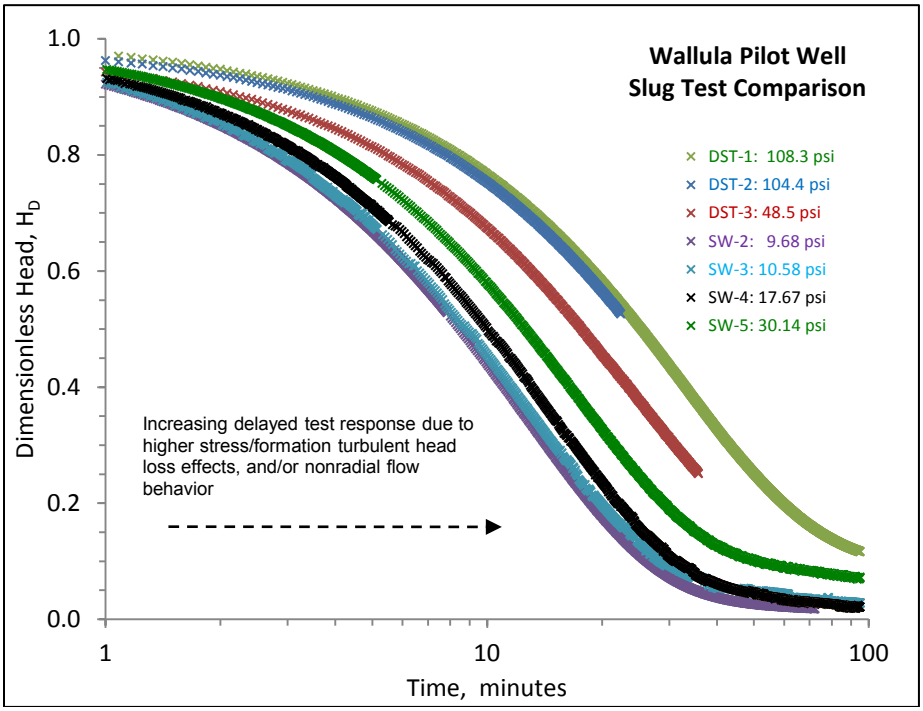

Figure 4.4. Comparison of Wallula Pilot Well Pneumatic Slug and Earlier Borehole Slug/Drill Stem Test Responses

Attempts to analyze the entire pneumatic slug test response for the individual slug tests using standard homogeneous formation and radial flow models were only partially successful. Figure 4.5 shows a typical slug test response and attempted type-curve match, which is based on homogeneous formation analytical solution (see Appendix A).

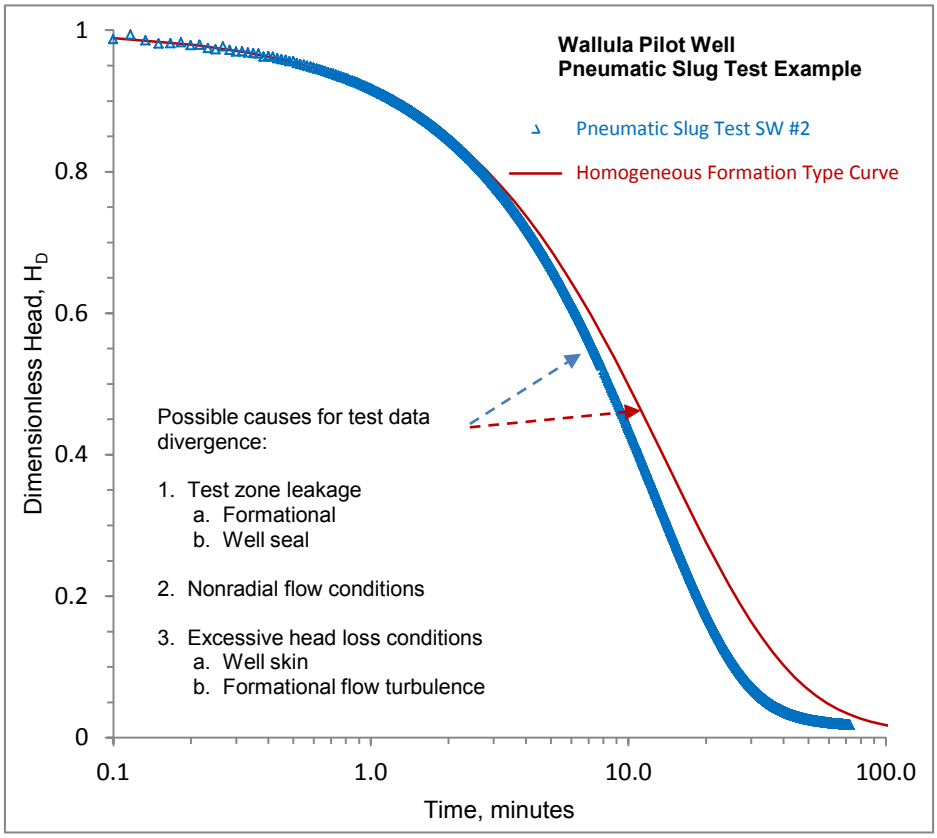

Figure 4.5. Pneumatic Slug Test Response Example

As shown, the observed slug test response diverges from the predicted type-curve solution during later test times after ~20 to 30% of the test recovery has occurred. A number of causes for the later test time divergence are possible, including test zone leakage, nonradial flow behavior, and excessive head loss conditions. It is not possible to distinguish between causative factors based solely on slug test response characteristics. However, based on diagnostic analysis of the subsequent constant-rate pumping test (discussed in Section 4.4), the cause for the divergent behavior appears to be attributed to nonradial flow behavior.

Nonradial slug test analysis methods are not available commercially. In an attempt to provide a range for hydraulic properties within near-well formation region, the early-time slug test responses were analyzed using standard homogenous formation and radial-flow analytical solutions (see Appendix A). Because Butler (1997) recommends use of low-stress slug tests for determining formation property conditions for test zones exhibiting slug stress dependence, pneumatic slug test SW-2 was initially examined. Figure 4.6 shows the composite dimensionless head and head derivative analysis, and associated type-curve and derivative plot match for this test. As indicated in the figure, the early-time analysis match provided the following hydraulic property estimates: transmissivity, T = 20.2 ft^2/day and hydraulic conductivity, K = 0.42 ft/day, based on an assumed storativity, S, of 1.0E-5, a well skin, s_K, of

0, and a contributing formation thickness, b, of 48 ft. The 14.6-m (48-ft) contributing thickness is based on previous testing observations made during the borehole characterization phase of the program (McGrail et al. 2009). Based on formation temperature and hydrostatic pressure conditions of 95°F and 1170 psi, respectively, and a calculated fluid dynamic viscosity of 0.70 cp, the intrinsic permeability, k, estimate based on this test analysis is 108 millidarcies (mD).

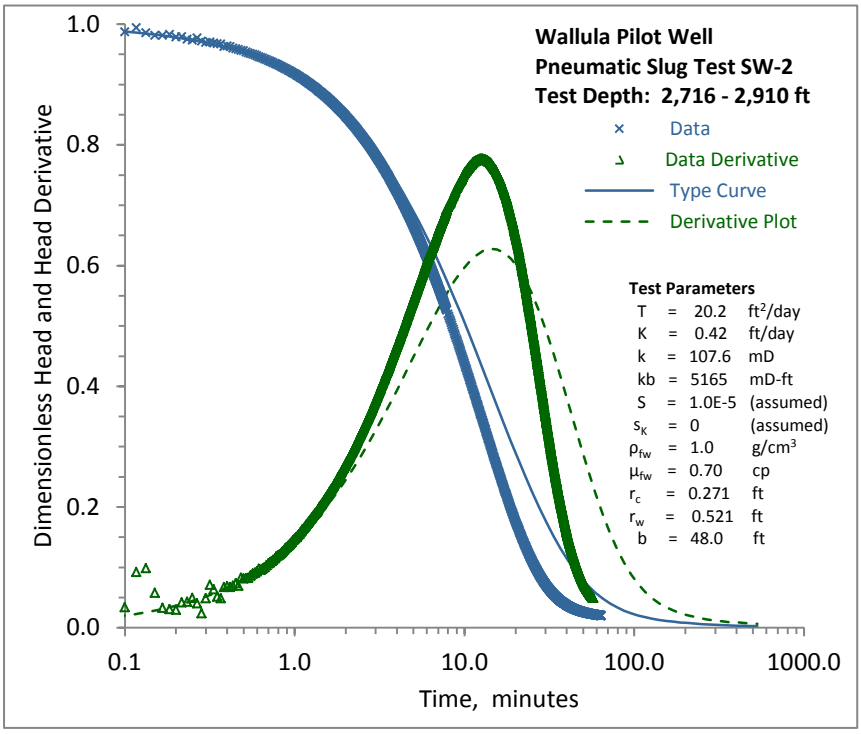

Figure 4.6. Pneumatic Slug Test SW-2 Analysis Plot: Homogeneous Formation Solution

As indicated in Figure 4.3, the delayed test response relationship for higher slug test stress levels would produce correspondingly lower estimates for hydraulic properties. For the highest stress test, SW-5, an associated T estimate of 13.0 ft^2/day and a k value of 69 mD were calculated using the aforementioned test conditions and assumptions. Analysis plots for the pneumatic slug withdrawal tests—SW-3, SW-4, and SW-5—are presented in Appendix B, Figures B4 through B6. For comparison purposes, the transmissivity range for the pneumatic slug tests (i.e., T = 13.0 to 20.2 ft^2/day) is similar to the range previously reported by McGrail et al. (2009) of T = 9.8 to 19.8 ft^2/day for all previous hydrologic tests conducted on the injection zone during the reconnaissance-level borehole testing campaign. These earlier analyses were based on the same analytical assumptions of a homogeneous formation/radial flow model conditions. The close correspondence of test results indicates that no adverse conditions were imposed on the Wallula pilot well injection reservoir by well completion activities (i.e., bottom borehole plug-back cementing and cementing of the overlying casing string).

4.3 Step-Drawdown Test

Following completion of the pneumatic slug tests, a 4-step drawdown test was planned, with each step lasting 2 hours in duration. The objectives for the step-drawdown test were to quantify well loss conditions for the Wallula pilot well and injection zone system, and to select an optimum pumping rate

for the following 7-day constant-rate pumping test. To conduct the test, a 5-horsepower Franklin Motor submersible pump was set using 2-7/8-in. outside diameter tubing at a depth of 453 ft (138 m) bgs, and a 300 psi In-Situ, Inc., vented-pressure probe was attached to the tubing pump column at a depth of 439 ft (133 m) (i.e., ~14 ft [4.2 m] above the pump intake) to provide real-time, shallow fluid column pressure response data. The frequency of recording the shallow fluid-column pressure response was varied to meet measurement needs during various periods of active drawdown test and subsequent test recovery (i.e., more frequent at the test beginning and immediately following pumping test termination). Downhole (near-formation depth) pressure response data were collected using a pair of CalScan USA (Badger model), silicon-crystal-based, absolute pressure memory gauges. The pressure sensor range was 0–1500 pounds-force per square inch absolute (psia), with a manufacturer-stated absolute accuracy 0.024% of full scale (0.36 psia) and a pressure resolution is 0.0003% of full scale (0.0045 psia). The downhole memory pressure gauges were installed at a depth of ~2584 ft (~787 m) bgs by suspending the gauges on separate wireline system below the submersible pump. Downhole pressure measurements were recorded at a fixed frequency of every 5 secs, which included both the step-drawdown test and the following 7-day constant-rate pumping test.

Surface pumping rates were monitored using a Great Plains Industries electronic digital flowmeter and totalizer (model #A109GMA100NA1), which was installed directly in-line within the surface discharge piping system within ~20-ft (~6-m) from the wellhead. Pumped groundwater was conveyed to a sanitary drain system at the Boise Inc. mill site, located approximately 300 ft from the well, which was then discharged to an approved disposal facility. Surface-discharge rates were occasionally checked manually by measuring the time required to fill a 5-gal (19-L) bucket at the discharge point to the sanitary drain system.

The step-drawdown test was initiated at 9:50 a.m. Pacific Standard Time (PST), on February 23, 2011, using a targeted pumping rate of ~5 gpm (~19 L/m). After 2 hours of pumping, the second step was started at 11:50 a.m. at a planned pumping rate of ~10 gpm (~38 L/min). Because of observed, excessive drawdown during the initial two steps, the test was redesigned as a three-step test. The third step was initiated at 1:50 p.m. with a targeted pumping rate of ~13 gpm. Three minutes into the third step (i.e., at 1:53 p.m.), the in-line electronic flowmeter stopped functioning, and flow measurements were monitored manually using the aforementioned manual-timed bucket measurement method. The third step was extended to 3.2 hours in duration and the test terminated at 5:00 p.m. on February 23, 2011. Average pumping rates and total volumes pumped for each step were as follows:

- Step 1 = 4.845 gpm (18.34 L/min)
- Step 2 = 10.489 gpm (39.7 L/min)
- Step 3 = ~13.1 gpm (~49.58 L/min).

The total estimated volume pumped was ~4,335 gal for the total 430 minutes of pumping. The step-drawdown test recovery was monitored until the start of the extended constant-rate pumping test, which commenced at 8:55 a.m. PST on February 28, 2011. Figure 4.7 shows the well-column drawdown pressure and initial part of the test recovery along with pertinent summary information concerning the step-drawdown test. As indicated in Figure 4.7, significant drawdown was exhibited during the test, as well as a general lack of drawdown stability by the end of each individual step (i.e., at the end of 2 hours of pumping). As a result, no quantitative extension of drawdown information could be derived from the

test for designing an optimal pumping rate for the following extended duration, constant-rate pumping test.

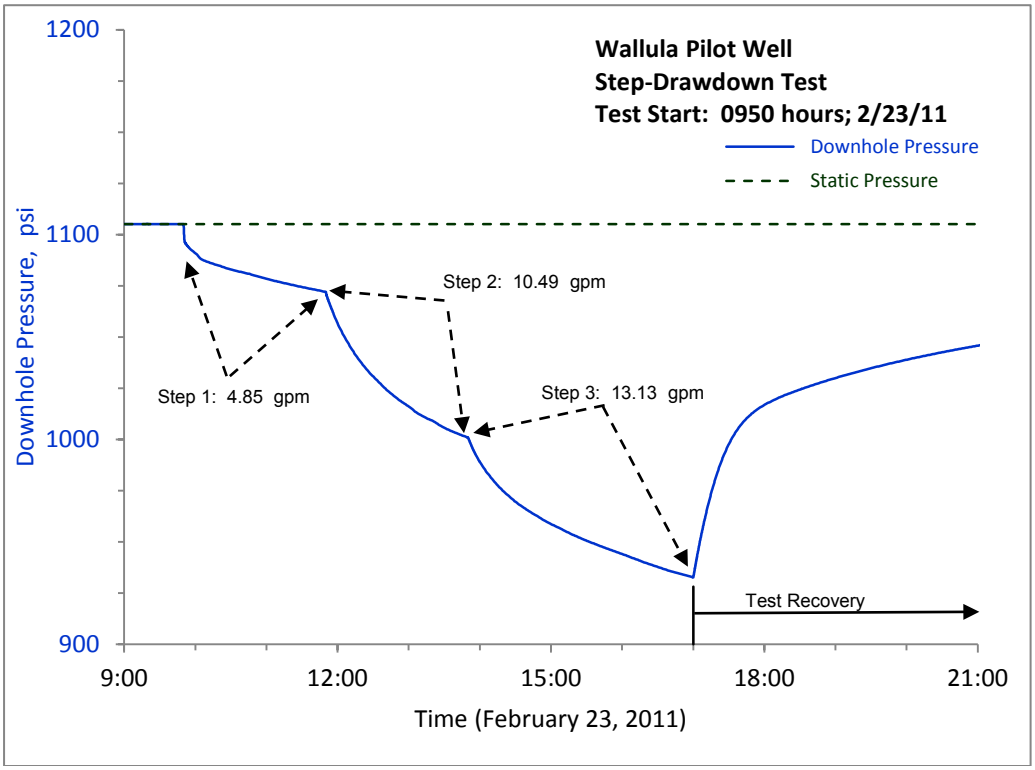

Figure 4.7. Step-Drawdown Test: Baseline Pressure Response Characteristics

In an attempt to provide insight into formation drawdown and well-loss conditions, the step-drawdown was analyzed using standard step-drawdown analysis methods described in Appendix A. Figure 4.8 shows specific drawdown (s/Q) relationship versus pumping rate (Q) observed for each of the three individual steps. A linear-regression line fit to the three-step test data points (i.e., measured at 2 hours), provides an Aquifer Loss (B) intercept of 8.514 ft and a Well Loss (C) slope parameter of 1.444 ft/gpm^2. Figure 4.9 shows the total drawdown analysis and associated drawdown contributions for aquifer and well loss components as a function of pumping rate (i.e., based on the linear-regression relationship shown in Figure 4.8). As indicated in Figure 4.9, nonformational well loss becomes the predominant component of drawdown at a pumping rate of <10 gpm. This can be better visualized by expressing the observed drawdown as the well efficiency relationship, which represents the percentage of the observed drawdown that is ascribed solely to formational factors, as described in Appendix A. Figure 4.10 shows the well efficiency plot for the test zone based on the step-drawdown, linear-regression results shown in Figure 4.8. As indicated in Figure 4.10, aquifer and well loss components both represent 50% of the observed drawdown at a pumping rate of ~6 gpm.

Discrete field samples of the pumped water were collected for limited field parameter determinations (i.e., F, pH, EC) at the beginning of the test and the end of each step using a collection-spigot/manifold system, which was installed in-line within the surface discharge piping system, downline from the surface flowmeter location. These field results, including results collected during the subsequent constant-rate test, are discussed in Section 4.4.

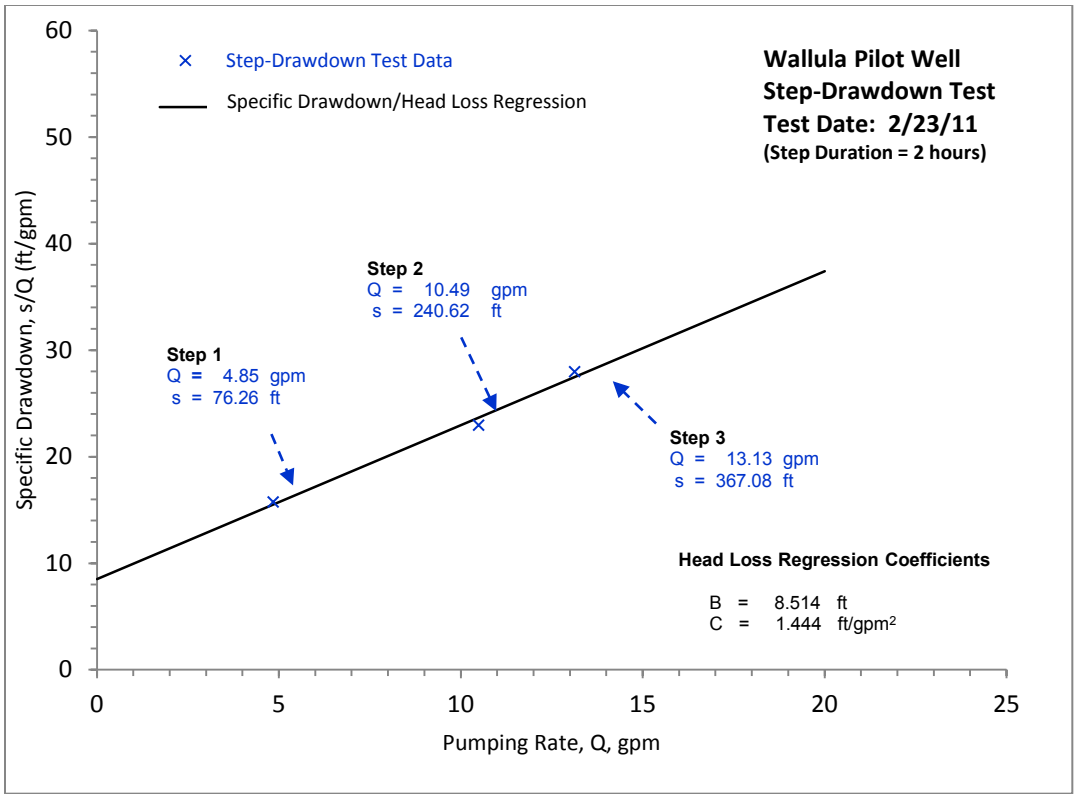

Figure 4.8. Step-Drawdown Test: Specific Drawdown/Head Loss Analysis

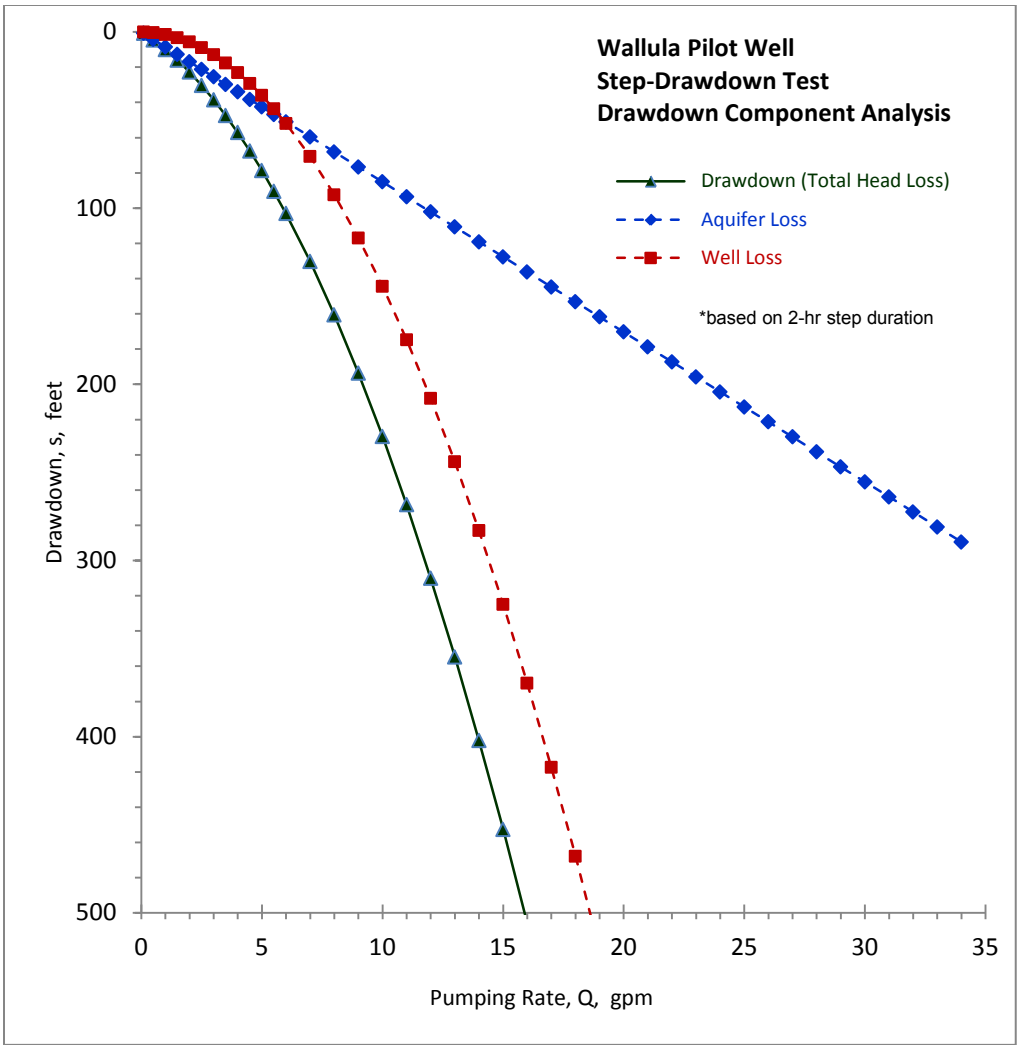

Figure 4.9. Step-Drawdown Test: Drawdown Component Analysis

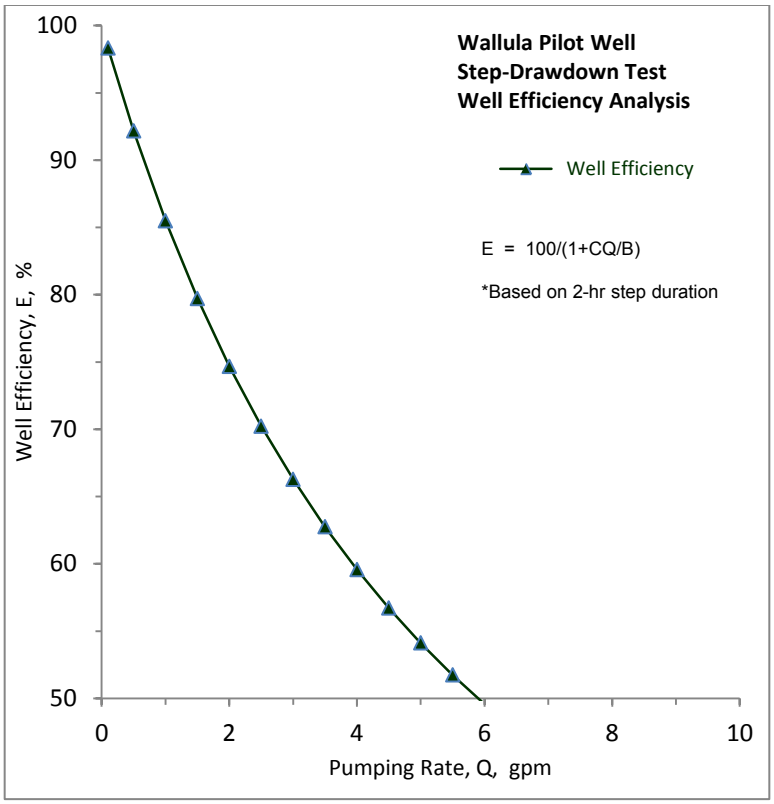

Figure 4.10. Step-Drawdown Test: Well Efficiency Analysis

4.4 Constant-Rate Test

Following approximately 4 days of step-drawdown test recovery, a 7-day constant-rate pumping test was initiated at 10:51a.m. PST on February 28, 2011, with a target pumping rate of ~4 gpm. The planned pumping rate of 4 gpm was selected based on a qualitative assessment of the short-term, step-drawdown test results described in Section 4.3, anticipated additional drawdown for the extended testing period, and available drawdown capacity for the given submersible pump setting (i.e., ~453 ft). The objectives for the extended constant-rate test were to support aquifer flow model identification, determine large-scale hydraulic properties, and detect the presence of surrounding hydrologic boundaries.

Test equipment and measurement systems employed during the constant-rate pumping test were the same as described in Section 4.3 for the step-drawdown test. The only modification was the installation of an additional surface flowmeter (Neptune T-10, flowmeter/totalizer, model #47284556) that was placed in-line with the repaired Great Plains Industries flowmeter/totalizer, which had stopped functioning previously during the later stages of the step-drawdown test.

Pumping rates were regulated and maintained at ~4.1 gpm after the first 5 minutes of pumping and allowed to slowly decline (i.e., the flow rate was not continually adjusted) during the 7-day test to a pumping rate of ~3.3 gpm at the time of test termination at 9:05 a.m., February 7, 2011, due to increasing drawdown (i.e., pumping head) during the course of the test. Figures B.7 and B.8 in Appendix B show the slow decline in pumping rate and total groundwater pumped over the duration of the test, respectively.

In total, 34,663 gal of groundwater were pumped from the well and test interval during the 9974 minute test, for an average pumping rate of 3.475 gpm.

Groundwater samples were collected periodically both for field and laboratory hydrochemical and microbial characterization. An in-line sampling-collection manifold system facilitated discrete and continuous sampling for these microbial and hydrochemical characterization activities. The sampling system (shown in Appendix C, Figures C.2 and C.3) was installed in-line within the surface discharge piping system, downline from both flowmeter locations. Sampling manifold valve manipulation during sampling caused some minor variations in surface pumping rates during the first day of pumping (see Appendix B, Figure B.6), and as a result, the location for discrete sample collection was moved to the distant end of the surface conveyance line that discharged to the sanitary drain system. Figure 4.11 shows the fluoride concentration for discrete groundwater samples collected periodically during the constant-rate pumping test, as well as during the preceding step-drawdown test as a function of the total volume pumped.

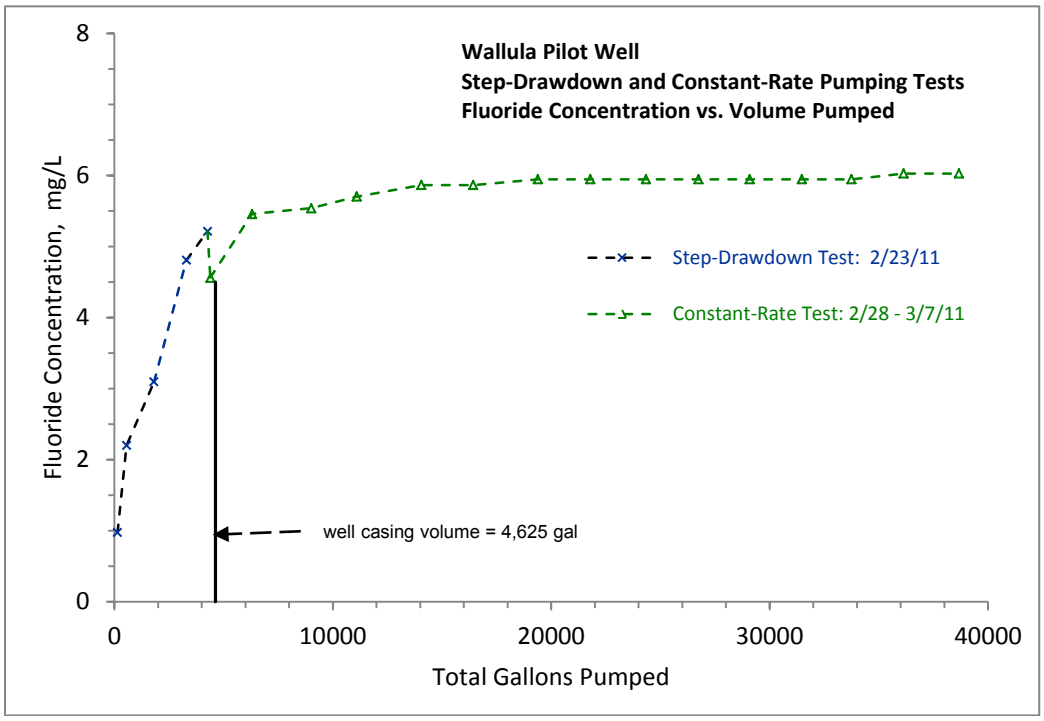

Figure 4.11. Fluoride Concentration Levels During Step-Drawdown and Constant-Rate Pumping Tests

As shown, fluoride concentrations exceeded MCLs for secondary and primary drinking water standards essentially after 1 borehole volume had been extracted from the well and remained relatively constant at a concentration value of 6.0 mg/L for the majority of the constant-rate pumping test. In addition, Figures B.9 and B.10 in Appendix B show elevated electrical conductivity and pH values, respectively, during the initial pumping period of the step-drawdown test. These elevated parameter values at the beginning of pumping are believed to be reflective of cementing activities that occurred during the earlier well completion in 2009. Formal laboratory hydrochemical results (major inorganics and trace elements, were collected at 10:20 a.m., March 4, 2011, and at 8:20 a.m., March 7, 2011. The major inorganic results indicate that groundwater within the injection zone is of a relatively dilute, sodium-carbonate hydrochemical water type, with individual chemical constituent levels nearly identical

to what was previously reported in McGrail et al. (2009) for the test interval during the borehole testing campaign. Laboratory isotopic and microbial analysis results obtained during the constant-rate pumping test will be reported in subsequent documents.

4.4.1 Diagnostic Test Analysis

To compare and analyze the drawdown and recovery responses, diagnostic composite log-log plots of the pressure change and its derivative data were prepared for data collected during and immediately following the termination of the extended constant-rate pumping test. As discussed in Appendix A, diagnostic derivative plot analysis is particular useful for identifying operative flow regime conditions during testing, establishment of infinite-acting radial flow conditions, and presence of hydrologic boundaries. Figure 4.12 shows the log-log pressure change comparison for the 7-day drawdown and 21-day recovery response, following termination of the pumping test.

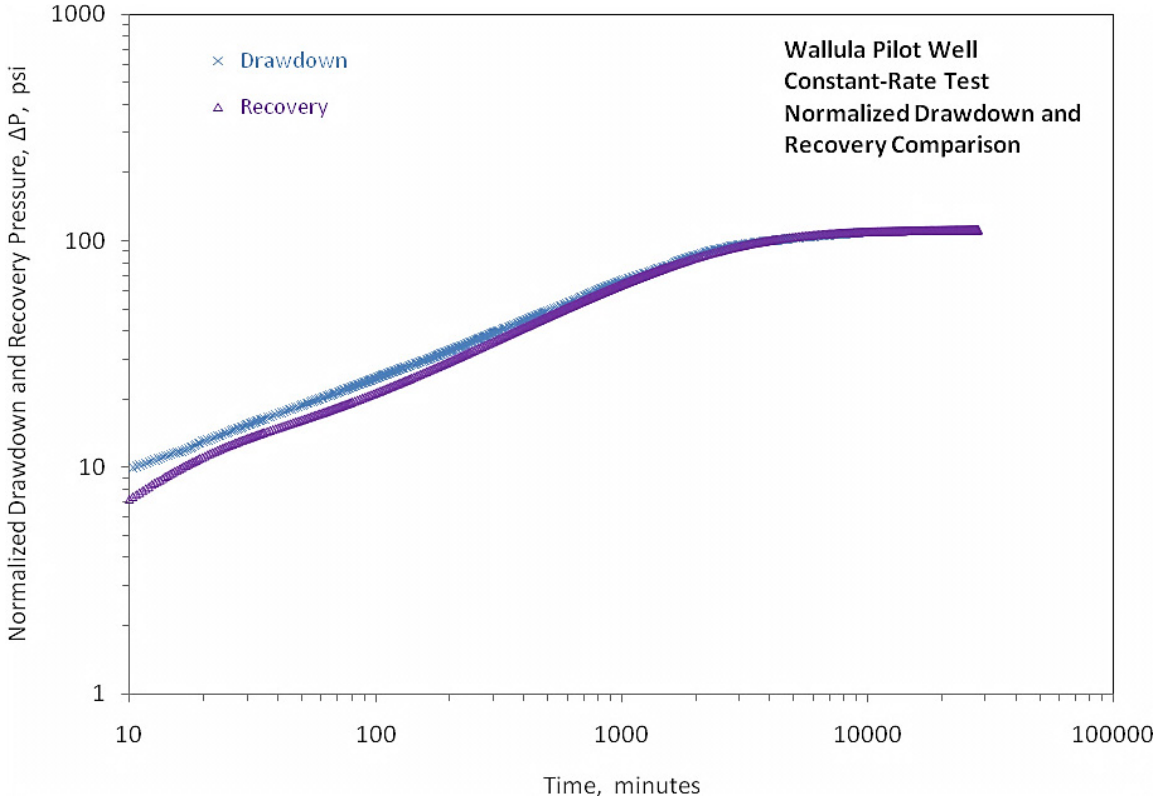

Figure 4.12. Comparison of Normalized Drawdown and Recovery Responses

The drawdown plot was corrected for variations in pumping rate decline that occurred during the course of the test by dividing the observed pressure change by the ratio of pumping rate over the pressure measurement period, and multiplying this quotient by average pumping rate for the entire test (i.e., 3.475 gpm). As discussed in Appendix A, this type of superposition correction is valid for tests where the pumping rate declines in an exponential fashion. As shown in Figure 4.12, the normalized drawdown and recovery response data indicate very similar patterns after the early-time flow manipulation during the drawdown period were completed; i.e., after ~7 minutes into the test.

Figure 4.13 shows the composite diagnostic plot of the normalized drawdown and drawdown derivative, along with identified test conditions.

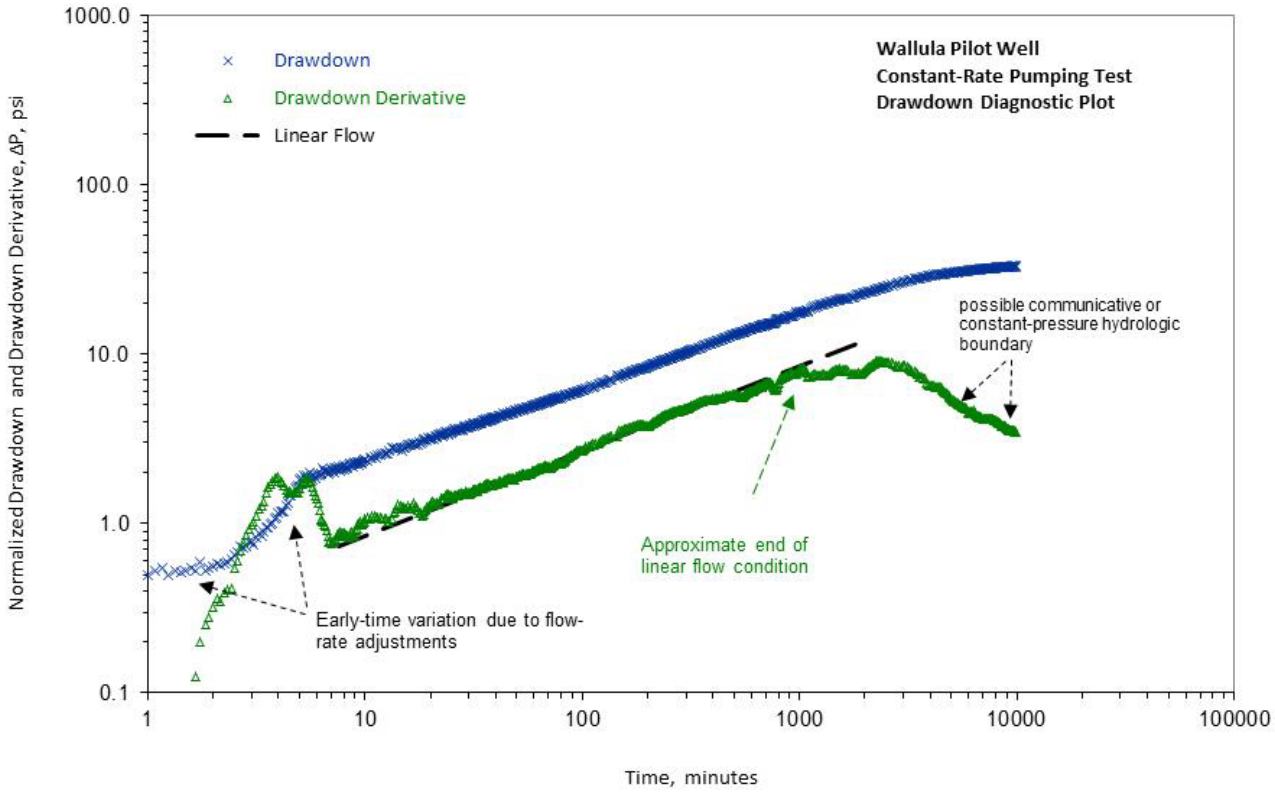

Figure 4.13. Diagnostic Composite Drawdown and Drawdown Derivative Plot

As indicated in the figure, three flow conditions are evident during the ~7-day pumping test: an early-time drawdown variation caused by pumping-rate adjustments (≤7 minutes); linear-flow regime conditions (7 to ~700 minutes); and a transitional flow-regime period (>700 minutes) indicated by the decline of the drawdown derivative. Radial flow conditions were not established near the end of the test, which may be attributed to the intersection of a communicative or constant-pressure boundary. As noted previously, surface flow rates were adjusted most significantly during the first few minutes of the test using the surface control valve in an effort to maintain pumping at the targeted 4 gpm rate. Pumping rates were significantly higher than 4 gpm during the initial minute of the test, which contributed to the rapid removal of wellbore storage effects from the drawdown response. The majority of the intermediate time period (i.e., 7 to ~700 minutes) indicates the establishment of a linear-flow regime (indicated by the one-half slope for the log –log derivative plot) in the surrounding well reservoir area. A linear one-half slope is shown superimposed on the derivative data. As discussed in Section 4.4.2, there are several plausible conceptual models that could be responsible for the observed linear-flow condition. After approximately 700 minutes into the test, the test data exhibit a flow transition pattern to an expected radial flow formational condition; however, the derivative plot indicates that radial flow conditions were never established and that a hydrologic boundary condition was likely responsible (i.e., test intersection of a communicative or constant-pressure hydrologic boundary).

Figure 4.14 shows the corollary composite diagnostic plot of recovery and recovery derivative with identified flow test conditions. As shown in Figure 4.14, five flow-regime conditions are evident during

the ~21 day recovery test period: an early-recovery time period dominated by wellbore-storage effects (<1 to ~50 minutes); a transitional flow-regime period (~50 to ~150 minutes); an established linear-flow regime condition (~150 to 700 minutes); a transitional period from linear-flow conditions (700 to ~3,000 minutes); and intersection of a communicative or constant-pressure boundary (≥3000 minutes). Early recovery time wellbore storage effects are indicated by a unit slope for log-log recovery and recovery derivative responses, and a unit slope is shown superimposed in Figure 4.14. The wellbore storage dominated recovery period transitions to a linear-flow controlled period in the surrounding well reservoir area, as indicated by the one-half slope for the log-log derivative plot. A linear one-half slope is shown offset from the recovery derivative data. As was indicated for the diagnostic drawdown discussion, after approximately 700 minutes into the recovery, the test data exhibits a flow-regime transition pattern. The recovery derivative plot indicates that radial flow conditions were never established and that a hydrologic boundary condition was intersected after ~3000 minutes of recovery. This boundary condition continued to be expressed until the end of the ~21 day recovery test.

Note that the drawdown and recovery data shown in the diagnostic analysis figures (i.e., Figures 4.12, 4.13, and 4.14) were not corrected for the effects of barometric fluctuations during the test. This is because the barometric corrections were relatively small (e.g., <0.15 m) in comparison to the associated test responses, due to existing formational and boundary conditions. As a result, no significant improvement in diagnostic analysis was achieved using barometric-corrected data.

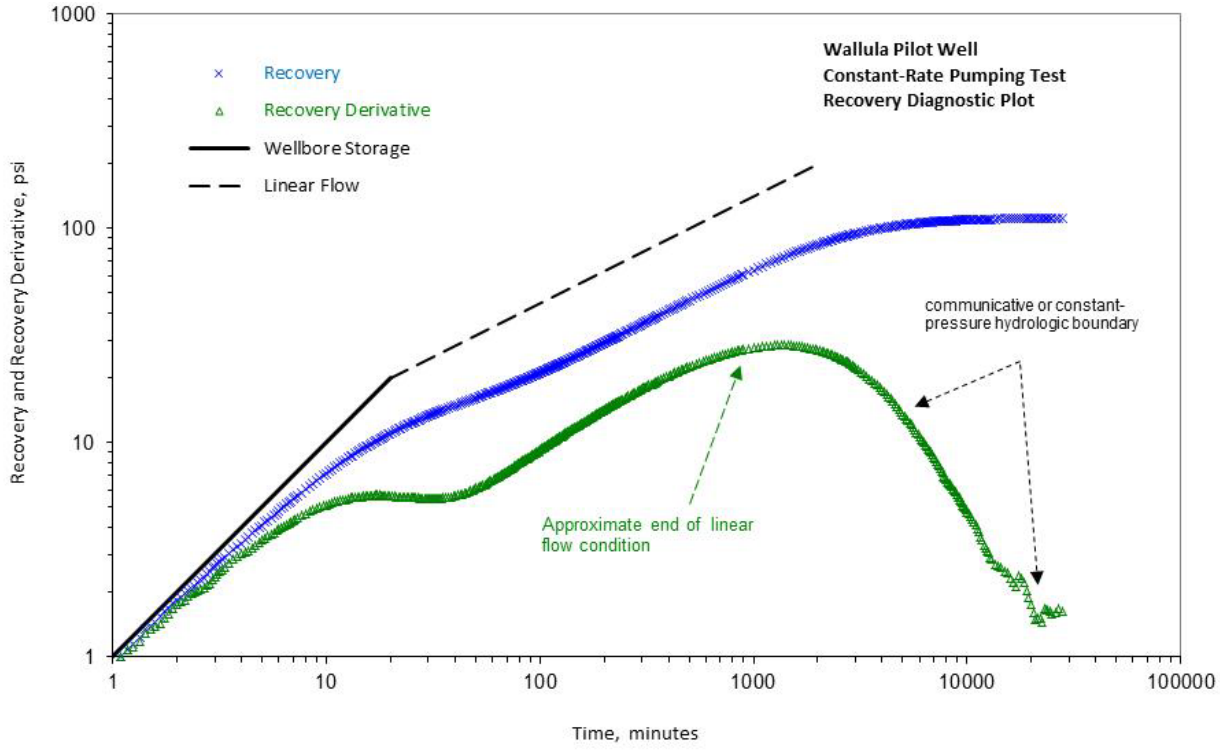

Figure 4.14. Diagnostic Composite Recovery and Recovery Derivative Plot

4.4.2 Linear-Flow/Boundary Conceptual Models

A number of causative features or conditions can produce the linear-flow regime response (i.e., one-half slope exhibited in the diagnostic pressure and derivative log-log plot) during the Wallula

constant-rate pumping test. These features or conditions include a transmissive horizontal or vertical fracture intersected by the well; a highly, horizontally anisotropic reservoir zone condition; or a linearly shaped, higher-permeability strip, pathway, or "embedded channel" within the interflow reservoir. Characterization information currently available cannot be used definitively to distinguish between the possible conceptual models that can produce the nonradial flow regime condition or the primary attributes (i.e., azimuth, width, length, thickness) of the feature producing the linear-flow behavior during the pumping test.

Figure 4.15 shows an areal conceptualization of the linear-flow region that develops surrounding a well that intersects an infinite-conductivity vertical fracture (i.e., conductivity of the fracture is orders-of-magnitude greater than the formation conductivity, $K_{frac} >> K_f$), that completely transects the aquifer. As discussed in Jenkins and Prentice (1991), because of the high conductivity of the intersected fracture, the fracture can be considered an extension of the well ("planar production surface") to which groundwater within the formation flows in parallel fashion (i.e., linearly) during a pumping test. As shown in Figure 4.15, an elliptical area immediately surrounding the well and fracture system illustrates the region where linear-flow conditions are established. Outside this elliptical area within the formation, groundwater flow may approach radial or pseudo-radial flow conditions.

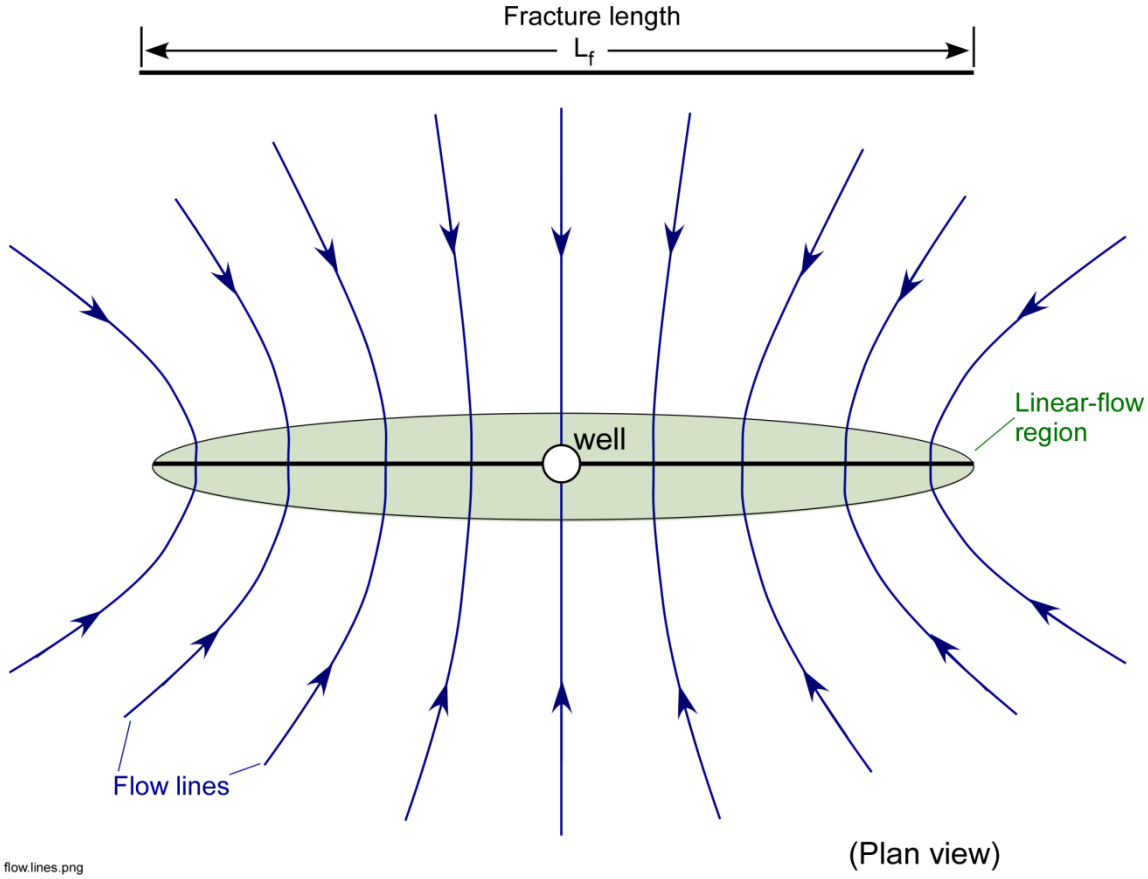

Figure 4.15. Areal Conceptualization of Developed Linear-flow Region Surrounding Well/Vertical Fracture

Besides spatial development of flow regions surrounding a well, flow regimes can also exhibit transient or temporal characteristics. Figure 4.16 shows the progressional development of flow regimes during the course of pumping test for the regions within and surrounding a lateral channel or strip aquifer that is intersected by a well, as reported in Butler and Liu (1991). In contrast to the previous example, the lateral channel/strip aquifer intersected by the well is of finite-conductivity, with a less significant contrast with the surrounding formation. As shown in Figure 4.16, flow to the well is bi-linear during early-test time (i.e., linear within the channel to the well and linear from the surrounding formation to the channel), followed by a transitional flow phase in both regions during intermediate-test time. If a pumping test is conducted for a sufficient period of time, pseudo-radial flow conditions may be exhibited as shown during late-test times within and outside the channel. The time required to attain pseudo-radial flow conditions is a function of the dimensional characteristics of the strip/channel aquifer and the hydraulic diffusivity properties within and outside the channel formation.

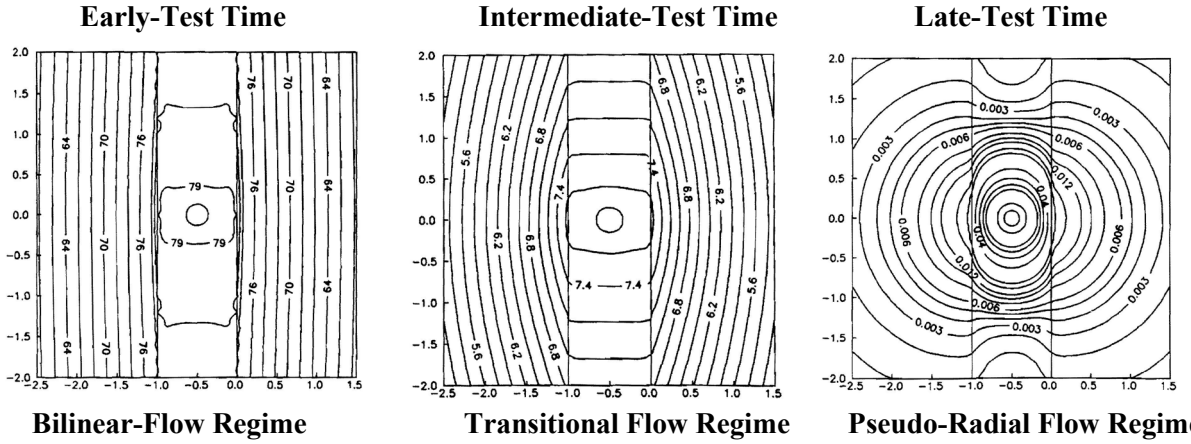

Figure 4.16. Map-View Comparison of Temporal, Test Flow-Regime Conditions for a Strip/Channel Aquifer (Butler and Liu 1991). (Note: Flow to well is orthogonal to equipotential lines.)

In addition to the establishment of a linear-flow regime, the presence of a hydrologic boundary condition is indicated by the distinctive diagnostic derivative plot pattern (i.e., declining pattern on diagnostic derivative log-log plot) during later test time (i.e., ≥3000 min). This type of boundary condition can be produced by a number of causative factors, including pervasive caprock leakage; presence of a vertical, communicative hydrologic feature (i.e., linear constant-pressure boundary); an abrupt lateral transmissivity change (i.e., abrupt boundary increase in reservoir hydraulic properties with distance from the well); and spherical flow. As for the case in identifying the cause for the observed linear-flow regime, the absence of observation and monitor well reservoir response data during the extended hydrologic test makes it difficult to definitively identify the cause of the observed hydrologic test boundary. Subtle distinguishing differences in the derivative response patterns for these identified boundary formational conditions suggest the boundary condition exhibited during the hydrologic test was not likely produced by either establishment of spherical flow conditions or due to pervasive caprock leakage. The most plausible explanation for the observed test boundary condition includes an intersection of a ***vertical***, crosscutting, communicative hydrogeologic feature (e.g., tectonic fracture) or a significant ***lateral*** increase in reservoir hydraulic/storage properties (i.e., hydraulic diffusivity [T/S]) at a distance from the well. Of these two hydrologic boundary-producing scenarios, the vertical crosscutting, communicative feature has the most adverse or limiting impact for emplacement of any subsequent CO_2 injection into the surrounding test reservoir. This boundary condition would restrict or limit the volume

and mass of CO_2 emplaced within the injection reservoir if vertical CO_2 migration to overlying basalt reservoirs (i.e., via the communicative feature) is to be avoided. Theoretically, the distance to a hydrologic boundary can be determined semi-quantitatively based solely on the test well response (and more precisely with multiple monitor well test data); however, this assumes radial reservoir flow conditions and knowing the effective well radius for the test well. Given the previously discussed linear-flow regime condition and unknown dimensional characteristics for the various possible causative mechanisms, boundary distance calculations are highly uncertain (e.g., ~50 to ≥300 ft).

4.4.3 Linear Fracture-Flow Test Analysis

Although the operative conceptual model responsible for the linear-flow condition during the extended Wallula pilot well pumping test is not known, two fracture analysis methods were applied to the test results as a preliminary analytical approach. The analytical approach included a general linear fracture-flow analysis and an example of a more quantitative type-curve analysis application.

As discussed in Appendix A, the linear arithmetic plot analysis approach is based on the method developed and presented in Jenkins and Prentice (1982) for general pumping test analysis. For this analysis pumping test drawdown data, s, is plotted on an arithmetic plot versus the square root of pumping time, $t_p^{½}$. For linear-flow conditions, the s versus $t_p^{½}$ relationship plots as a straight line. The slope of the established linear drawdown analysis ($s/t_p^{½}$), is directly related to the parameter grouping, $Q/L_f(\pi TS)^{½}$, which can be expressed as Equation (4.1):

$$L_f(TS)^{½} = (Q/s)(t_p/\pi)^{½} \quad (4.1)$$

where Q is the pumping rate and L_f, T, and S are the fracture length, transmissivity, and storativity of the feature causing the linear-flow regime condition to the well.

Figure 4.17 shows the analysis for the indicated linear-flow region prior to interception of the later-test time boundary condition. As indicated in the analysis figure, the interception of linear flow and later boundary condition occurs at a $t_p^{½}$ value of ~54, which is equivalent to a test time of ~2920 min. This is similar to the diagnostic analysis value previously identified in Section 4.4.1 of ~3000 min. A similar boundary intersection time result was obtained from the arithmetic linear plot extension for recovery data shown in Appendix B, Figure B.9.

As indicated in Figure 4.17, an estimate value for $L_f(TS)^{½}$ of 2.25 $ft^2/day^{½}$ was derived for the general linear-flow feature analysis. Jenkins and Prentice (1982) state that for pumping well test analysis without benefit of monitor well data (and if L_f is unknown), a unique value for T is not attainable, and "…values of T determined using estimated L_f and S values should be used with caution." Given this cautionary comment by Jenkins and Prentice (1982), plausible values for S and L_f were used purely as a qualitative indication of possible combinations for fracture length, L_f, and test zone transmissivity, T. For rigid, confined aquifer systems (and a thickness range: b = 10 to 100 ft), storativity values would be expected to range between 10^{-4} and 10^{-6}. Based on this range for injection zone storativity, Figure 4.18 shows the relationship of L_f versus T for this given S range.

Based on fluid and formation compressibility relationships presented in Appendix A, and anticipated test zone thickness (b = 48 ft) and porosity conditions (i.e., 5 to 15%), a realistic S estimate range of between 10^{-4} and 10^{-5} would be expected for the Wallula pilot well injection reservoir.

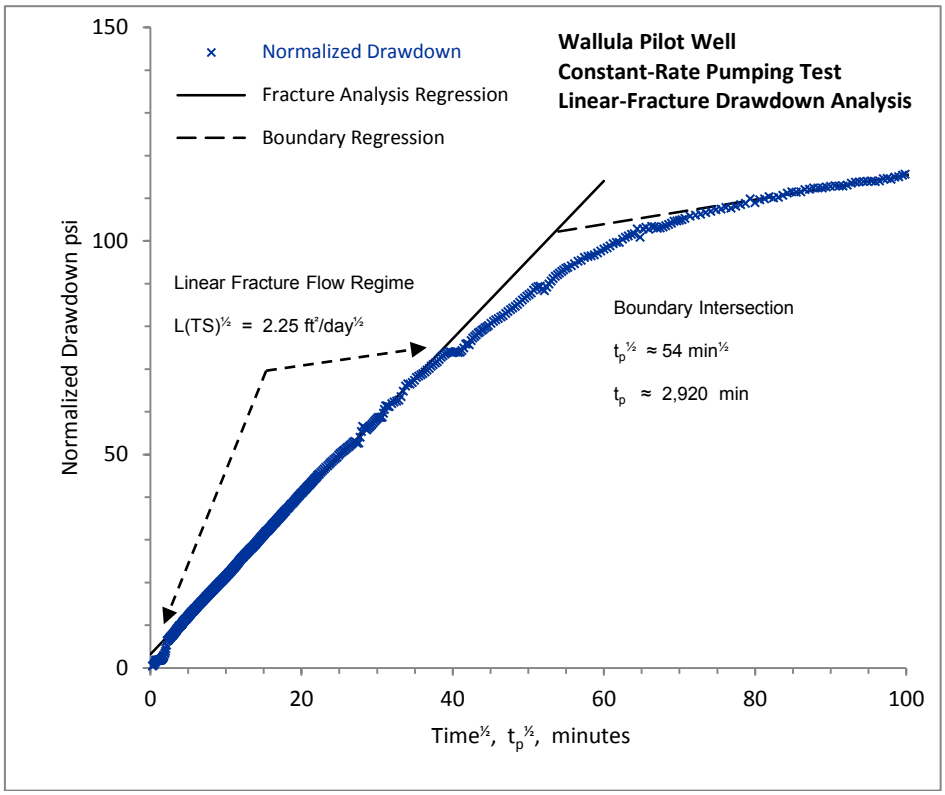

Figure 4.17. Constant-Rate Pumping Test: General Linear-Fracture Drawdown Analysis

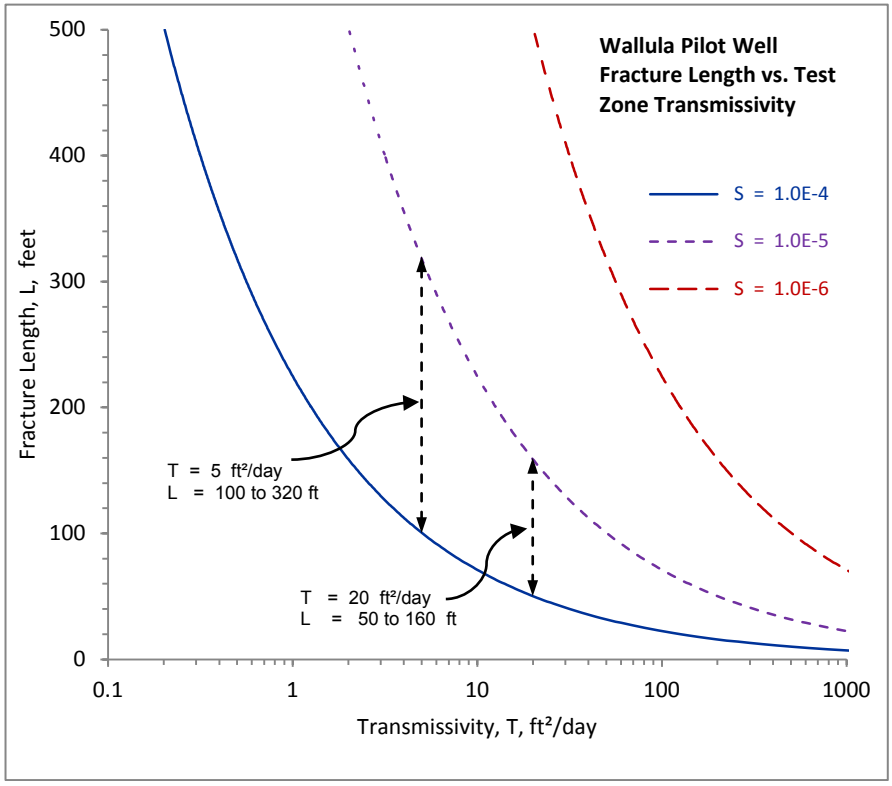

Figure 4.18. Qualitative Assessment of Fracture Length Versus Test Zone Transmissivity

If the test zone transmissivity is within the range of 5 and 20 ft^2/day, then estimates for vertical fracture length extending from the well would range between ~ 100 and 160 ft and ~50 and 320 ft from the well, respectively, given the storativity relationships (i.e., for 10^{-4} and 10^{-5}) shown in Figure 4.18. This is highly speculative exercise in estimating fracture length, but it is useful in assessing likely ranges for fracture length extending from the well. Similar results were obtained based on a general linear fracture-flow analysis for the observed recovery data (Appendix B, Figure B.11). As indicated in Appendix B, Figure B.11, an estimate value for $L_f\,(TS)^{½}$ of 2.17 $ft^2/day^{½}$ and a boundary intersection time of ~3025 min were derived for the general linear fracture- flow analysis, which are very similar to the drawdown derived relationship values.

The following type-curve analysis method is intended as an example to demonstrate analytical capabilities that would be available if the operative conceptual model for the observed linear-flow condition were known. For example purposes, the horizontal, discrete fracture model originally presented in Gringarten and Ramey (1974a) was used to analyze the Wallula pumping test drawdown results. As discussed in Appendix A, the horizontal fracture model is a realistic condition for the observed linear-test response; this is due to common observations of thin "enhanced pathways" within brecciated interflow zones, as determined from dynamic fluid logs (flowmeter and fluid temperature surveys) obtained during pumping tests conducted within deep basalt boreholes on the Hanford Site as part of the Basalt Waste Isolation Project during the 1980s (Strait and Spane 1982, 1983). Figure 4.19 shows a surface basalt exposure exhibiting this type of discrete, high-permeability horizontal fracture pathways that may be representative for the Wallula injection zone condition. While it is recognized that the described, thin horizontal pathway model is a function of the natural basalt flow emplacement process, the horizontal fractures imposed by natural tectonic stress distribution is also a mechanism for creating a horizontal zone of enhanced permeability within the Wallula injection zone. As reported in Sublette (1986) and summarized in DOE (1988), the natural in-situ stress field measured for 13 basalt test intervals (i.e., depths between 3020 and 3920 ft) within deep boreholes at the nearby Hanford Site indicates a maximum average horizontal to vertical stress ratio of 1.77 ± 0.2. This established high horizontal to vertical mean stress ratio indicates that any imposed post emplacement, basalt fracturing at comparable depths within the Pasco Basin would be horizontal in alignment and parallel the maximum horizontal stress field condition; i.e., a north/south direction as discussed in DOE (1988).

Figure 4.20 shows a composite drawdown and drawdown derivative analysis using the horizontal fracture-based type curve method described in Gringarten and Ramey (1974a). The type curve and derivative plots were generated using the AQTESOLV (Pro 4.50) hydrologic test software, described in Duffield (2007, 2009) and in Appendix A. Several hydrologic parameters were held constant and automated composite curve fitting features of the software program allowed a "best-estimate" fit to be achieved by statistical error and residual reduction analysis. For this demonstrated analysis application, the vertical and horizontal anisotropy ratios (K_v/K_h and K_x/K_y) for the injection zone were arbitrarily set at .01 and 1.0, respectively, and a linear, constant-pressure hydrologic boundary placed at a distance of 100 ft from the test well location. The horizontal fracture was placed in the middle of the assigned 48-ft injection zone thickness as recommended in Gringarten and Ramey (1974a) for natural fracture systems. As indicated in the figure, the example analysis provided a radial horizontal fracture width, R_f, of 158 ft, and injection zone estimates of transmissivity, T, and storativity, S, of 0.63 ft^2/day and 2.5E-4, respectively.

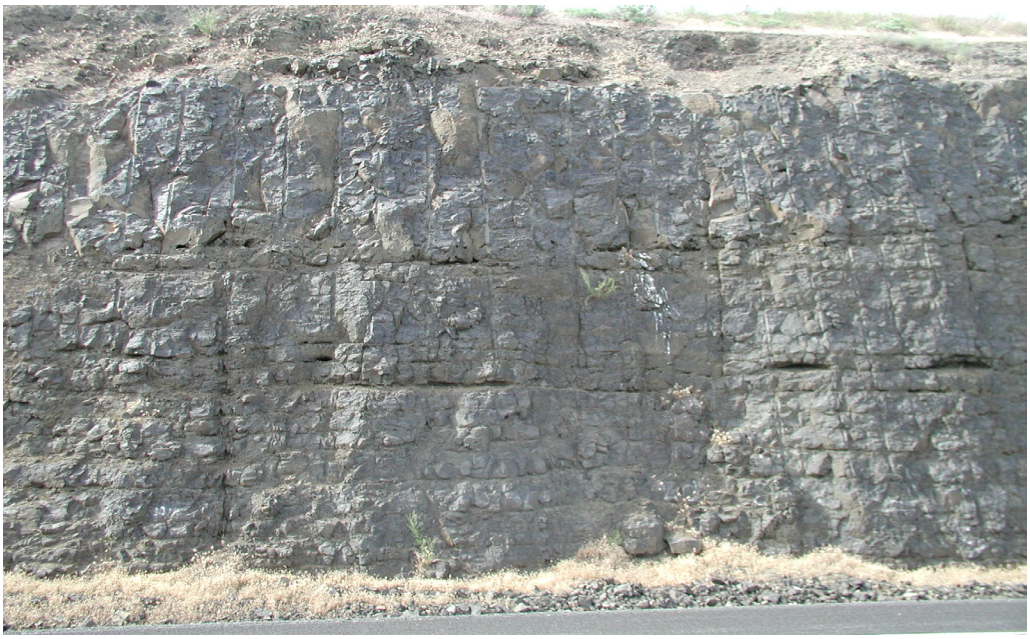

Figure 4.19. Surface Exposure Showing Two High Permeability, Horizontal Fracture Planes with Basalt Flow (photo courtesy of S. Reidel)

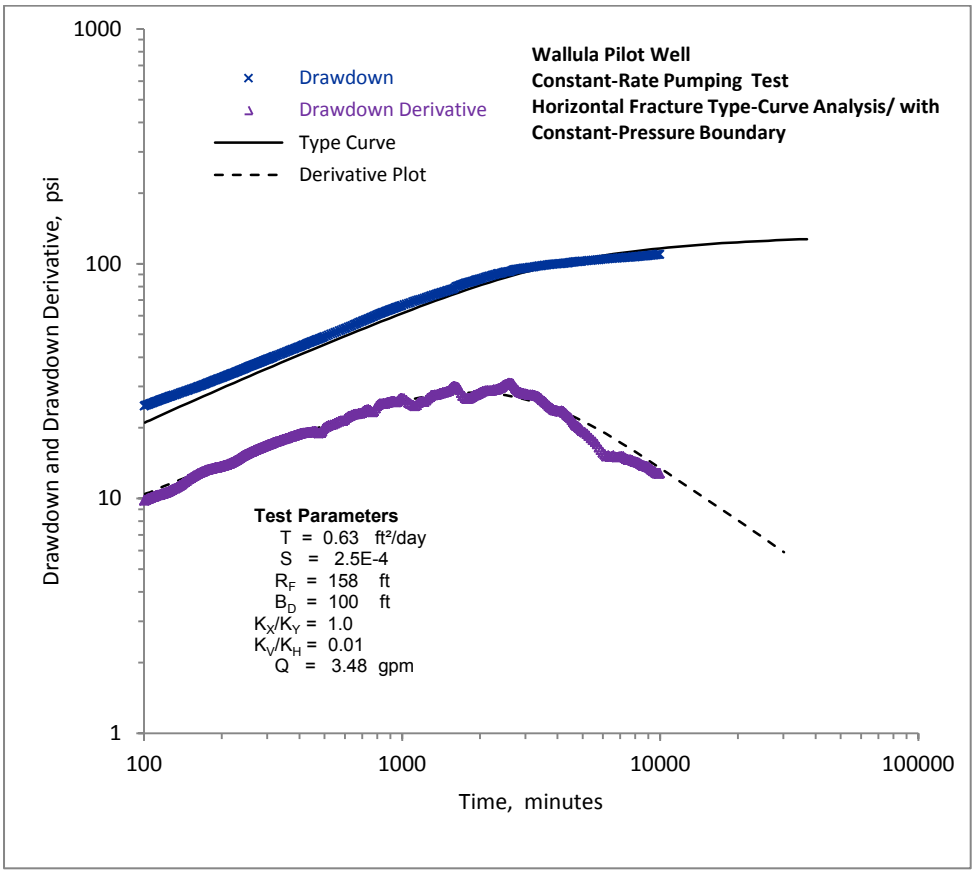

Figure 4.20. Horizontal Fracture Type-Curve Analysis with Constant-Pressure Boundary

For a comparison of different fracture model type-curve analyses, the drawdown and drawdown derivative data were reanalyzed using the ***vertical*** fracture-based type-curve method described in Gringarten and Ramey (1974b). As for the previous analysis example, the type curve and derivative plots were generated using the AQTESOLV (Pro 4.50) hydrologic test software, and the same hydrologic parameters and imposed boundary condition were held constant during the automated composite test analysis. The results of the vertical fracture type-curve and derivative plot analysis are shown in Figure 4.21. As indicated in Figure 4.21, the example analysis provided a vertical fracture length, L_f, of 450 ft (i.e., radial fracture width, X_f, of 225 ft), and injection zone estimates of transmissivity, T, and storativity, S, of 0.27 ft²/day and 8.0E-5, respectively.

As for the previous general linear-fracture analysis, the fracture type-curve analysis examples are provided to demonstrate the ability to determine specific properties of the injection reservoir if the operative linear-flow regime model and specific hydrologic boundary conditions are known. Available hydrogeologic data are currently not sufficient to select between possible linear-flow regime models (discussed in Section 4.4.2) or hydrologic conditions responsible for the hydrologic boundary exhibited during the constant-rate pumping test. Recommended hydrologic characterization tests that will aid in model and boundary identification, and therefore reduce the uncertainty of existing reservoir conditions, are presented in Section 6.0.

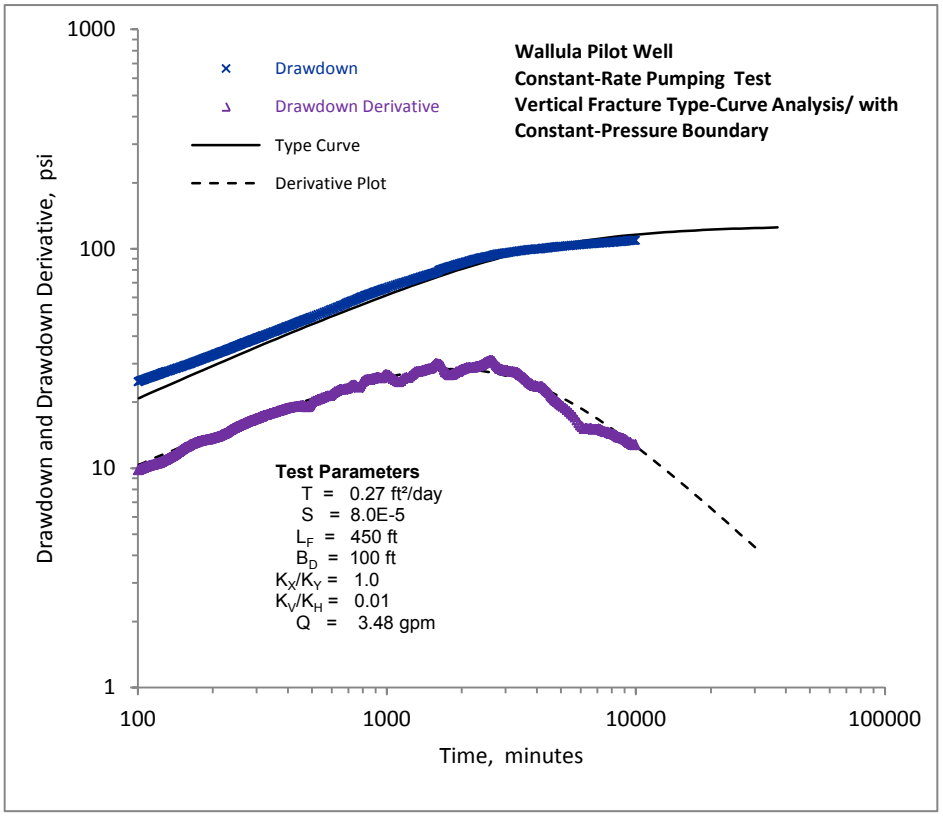

Figure 4.21. Vertical Fracture Type-Curve Analysis with Constant-Pressure Boundary

5.0 Conclusions

Hydrologic characterization information at the Wallula pilot well site was obtained during three sequential characterization phases:

- Initial hydrogeologic reconnaissance-level characterization information obtained during the borehole drilling/advancement phase (January–May 2009)
- Extended baseline pressure monitoring of the Wallula pilot well injection reservoir to assess background formation dynamics (June 2009–December 2010)
- Detailed hydrologic testing of the Wallula pilot well injection reservoir conducted for large-scale hydraulic property determination and hydrologic boundary delineation (January–March 2011).

Preliminary characterization results obtained during the initial borehole drilling campaign were previously published in McGrail et al. (2009). Based on reconnaissance-level hydrogeologic information obtained during borehole drilling/advancement, a candidate injection reservoir zone was identified between the depth interval of 2716 and 2910 ft bgs. Specific criteria used in the reservoir zone selection included in-situ, static formation fluid temperature and pressure conditions above supercritical CO_2 levels; the presence of nonpotable drinking water within the candidate injection zone (i.e., existing dissolved chemical constituents exceeding primary and secondary drinking water standards); and the presence of sufficient reservoir formation injectivity (i.e., hydraulic properties) and overlying caprock sealing characteristics to facilitate the planned injection and sequestration of CO_2 during a subsequent field pilot study phase.

Following well completion activities, baseline pressure monitoring of the Wallula pilot well injection reservoir zone between June 2009 and December 2010 provided temporal and seasonal response information. Salient findings obtained from the baseline monitoring characterization phase indicated the following:

- Significant long-term, seasonal hydraulic head (pressure) fluctuation pattern within the injection zone of approximately 2.15 m over the 1.5-year monitoring period
  - Contributory human-related factors influencing the natural seasonal pattern include agricultural pumping within the basin, and a possible minor hydraulic communicative response to more distant Columbia River stage-elevation fluctuations
- Associated, short-term, temporal response to natural external stresses (i.e., barometric and earth-tide fluctuations), but no apparent, direct short-term relationship to nearby, McNary Dam reservoir elevation and loading fluctuations
- Detailed barometric response analysis that suggests the presence of formational leakage or presence of a communicative hydrologic boundary condition within the surrounding reservoir.

Following the baseline monitoring period, hydrologic well tests were conducted during late December 2010 and March 2011 to identify the operative aquifer model; determine large-scale hydraulic properties; and delineate the presence of surrounding hydrologic boundaries within the targeted Wallula pilot well injection reservoir. Diagnostic derivative analysis of the 7-day constant-rate pumping test and ~3-week recovery period response indicated a nonradial, linear-flow regime to the well, and the presence of a hydrologic boundary condition. The lack of surrounding observation and monitor well data within the

test reservoir during the extended test makes it difficult to identify the causative factor(s) responsible for either the linear-flow regime condition or the observed hydrologic boundary.

Possible causative mechanisms or features that could produce the linear-flow regime response (i.e., one-half slope on diagnostic pressure and derivative log-log plot) during hydrologic testing include a transmissive horizontal or vertical fracture intersected by the well; the presence of a highly, horizontally anisotropic reservoir zone condition; or the presence of a linearly shaped, higher-permeability pathway or "embedded channel" within the interflow reservoir. Characterization information currently available cannot be used to definitively distinguish between the possible conceptual models that can produce the nonradial flow-regime condition or the attributes of the primary feature (i.e., azimuth, width, length, thickness). The main impact of the dominant linear-flow regime condition within the well and formation system would be the nonradial emplacement of injected CO_2 into the surrounding test reservoir. Although some general directional CO_2 emplacement information may be achieved from injection well geophysical surveys to be conducted immediately after CO_2 injection, the level of characterization may not be sufficient to design and deploy future re-entry and coring into the injection reservoir to retrieve geologic cores for CO_2 and basalt rock reaction assessment (McGrail et al. 2009). Earlier plans for this post-injection characterization activity assumed a homogeneous reservoir, with essentially a nondirectional (i.e., radial) dependence for the injected CO_2. Given the heterogeneous characteristics of the feature producing the linear-flow regime, it is inherent these directionally-dependent properties be known in advance to assure a high probability of intersecting the CO_2 reactive reservoir areas during future re-entry and coring activities.

The presence of the hydrologic boundary condition indicated by the distinctive diagnostic derivative plot pattern (i.e., declining pattern on diagnostic derivative log-log plot), can be produced by a number of causative factors, including the following:

- Pervasive caprock leakage
- Presence of a vertical, communicative hydrologic feature (i.e., linear constant-pressure boundary) or significant lateral transmissivity change boundary (i.e., significant/abrupt increase in reservoir hydraulic properties with distance from the well)
- Spherical flow.

As for flow-regime cause identification, the absence of observation and monitor well reservoir response data during the extended hydrologic test makes it difficult to definitively identify the cause of the observed hydrologic boundary response. Subtle distinguishing differences in the derivative response patterns for these identified boundary/formational conditions, however, suggest the boundary condition exhibited during the hydrologic test was not likely produced by either establishment of spherical flow conditions or due to pervasive caprock leakage. The most plausible explanation for the observed test boundary condition includes an intersection of a vertical, crosscutting, communicative hydrogeologic feature (e.g., tectonic fracture), or a significant lateral increase in reservoir hydraulic and storage properties (i.e., hydraulic diffusivity [T/S]) at a distance from the well. Of these two hydrologic boundary-producing scenarios, the vertical, crosscutting, communicative feature has the most adverse or limiting impact for emplacement of any subsequent CO_2 injection into the surrounding test reservoir. This boundary condition would restrict or limit the volume/mass of CO_2 emplaced within the injection reservoir if vertical CO_2 migration to overlying basalt reservoirs (i.e., via the communicative feature) is to be avoided. Theoretically, the distance to a hydrologic boundary can be determined semi-quantitatively

based solely on the test well response (and more precisely with multiple monitor well test data); however, this assumes radial reservoir flow conditions and knowing the effective well radius for the test well. Given the previously discussed linear-flow regime condition and unknown dimensional characteristics for the various possible causative mechanisms, boundary distance calculations are highly uncertain (e.g., ~50 to ≥300 ft).

6.0 Recommendations

To improve the design of the subsequent CO_2 injection and post-injection coring phases of the field pilot study, identifying the causative mechanism for the linear-flow regime and nature (type and distance) of the exhibited hydrologic boundary within the injection reservoir is of primary importance. This can be best resolved with construction of additional surrounding monitor wells within the injection reservoir and in overlying reservoir horizons and performing high-stress, multi-well interference hydrologic tests. However, because of the inherent costs and time required to implement this type of hydrologic test characterization, it is recommended that more rapid and less invasive techniques be used to reduce the uncertainty of the possible injection reservoir conditions identified in previous test characterization phases. With this objective, the following test characterization recommendations are provided in-lieu of constructing additional monitor wells and conducting multi-, inter-well hydrologic tests. The two primary test characterization recommendations include conducting the following:

- Dynamic fluid-logging survey of the open injection zone horizon
- Extended, high-stress (drawdown), constant-rate pumping test in concert with active surface gravity and land deformation surveys.

The dynamic fluid-logging survey entails extracting groundwater from the test interval (e.g., pumping), and monitoring the influx of groundwater from the intersected open reservoir section to the wellbore by high-precision flowmetering (e.g., electromagnetic flowmeter) and indirectly by fluid temperature logging, which indicates regions of groundwater influx by the distortion of the fluid-temperature profile from equilibrated, static, fluid-column temperature conditions. The primary objective of the dynamic fluid-logging survey is to establish the relative vertical distribution of permeability within the open injection well section from which a refined conceptualization can be obtained for the mechanism responsible for linear-flow conditions within the reservoir; i.e., between horizontal and vertical fractures and an embedded higher permeability channel. An example of a successfully applied dynamic fluid-logging survey for identifying permeability distribution characteristics within a deep (i.e., ~9000 ft) carbon sequestration borehole is presented in Spane et al. (2006).

The second recommended hydrologic test involves performing repeated high-precision surface gravity and land deformation surveys during the course of conducting an extended (e.g., 14-day), high-stress (~450 psi), constant-rate pumping test. The main objective for this characterization test is to delineate the lateral region impacted directly by groundwater extraction and formation pressure decline (i.e., the nonradial area of investigation) during the extended high-stress pumping test. Determining the density distribution of subsurface materials and its evolution with time potentially provides a cost effective monitoring technique to determine field-scale displacements of fluids induced by the extraction of groundwater and the associated decline in formation pressure. More importantly, the accurate measurement of the associated, temporal ground deformation due to groundwater withdrawal during an extended pumping test reflects the spatial geomechanical formational responses imposed by the test. Recent developments in space geodesy and gravimetry now provide an economical and rapid means of mapping deformation of the ground surface and displacement of groundwater in the subsurface over large areas with the required level of accuracy. Due to the availability of both high-precision gravity meters and newly acquired satellite-based positioning techniques (differential global position system), it is now possible to map very small gravity anomalies and their time variations over large areas. Displacements of the ground surface can also be measured very precisely through satellite radar interferometry

(interferometric synthetic aperture radar [InSAR] and polarization-interferometric synthetic aperture radar [P-InSAR]). Each of these methods has been successfully applied for assessing areal impacts associated at active natural gas storage fields or CO_2 pilot storage sites (e.g., Ferguson et al. 2007; Chapman et al. 2008; Davis et al. 2008) and recently for InSAR applications at a commercial sequestration site at In Salah, Algeria (Vasco et al. 2010).

The objective for the recommended Wallula extended high-stress, constant-rate pumping test is to create a large areal distortion pattern due to groundwater extraction that, if successfully delineated using the aforementioned characterization methods, may provide direct evidence as to the nature and location of the hydrogeologic feature responsible for producing the hydrologic boundary condition exhibited during the recent, lower stress (~190 psi) constant-rate pumping test. Physical measurement of the distortion and deformation of the land surface during pumping tests is an established hydrologic technique for assessing aquifer storage characteristics (e.g., Peterson 1967; Robson and Banta 1990) using more traditional measurement techniques (e.g., extensometers or tiltmeters). Recent development of the InSAR technology has extended surface distortion detection applications for mapping subsurface areal permeability patterns (Vasco et al. 2001) and the presence of hydrogeologic structures (Burbey 2008) during extended hydrologic tests. However, these previous applications were commonly applied within more compressible sedimentary aquifer settings, which is in contrast to highly rigid basalt formation conditions. It would be expected that basalt formations, due to their inherently higher rigidity, would exhibit associated formation dilation responses that would be comparably smaller than for highly compressible formations. Nevertheless, success in applying these techniques for determining areal deformation associated with a large-scale aquifer storage and recovery project within basalts in nearby Pendleton, Oregon, has been recently demonstrated (Bonneville et al. 2011). Similar successful results are expected for the recommended smaller-scale characterization test to be conducted at the Wallula pilot well site location.

The best results for this recommended extended pumping test are expected when background seasonal reservoir pressure trend effects are at a minimum. As shown in Section 3.1, background seasonal effects at the Wallula pilot well are at a minimum for the injection reservoir during two time periods: April through March and to a less extent, September through October). To achieve the intended test objective, InSAR data will be collected before, during, and after the hydrologic test campaign. The collection and processing of these data will be done by the NASA Jet Propulsion Laboratory with whom a collaborative agreement was established in 2009 for support activities associated with the previously mentioned Pendleton, Oregon, aquifer storage and recovery project. Based on an earlier accepted proposal with the European Space Agency, programmed use of two satellites (X-band TerraSAR-X and C-band Radarsat-2 polarimetric SAR) has been granted covering the area surrounding Pendleton for 3 years, starting in January 2011. The satellite radar coverage extends 200 km, and includes the area within the Wallula pilot well vicinity. This coverage provides for generating a high precision, land-surface elevation areal image to be generated every 2 weeks. Timing of the extended constant-rate pumping test will be coordinated with the satellite scheduled coverage to maximize development of a good pretest baseline, testing deformation profile, and recovery rebound series.

In addition to the InSAR survey data, a series of differential global position system and gravity measurements along two profiles radial to the Wallula pilot well will be performed at a frequency of every 2 days. The exact locations of these radial profile lines and measurement stations will be determined after completing an initial detailed gravity map of the area immediately surrounding the

Wallula pilot well. Radial profile line orientation will be selected on basis of background noise level, and the presence of any identifiable subsurface density anomalies (e.g., basalt dikes).

While the dynamic fluid-logging and extended constant-rate pumping tests represent the primary recommended field test characterizations, several "follow-on" analysis recommendations are also identified that do not require additional field testing. As discussed in Section 3.0 concerning preliminary baseline monitoring results, the Wallula pilot well injection reservoir exhibited a significant long-term, seasonal response pattern and a well-defined, associated temporal response to natural stress factors (i.e., barometric and earth tides). As previously discussed, the long-term seasonal reservoir response appears to exhibit a pattern that is generally correspondent to expected agricultural groundwater withdrawal pumping usage within the basin. It is recommended that an inventory of large-production agricultural wells within the lower Pasco and lower Walla Walla basins be developed, and background information assembled concerning the stratigraphic well completion and general pumping and usage practices for the respective well locations. In addition, the possible casual communicative association exhibited between Columbia and Snake River stages below McNary and Ice Harbor Dams, respectively, need to be more quantitatively evaluated. While this association appears to be coincidental during part of the seasonal cycle (i.e., during the groundwater recessional period between May and October), more detailed analysis should be applied to see if river or reservoir elevation stage boundary fluctuations represent a secondary contributing factor to the seasonal Wallula pilot well response pattern. Establishing the relevance of this possible hydrologic boundary condition will provide information pertaining to the ultimate fate of CO_2 sequestered at the Wallula pilot well location, as well as the feasibility of the general CO_2 storage within shallow basalts (i.e., $\leq$3000 ft) within the lower Pasco Basin.

The demonstrated high correspondence of reservoir zone pressures to short-term natural stress effects (i.e., barometric pressure and earth tides), as discussed in Section 3.2, also provides the opportunity to characterize the storage properties of the Wallula pilot well injection reservoir, without the need to perform multi-well interference tests. While this hydrologic technique has been an established method, albeit with mixed results (e.g., Bredehoeft 1967; Hsieh et al. 1987, 1988; Merritt 2004), recent refinements in the combined barometric and earth tide approach applied by Cutillo and Bredehoeft (2011) represent promise in characterizing the storage properties within highly rigid formations such as basalt. It is recommended the existing baseline well record be analyzed using this approach to estimate the specific storage, S_s, of the Wallula pilot well injection reservoir. Knowing the reservoir storage properties more precisely would greatly refine modeling estimates of the impacted area following CO_2 injection.

If the recommended field tests provide sufficient detail to identify characteristics of the interflow zone feature producing the linear-flow regime condition (i.e., dimensional characteristics) and apparent hydrologic boundary condition (e.g., distance from the well to the causative boundary), then additional numerical computer runs using STOMP-H_2O-CO_2-NaCl model (White and Oostrom 2006) should be implemented that capture these new Wallula pilot well injection reservoir properties. McGrail et al. (2009) previously ran the STOMP (Subsurface Transport Over Multiple Phases) model simulations based on a homogenous formation and radial flow regime. These recommended model reruns will improve the delineation of CO_2 physical emplacement within the Wallula injection reservoir and provide volumetric limitations to the injection if the hydrologic boundary is identified as a nearby vertically conductive feature.

7.0 References

40 CFR 141.62. 2009. "National Primary Drinking Water Regulations, Maximum Contaminant Levels for Inorganic Contaminants." *Code of Federal Regulations*, U.S. Environmental Protection Agency.

Bonneville A, EC Sullivan, E Heggy, J Dermond, M Sweeney, K Parker and C Strickland. "INSAR and Gravity Surveys of a Large Aquifer Storage and Recovery Site in Pendleton, OR: Application to Large CO_2 Storages." *8th Washington Hydrogeology Symposium*, Tacoma, Washington, April 2011.

Bower DR and KC Heaton. 1978. "Response of an Aquifer Near Ottawa to Tidal Forcing and the Alaskan Earthquake of 1964." *Canadian Journal of Earth Sciences* 15(3):331-340.

Bredehoeft JD. 1967. "Response of Well-Aquifer Systems to Earth Tides." *Journal of Geophysical Research* 72(12):3075-3087.

Burbey TJ. 2008. "The Influence of Geologic Structures on Deformation due to Ground Water Withdrawal." *Ground Water* 46(2):202-211.

Butler JJ, Jr. 1997. *The Design, Performance, and Analysis of Slug Tests*. Lewis Publishers, CRC Press, Boca Raton, Florida.

Butler, JJ, Jr. and WZ Liu. 1991. "Pumping Tests in Non-Uniform Aquifers - The Linear Strip Case." *Journal of Hydrology* 128:69-99.

Chapman DS, E Sahm, and P Gettings. 2008. "Monitoring Aquifer Recharge Using Repeated High-Precision Gravity Measurements: A Pilot Study in South Weber, Utah." *Geophysics* 73(6): WA83-WA93.

Chien YM, RW Bryce, SR Strait, and RA Yeatman. 1986. "Elimination of Frequency Noise from Groundwater Measurements." In *High-Level Nuclear Waste Disposal*, ed. HC Burkholder, pp. 389–400, Battelle Press, Richland, Washington.

Cutillo PA and JD Bredehoeft. 2011. "Estimating Aquifer Properties from the Water Level Response to Earth Tides." *Ground Water* 49(4):600-610.

Davis K, Y Li, and M Batzle. 2008. "Time-Lapse Gravity Monitoring: A Systematic 4D Approach with Application to Aquifer Storage and Recovery." *Geophysics* 73(6): WA61-WA69.

Diodata DM. 1998. "Software Spotlight – Minitab 12." *Groundwater* 36 (5):716-717.

DOE. 1988. *Site Characterization Plan, Reference Repository Location, Hanford Site, Washington*. DOE/RW-0164, Vol. 2, U.S. Department of Energy, Washington, D.C.

Duffield GM. 2007. *AQTESOLV for Windows Version 4.5 User's Guide*. HydroSOLVE, Inc., Reston, Virginia (http://www.aqtesolv.com).

Duffield GM. 2009. "Upgrading Aquifer Test Analysis, by William C. Walton." *Ground Water - Comment Discussion Paper* 47(6):756-757.

Eslinger PW. 1986. *Probability Distribution of Horizontal Hydraulic Conductivity in Grande Ronde Basalt Flow Interiors*. Computational Brief, CB No. 550, Rockwell Hanford Operations, Richland, Washington.

Ferris JG. 1963. "Cyclic Fluctuations of Water Level as a Basis for Determining Aquifer Transmissibility." *Water-Supply Paper* 1536-I, U.S. Geological Survey, pp. 305–318.

Ferguson JF, T Chen, J Brady, CLV Aiken and J Seibert. 2007. "The 4D Microgravity Method for Waterflood Surveillance II - Gravity Measurements for the Prudhoe Bay Reservoir, Alaska." *Geophysics* 72(2): I33-I43.

Gephart RE, RC Arnet, RG Baca, LS Leonhart, and FA Spane. 1979. *Hydrologic Studies within the Columbia Plateau, Washington: An Integration of Current Knowledge*. RHO-BWI-ST-5, Rockwell Hanford Operations, Richland, Washington.

Gringarten AC and Ramey HJ, Jr. 1974a. "Unsteady-State Pressure Distribution Created by a Well with a Single Horizontal Fracture, Partial Penetration, or Restricted Entry." *Society of Petroleum Engineers Transactions* 257:413-426.

Gringarten AC and Ramey HJ, Jr. 1974b. "Unsteady-State Pressure Distribution Created by a Well with a Single Infinite-Conductivity Vertical Fracture." *Society of Petroleum Engineers* SPE Paper 4051, presented at the SPE-AIME 47 Annual Fall Meeting, San Antonio, Texas, October 8-11, 1972.

Hsieh PA, JD Bredehoeft, and JM Farr. 1987. "Determination of Aquifer Transmissivity from Earth Tide Analysis." *Water Resources Research* 23(10):1824-1832.

Hsieh PA, JD Bredehoeft, and SA Rojstaczer. 1988. "Response of Well Aquifer Systems to Earth Tides: Problem Revisited." *Water Resources Research* 24(3):468-472.

Hydrotechnique Associates. 1984. *Evaluation of Barometric and Earth Tide Effects in Well Records: Documentation.* Report prepared for Rockwell Hanford Operations by Hydrotechnique Associates, Berkeley, California.

Jenkins DN and JK Prentice. 1982. "Theory of Aquifer Test Analysis in Fractured Rocks Under Linear (Nonradial) Flow Conditions." *Ground Water* 20(1):12-21.

McGrail, BP, EC Sullivan, FA Spane, DH Bacon, G Hund, PD Thorne, CJ Thompson, SP Reidel, and FS Colwell. 2009. *Preliminary Hydrogeologic Characterization Results from the Wallula Basalt Pilot Study*. PNWD-4129, Pacific Northwest National Laboratory, Richland, Washington.

Merritt ML. 2004. *Estimating Hydraulic Properties of the Floridan Aquifer System by Analysis of Earth-Tide, Ocean-Tide, and Barometric Effects, Collier and Hendry Counties, Florida*. U.S. Geological Survey Water-Resources Investigations Report 03-4267.

Minitab, Inc. 2007. "Minitab 15 Statistical Software." Minitab, Inc., State College, Pennsylvania.

Nevulis RH, DR Davis, and S Sorooshian. 1989. "Analysis of Natural Groundwater Level Variations for Hydrogeologic Conceptualization, Hanford Site, Washington." *Water Resources Research* 25(7):1519-1529.

NAVD88. 1988. *North American Vertical Datum of 1988*.

NGVD 29/47. 1973. *National Geodetic Vertical Datum of 1929*.

Peterson FL. 1967. *Short-Term Responses in the Vicinity of Flowing Wells*. Ph.D. Dissertation, Stanford University, Palo Alto, California.

Pinder GP, JD Bredehoeft, and HH Cooper, Jr. 1969. "Determination of Aquifer Diffusivity from Aquifer Response to Fluctuations in River Stage." *Water Resources Research* 3(4): 850–855.

Rasmussen TC and LA Crawford. 1997. "Identifying and Removing Barometric Pressure Effects in Confined and Unconfined Aquifers." *Ground Water* 35(3):502-511.

Reidel SP, VG Johnson, and FA Spane. 2002. *Natural Gas Storage in Basalt Aquifers of the Columbia Basin, Pacific Northwest USA: A Guide to Site Characterization*. PNNL-13962, Pacific Northwest National Laboratory, Richland, Washington.

Reidel SP, FA Spane, and VG Johnson. 2005. *Potential for Natural Gas Storage in Deep Basalt Formations at Canoe Ridge, Washington State: A Hydrogeologic Assessment*. PNNL-15386, Pacific Northwest National Laboratory, Richland, Washington.

Robson SG and ER Banta. 1990. "Determination of Specific Storage by Measurement of Aquifer Compression Near a Pumping Well." *Ground Water* 28(6):868-874.

Schroder RA and SR Strait. 1987. *Fluid Temperature Data from Selected Boreholes on the Hanford Site*. SD-BWI-DP-065, Westinghouse Hanford Company, Richland, Washington.

Spane FA. 1982. "Hydrologic Studies within the Pasco Basin." In *Proceedings of 1982 National Waste Terminal Storage Program Information Meeting*, U.S. Department of Energy, DOENWTS-30, pp. 23–28.

Spane FA. 1999. *Effects of Barometric Fluctuations on Well Water-Level Measurements and Aquifer Test Data*. PNL-13078, Pacific Northwest Laboratory, Richland, Washington.

Spane FA. 2002. "Considering Barometric Pressure in Groundwater Flow Investigations." *Water Resour. Res.* 38(6):14/1–18.

Spane FA. 2008. *Results of Detailed Hydrologic Characterization Tests Conducted within Ohio Geological Survey CO_2 No. 1 Well*. PNWD-4000, Battelle Pacific Northwest Division, Richland, Washington.

Spane FA and K Didricksen. 2005. "Identification of Leakage Effects During Site Characterization Studies at the Proposed Black Rock Reservoir Site." PNWD-SA-6937, 5th Hydrogeology Symposium of Washington, April 12–14, 2005.

Spane FA and RD Mackley. 2010. "Removal of River-Stage Fluctuations from Well Response Using Multiple-Regression." *Ground Water*, DOI: 10.1111/j.1745-6584.2010.00780.x.

Spane FA and RB Mercer. 1985. *HEADCO: A Program for Converting Observed Water Levels and Pressure Measurements to Formation Pressure and Standard Hydraulic Head.* RHO-BW-ST-71P, Rockwell Hanford Operations, Richland, Washington.

Spane FA and PD Thorne. 1986. *Comparison of Calculated and Observed Hydrostatic Pressure Measurements at Borehole DC-8.* RHO-BW-ST-74P, Rockwell Hanford Operations, Richland, Washington.

Spane FA, Jr. and PD Thorne. 2000. *Analysis of the Hydrologic Response Associated with Shutdown and Restart of the 200-ZP-1 Pump-and-Treat System*. PNNL-13342, Pacific Northwest National Laboratory, Richland, Washington.

Spane FA, BP McGrail, EC Sullivan, DS Goldberg, TL McLing, RS Weeks, and RW Smith. 2008. *Field Activity Plan: Characterization Test for CO_2 Sequestration in the Columbia River Basalt Group*. PNWD 3844, Revision 1, Battelle Pacific Northwest Division, Richland, Washington.

Spane FA, PD Thorne, N Gupta, P Jagucki, TS Ramakrishnan, and N. Mueller. 2006. "Results Obtained from Reconnaissance-Level and Detailed Reservoir Characterization Methods Utilized for Determining Hydraulic Property Distribution Characteristics at Mountaineer AEP #1." In *Proceedings, CO2SC Symposium 2006*, Lawrence Berkeley National Laboratory, Berkeley, California, March 20-22, 2006.

Strait SR and FA Spane, Jr. 1982. *Preliminary Results of Hydrologic Testing the Composite Umtanum Basalt Flow Top at Borehole RRL-2*. SD-BWI-TI-105, Rev. 0, Rockwell Hanford Operations, Richland, Washington.

Strait SR and FA Spane, Jr. 1983. *Preliminary Results of Hydrologic Testing the Umtanum Basalt Fracture Zone at Borehole RRL-2*. SD-BWI-TI-89, Rev. 0, Rockwell Hanford Operations, Richland, Washington.

Sublette WR. *Rock Mechanics Data Package*. RHO-BWI-DP-41, Rev. 1, Rockwell Hanford Operations, Richland, Washington.

Toll NJ and TC Rasmussen. 2007. "Removal of Barometric Pressure Effects and Earth Tides from Observed Water Levels." *Ground Water* 45 (1): 101–105.

Vasco DW, K Karasaki, and K Kishida. 2001. "A Coupled Inversion of Pressure and Surface Displacement." *Water Resources Research* 37(12):3071–3089.

Vasco DW, A Rucci, A Ferretti, F Novali, RC Bissell, PS Ringrose, AS Mathieson, and IW Wright. 2010. "Satellite-Based Measurements of Surface Deformation Reveal Fluid Flow Associated with the Geological Storage of Carbon Dioxide." *Geophysical Research Letters* 37, L03303, doi:10.1029/2009GL041544.

WAC 173-218-115. "Specific Requirements for Class V Wells Used to Inject Carbon Dioxide for Permanent Geologic Sequestration. " Last accessed December 30, 2009, at http://apps.leg.wa.gov/WAC/default.aspx?cite=173-218-115.

White MD and M Oostrom. 2006. *STOMP Subsurface Transport over Multiple Phases, Version 4.0, User's Guide*. PNNL-15782, Pacific Northwest National Laboratory, Richland, Washington.

Appendix A

Hydrologic Test Methods

Appendix A

Hydrologic Test Methods

The general hydraulic test characterization discussion presented in this appendix is taken from Reidel et al. (2002), Spane (2008), Spane et al. (2008), and McGrail et al. (2009), and has been revised to support various hydrologic testing activities conducted at the Wallula pilot well. These hydrologic test methods pertain primarily to single-well field tests designed for the determination of hydraulic/storage properties of selected reservoir and caprock horizons. This discussion lists those methods applied or planned for use at the Wallula pilot well for the assessment of basalt interflow zones and flow interior/caprock horizons. Table A.1 lists the various hydrologic test methods discussed in this section, the hydrologic parameter(s) derived from their analysis, and the relative *radius-of-investigation* (test scale) as it relates to the Wallula pilot borehole.

Table A.1. Summary of Hydrologic Test Methods Used for Wallula Pilot Test Site Characterization Investigation (modified from Reidel et al. 2002, and Spane 2008)

Test Method	Hydrologic Parameter[(a)]						Test Scale		
	T	K_h	S	s_k	W_L	L	Local	Intermed.	Large
Slug	√	√	x	x			√		
DST[(b)]	√	√	√	√		√	√	√	
Step-Drawdown/ Recovery	√	√	√	√	√	√		√	
Constant-Rate Pumping – Drawdown and Recovery	√	√	√	√		√		√	√
Multistep, Constant-Head Injection[(c)]	√	√		√		x	√		

(a) Hydrologic parameter nomenclature.
(b) DST = Drill stem test.
(c) Low-permeability, caprock test method.

T = Test interval transmissivity
K_h = Equivalent hydraulic conductivity; equal to T divided by test interval length or aquifer thickness
S = Storativity; dimensionless
s_k = Well skin, dimensionless
W_L = Well loss
L = Leakage response.

Note: √ = Provides quantitative information.
x = Only provides inferential/qualitative information.

In addition to hydraulic/storage properties, the Wallula pilot study also includes hydrochemistry/microbiological sampling, and hydraulic head characterization determination for selected basalt interflow zones. These three characterization elements (i.e., hydraulic/storage properties, hydrochemical/isotopic content, microbiological sampling, and hydraulic head determination) can be readily included in a test strategy adopted for individual borehole characterizations. How they are integrated within the overall hydrologic test characterization strategy is primarily a function of each

characterization element's importance in meeting recognized objectives of the field testing program. A general discussion of several testing strategies commonly employed for deep borehole characterization studies (and their implementation in the initial Wallula pilot borehole characterization program) is presented in McGrail et al. (2009) and is not repeated in this report.

A.1 Slug/Drill-Stem-Tests

Because of their ease of implementation and relatively short duration, slug tests are commonly used to provide initial estimates of hydraulic properties (e.g., range and spatial/vertical distribution of hydraulic conductivity, K). Because of the small displacement volumes employed, hydraulic properties determined using slug testing are representative of conditions relatively close to the borehole. For this reason, slug-test results are normally used in the design of subsequent hydrologic tests having greater areas of investigation (e.g., slug interference [Novakowski 1989; Spane 1996] and constant-rate pumping tests [Butler 1990; Spane 1993]).

To conduct this test, a known volume of water is instantaneously removed (slug withdrawal) or added (slug injection) from the test interval. For tests conducted in 2009 during the Wallula pilot borehole characterization phase, most slug tests were initiated by simply removing or adding water to the packer-test tubing system and opening the downhole shut-in tool. The shut-in tool remained open during the active slug test recovery period. For slug tests conducted in 2011, the tests were performed without using a downhole packer-test tubing system, and were conducted only for the completed Wallula well open-borehole/injection zone section (i.e., 2716 to 2910 ft). The well configuration during the 2011 slug testing is shown in Figure 1.2 of this report. For these recently completed well tests, the slug tests were conducted pneumatically by using a sealed surface wellhead that was attached with a surface flange/seal to the top of the 7-in. well casing (see Appendix C, Figure C.1). The fluid column within the well was depressed pneumatically using regulated compressed air cylinders, and in-well fluid levels were monitored using a surface-based 50-psig strain-gauge pressure transducer that was installed a short distance below the projected fluid-column depression. After the depressed fluid-column pressure had stabilized, the compressed air inside the sealed well column was released as quickly as possible by opening wellhead ball valves (see Appendix C, Figure C.1), thereby initiating a slug withdrawal test caused by the depressed water column. A detailed description of the general design, performance, and analysis of slug test characterizations is presented in Butler et al. (1996) and Butler (1997). Additional discussion concerning specific design considerations for performing pneumatic slug tests is in Spane et al. (1996).

Analysis of the slug test recovery response provides an estimate of the test-interval transmissivity (T), average hydraulic conductivity (K), and storativity (S). However, estimates for storativity are less certain, due to the test method's lower sensitivity to S and impact of well skin, s_K, effects. The slug-test responses were analyzed using manual type-curve plots matching slug-test type curves generated using the Kansas Geological Survey (KGS) software program described in Liu and Butler (1995). Derivative plots for the slug test responses and type-curves were generated using the DERIV software program described in Spane and Wurstner (1993). The KGS model can account for a wide-range of well or formational conditions, including unconfined/confined aquifer conditions, partial well penetration, vertical anisotropy, and the presence of infinitesimal and finite-thickness well skin. However, note the KGS model is only valid for homogeneous formation tests exhibiting radial flow conditions. In addition, the KGS model and derivative plot options within the AQTESOLV (Pro 4.50) hydrologic test software (described in Duffield

2007 and 2009) were also employed for analysis of the 2011 pneumatic slug test results. A distinct advantage of using AQTESOLV is the automated type-curve/derivative plot matching analysis capability for observed test results. Other relevant papers discussing the general analysis of the slug tests or the slug-test phase of DST tests are provided in Ramey et al. (1975), Karasaki et al. (1988), and Ostrowski and Kloska (1989).

A DST can be implemented during the progress of the slug test recovery by closing a downhole shut-in tool to isolate the test formation from the open wellbore/test system. The closing of the downhole shut-in tool causes an acceleration of the slug test recovery response back to pretest, static formation conditions. This accelerated, closed-system recovery is caused by the significant reduction in test-system wellbore storage. The closed-system, slug test recovery phase following closing of the downhole shut-in tool constitutes the recovery phase of a DST. Normally, the DST shut-in recovery is initiated after the open-system, fluid-column recovery during the slug test has reached a value of approximately 50% of the applied initial slug stress (i.e., in relationship to pretest, static formation conditions). This can be directly monitored using a downhole, real-time test zone pressure sensor. An analysis of the recovery buildup during later stages of the DST recovery can be used to provide estimates of T, K, S, s_K, and (if pretest trend conditions are adequately accounted for) the recovery can be projected to estimate static formation pressure conditions. Wallula pilot borehole DST results for tests conducted during 2009 were analyzed using standard procedures presented in Earlougher (1977). These DST results were previously presented in McGrail et al. (2009). Since the 2011 pneumatic slug tests were performed within the completed well and without using a downhole packer/shut-in tool system, no DST tests were conducted during this characterization phase. Other relevant discussions pertaining to the recovery (shut-in) phase of DST testing are also presented in Correa and Ramey (1987) and Karasaki (1990).

A.2 Constant-Rate Pumping Test

During constant-rate pumping tests, groundwater is withdrawn from a well with discharge regulated and maintained at a uniform rate. The water-level (pressure) response within the well is monitored during the active pumping phase and during the subsequent recovery phase following termination of pumping. The analysis of the drawdown and recovery water-level response provides a means for estimating hydraulic properties (see Table A.1) of the interflow zone(s) tested, as well as for discerning formational and nonformational flow conditions (e.g., wellbore storage, skin effects, presence of boundaries and leakage). Standard analytical methods used for the analysis of constant-rate tests include type-curve matching and straight-line methods.

To support selection of proper analytical models and identification of test response complexities (e.g., radial/nonradial flow, hydrologic boundaries), diagnostic derivative analysis must be performed on the constant-rate test results prior to formal hydrologic test analysis. To conduct diagnostic derivative analysis of the drawdown and recovery test responses, composite log-log plots of the pressure change and its derivative data are prepared for data collected during and immediately following the termination of constant-rate pumping tests. Derivative plots can be generated using the DERIV program described in Spane and Wurstner (1993). The use of derivative plots has been shown to significantly improve the diagnostic and quantitative analysis of various hydrologic test methods (Bourdet et al. 1989; Spane 1993; Spane and Wurstner 1993). The improvement in test analysis is attributed to the sensitivity of pressure derivatives to various test/formation/boundary conditions.

As noted in Spane and Wurstner (1993), specific applications for which derivatives are particularly useful include the following:

- Identifying established flow-regimes, formation-response characteristics (nonleaky or leaky; confined or unconfined aquifer) and presence of surrounding boundary conditions (impermeable or constant head)
- Assisting in the selection of the appropriate type-curve solution through combined type-curve/derivative plot matching
- Determining when infinite-acting, radial flow conditions are established, and therefore when straight-line analysis methods are applicable.

Figure A.1 shows a limited selection of composite log-log drawdown and derivative response examples that are characteristic of some commonly encountered formation conditions during constant-rate pumping tests.

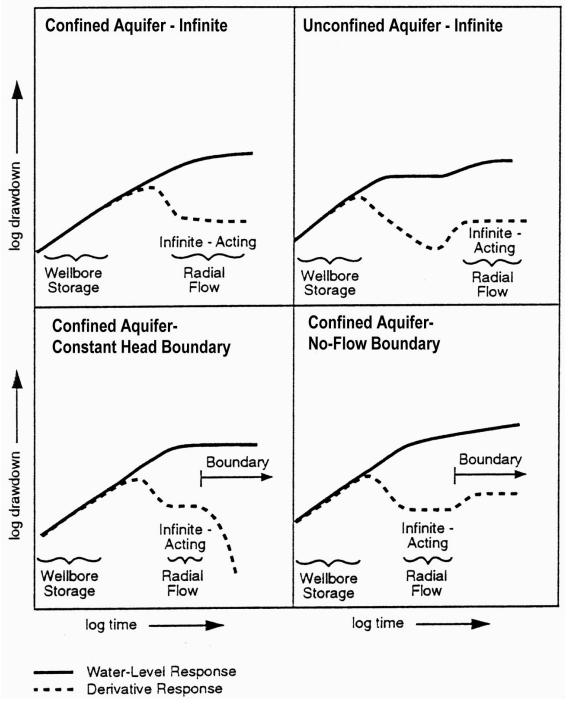

Figure A.1. Characteristic Log-Log Drawdown and Drawdown Derivative Plots for Selected Hydrogeologic Formation and Boundary Conditions (adapted from Spane and Wurstner 1993)

The plots are equally applicable for injection buildup and recovery analysis. Spane (1993) and Spane and Wurstner (1993) provide a summary discussion on the use of standard and derivative-based analytical methods for constant-rate tests. A more extensive listing of diagnostic derivative plots for various formation and boundary conditions is presented in Horne (1990) and Renard et al. 2009). These diagnostic plot procedures were applied for constant-rate pumping tests conducted during the initial 2009 Wallula pilot borehole characterization phase, as well as the extended 7-day pumping test conducted in 2011 for the Wallula pilot well injection interval.

Of particular relevance to the 2011 extended pumping test is the quantitative application of derivative plot analysis to identify established flow regimes during a constant-rate pumping test; e.g., radial versus nonradial flow conditions (i.e., linear, bi-linear, and spherical). As discussed in Ehlig-Economides et al. (1994), various flow regimes during constant-rate tests exhibit distinctive derivative plot patterns. Figure A.2 provides a useful flow-regime identification tool that can be used to discern established flow regimes and their transition to other flow conditions during the course of testing.

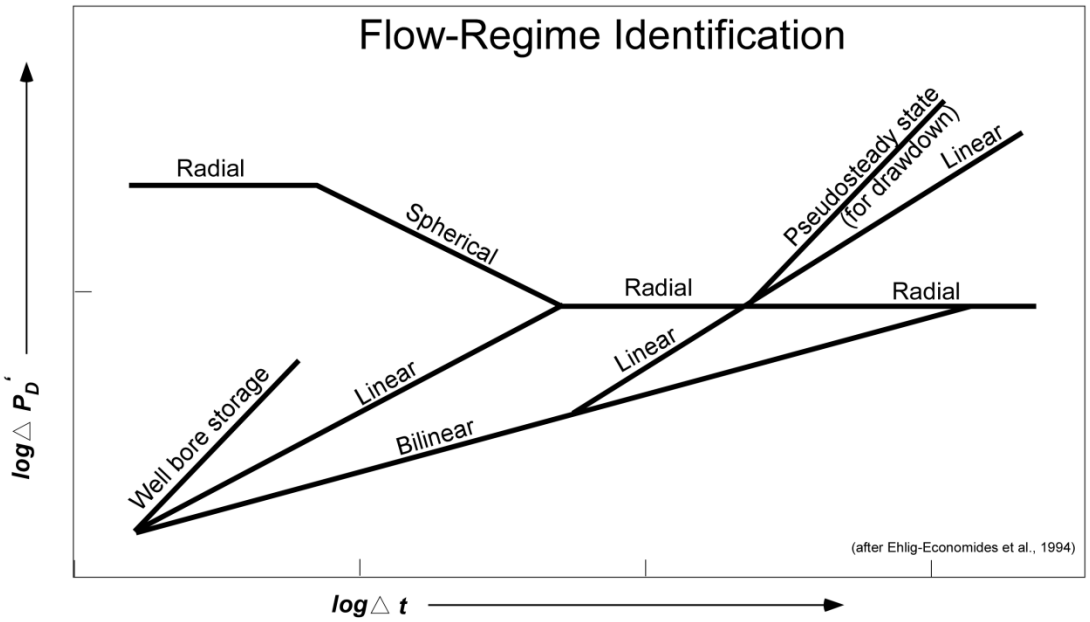

Figure A.2. Characteristic Derivative Plot Patterns for Selected Constant-Rate Test Flow-Regime Conditions (adapted from Ehlig-Economides et al. 1994)

As indicated in Figure A.2, the following flow regimes and conditions are indicated by their associated log-log derivative versus time-slope pattern values:

Flow-Regime/Condition	**Log-Log Derivative/Time Slope**
Wellbore Storage	1
Radial Flow	0
Linear Flow	½
Bi-Linear Flow	¼
Spherical Flow	-½

Examples of well/formation conditions that may be responsible for establishment of these various flow-regime conditions and their associated test analysis are provided in the following reports: Bourdet et al. (1989) for wellbore storage and radial flow; Gringarten and Ramey (1974a, 1974b), Jenkins and Prentice (1982) for linear flow; Cinco-Ley and Samaniego-V (1981) and Butler and Liu (1991) for bi-linear flow; and Ehlig-Economides et al. (1994) for spherical flow.

Analytical procedures for constant-rate pumping tests exhibiting wellbore storage and radial flow conditions are well established in groundwater literature. Type-curve-matching methods that are commonly used in the analysis of pumping test responses include Theis (1935), Hantush (1964), and Neuman (1975). Analyses using constant-rate test type curves for Wallula pilot test intervals exhibiting radial-flow conditions were generated using the WTAQ program described in Moench (1997), and Barlow and Moench (1999). Straight-line analysis methods, where the change of water levels within the well during drawdown and/or recovery is plotted against the log of time, can be applied to estimate hydraulic properties for test data sections exhibiting infinite-acting radial flow conditions (i.e., derivative slope = 0). Because well-skin effects are constant with time during constant-rate tests, straight-line methods can be used to quantitatively analyze the water-level response at both pumping and any nearby observation wells. No observation wells were available for test characterizations conducted within the Wallula pilot borehole during the 2009 and 2011 test characterization phases. The semilog, straight-line analysis techniques commonly used are based either on the Cooper and Jacob (1946) method (for buildup analysis) or the Horner (1951) method for recovery analysis. Note the Horner method, which is commonly used in the petroleum industry, is identical to the Theis (1935) recovery method used in groundwater hydrology. These methods are theoretically restricted to the analysis of test responses from wells that fully penetrate nonleaky, homogeneous, isotropic, confined aquifers. Straight-line methods, however, may be applied under nonideal well and aquifer conditions if infinite-acting, radial flow conditions exist. Infinite-acting, radial flow conditions are indicated during testing when the change in pressure—at the point of observation—increases proportionately to the logarithm of time. The establishment of infinite-acting, radial flow conditions is also indicated by a constant (flat) pressure derivative pattern on the log-log diagnostic plot.

The preceding discussion assumes that the pumping test was conducted at a constant-rate. For tests where varying discharge rates occur during the course of the test, several methods are available to correct the observed drawdown and recovery data for flow-rate change conditions. For tests where significant/abrupt changes in flow-rate occur, these discrete periods of different pumping rates can be addressed using the principle of superposition (e.g., Reilly et al. 1987). This is the approach used in the AQTESOLV software program for constant-rate test analysis. In addition, the superposition time function relationships described in Bourdet et al. (1989) and Cinco-Ley and Samaniego-V (1989) can also be used to manually correct observed test data directly for flow variations during testing.

For many pumping tests, discharge rates vary gradually during the course of the test. This condition is commonly associated with the increase in head differential that occurs over the test time, due to gradual increases in drawdown. This was the test condition observed during the 2011 Wallula injection zone, extended constant-rate test. In these test situations, the observed drawdown can be corrected for small variations in pumping rate (i.e., discharge decline) by dividing the observed pressure change by the ratio of pumping rate over the pressure measurement period, and multiplying this quotient by the average pumping rate for the entire test, as shown in Equation (A.1):

$$\Delta s_{cor} = (\Delta s_{obs}/Q_{obs})Q_{avg} \qquad \text{(A.1)}$$

This type of superposition approach is valid for tests where the pumping rate decreases (or increases) in an exponential fashion, and can be demonstrated by comparing a standard constant-rate solution (e.g., Theis 1935) to analyze a constant-drawdown test where observed flow rate declines over test time. Figure A.3 shows the well-known constant-drawdown test example presented in Lohman (1972), where

an artesian well (with a positive shut-in gauge pressure, Δs_{obs}, equivalent to 92.33 ft of water) was opened for surface discharge and allowed to flow freely over a 112-minute test period. Surface discharge declined steadily from an initial rate of 7.28 gpm observed 1 minute into the test to 4.88 gpm measured at test termination (i.e., a 33% decline in flow rate) and averaged 5.23 gpm for the entire test period. The varying flow rate versus time data observed for the reported Lohman test example were converted to a corrected drawdown, Δs_{cor}, based on the Equation (A.1) relationship. The predicted drawdown, Δs, based on the constant-rate test solution for the listed aquifer/test conditions reported in Lohman (1972) is superimposed on the converted test data. In addition, the converted constant-drawdown solution described in Jacob and Lohman (1952) and Lohman (1972) using Equation (A.1) is also shown for comparison purposes. As indicated in Figure A.3, a high correspondence between the solutions and the converted test data is evident. This high level of correspondence indicates the data correction relationship listed in Equation (A.1) is valid for correcting pumping test data for the effects of gradually decreasing flow rate, and analyzing the test data using standard constant-rate pumping test methods.

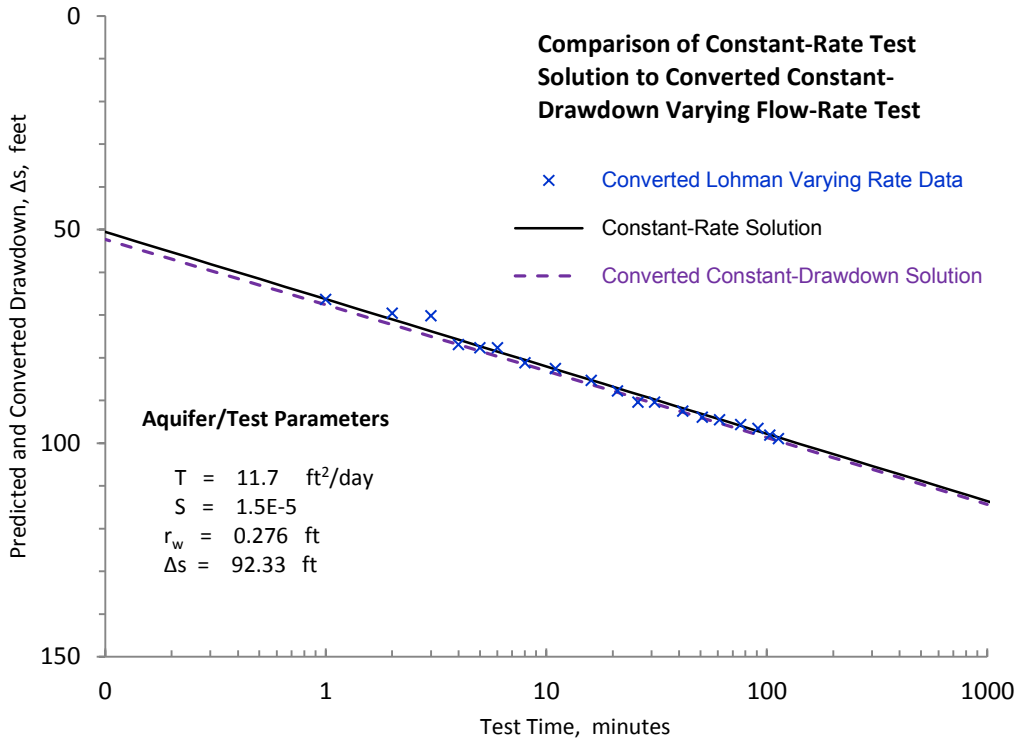

Figure A.3. Comparison of Constant-Rate Solution to Converted Constant-Drawdown Data

Note the previous discussions in this appendix pertain specifically to the analysis of the drawdown phase of constant-rate pumping tests. For the analysis of recovery data following termination of constant-rate tests, the equivalent time function of Agarwal (1980) may be used, which accounts for the preceding effects of pumping duration on the observed recovery response over time. Use of the Agarwal equivalent time function allows the converted recovery data to be analyzed using the same methods as employed for constant-rate drawdown test data analysis. However, use of the Agarwal equivalent time function for recovery test data is limited to constant-rate pumping tests that also exhibit radial flow conditions during the drawdown pumping phase, as noted in Cinco-Ley and Samaniego-V (1989).

For the completed Wallula well zone that exhibited nonradial (linear) flow regime conditions during the 2011 extended constant-rate test, various flow-model options contained in AQTESOLV (Duffield 2007, 2009) were employed. However, quantitative analysis of nonradial constant-rate tests require that additional geometric information be available for the formation feature causing nonradial flow conditions to the test well (e.g., length/width attributes for fractures or embedded channel/strip aquifer). These geometric attributes are currently not available for the Wallula pilot well injection zone. Recommended tests to help identify the cause of the nonradial flow condition for the Wallula well injection zone, and to determine various geometric/spatial characteristics of the controlling feature, are discussed in Section 6.0 of the main report.

In addition to the linear-flow type-curve model analysis approach available in AQTESOLV, the general arithmetic plot analysis approach based on the method developed and presented in Jenkins and Prentice (1982) for constant-rate tests exhibiting linear fracture-flow conditions was also used in analyzing the 2011 Wallula pilot well extended constant-rate test. For this analysis method, pumping test drawdown data, s, are plotted on an arithmetic plot versus the square root of pumping time, $t_p^{1/2}$. As discussed in Jenkins and Prentice (1982), for linear-flow conditions, the s versus $t_p^{1/2}$ relationship plots as a straight line. The slope of the established linear drawdown analysis ($s/t_p^{1/2}$), is directly related to the parameter grouping, $Q/ L_f (\pi TS)^{1/2}$, which can be expressed in Equation (A.2):

$$L_f(TS)^{1/2} = (Q/s)(t_p/\pi)^{1/2} \qquad (A.2)$$

where: Q = pumping rate
L_f = fracture length
T = fracture transmissivity
S = fracture storativity

As noted by Jenkins and Prentice (1982), for pumping well test analysis without benefit of monitor well data (and if L_f is unknown), a unique value for T is not attainable and "…values of T determined using estimated L_f and S values should be used with caution."

A.3 Step-Drawdown Test

Step-drawdown tests are normally conducted to assess well/aquifer head loss performance and for guidance in selecting an optimum pumping rate for subsequent, longer-duration, constant-rate pumping tests. The test is conducted as a series of sequential, short-duration constant-rate pumping tests (e.g., 1 to 4 hours in length), with each rate step being of uniform duration and at progressively higher pumping rates. A minimum of three steps is required, and four or more steps are generally preferred.

Step-drawdown testing was performed on Zone 1 during the 2009 Wallula pilot borehole characterization phase (as part of the Boise Inc. mill aquifer storage project) and immediately prior to the 2011 extended constant-rate test for the Wallula pilot well injection zone. Well loss for these tests was assessed by comparing discharge, Q, and the drawdown/pumping-rate ratio, s_w/Q, (i.e., drawdown/discharge). Using the standard head-loss analysis plot procedure originally described by Jacob (1946) and Rorabaugh (1953), a nonlinear, increasing s_w/Q versus Q pattern is indicative of turbulent well-loss conditions while a constant, linear relationship versus Q indicates that well losses exhibited during pumping are laminar in nature.

Jacob (1946) presented the following well head loss/drawdown relationship used to assess well-discharge performance (Equation A.3):

$$s_w = BQ + CQ^2 \quad (A.3)$$

where BQ = laminar aquifer head loss, and CQ^2 = turbulent well head loss.

As shown in Figure A.4, a linear-regression slope fit through the step-drawdown test data provides coefficients for the head loss Equation (A.3), with the intercept value equal to coefficient B, and the linear-regression slope equivalent to coefficient C. Note that the laminar aquifer head loss, BQ, includes the effects of true formational aquifer characteristics (i.e., head loss due to hydraulic properties) and those attributable to well-skin effects (i.e., damage associated with drilling/well construction process).

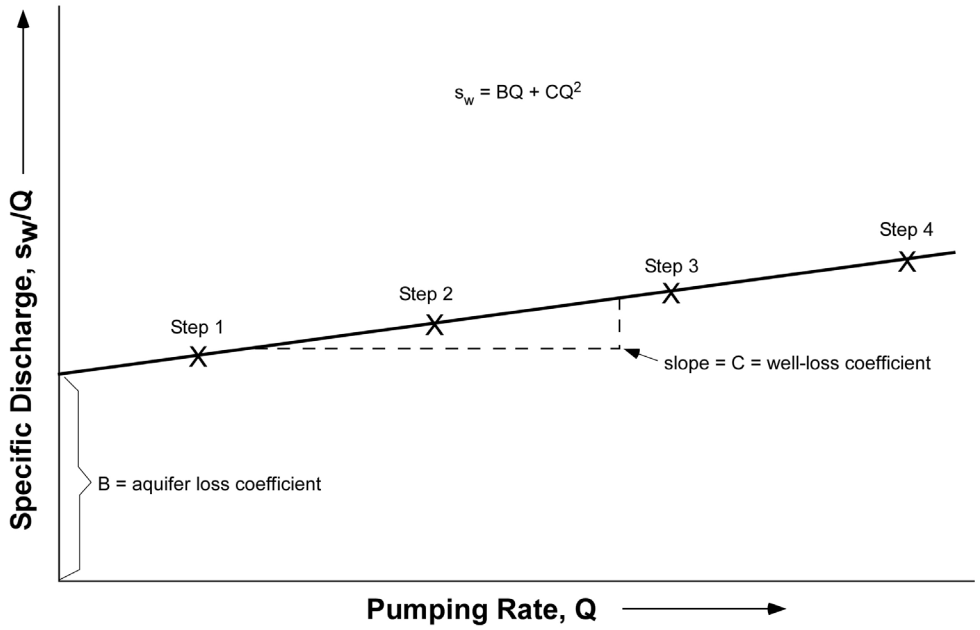

Figure A.4. Specific Drawdown Plot Relationships for Calculating Formation Loss (B) and Well Loss (C) Coefficients from Step-Drawdown Test Data (adapted from Spane and Newcomer, 2009)

Well efficiency, E, or percentage of the observed drawdown within the pumping well not attributed to turbulent well loss components can be calculated based on the following relationship (Equation A.4) provided in Roscoe Moss Company (1990):

$$E = 100/(1 + CQ/B) \quad (A.4)$$

where equation parameters were previously defined.

Equations (A.3) and (A.4) were used to correct and remove the nonformational head loss from the drawdown data observed during the ~24 constant-rate pumping test for Zone 1 that occurred following completion of the step-drawdown recovery period. This was due to the high pumping rates and observed

head loss conditions associated with this test zone characterization. They were not used to correct drawdown data obtained during the 2011 extended constant-rate test, since these correction methods are only applicable to tests exhibiting radial-flow conditions.

A.4 Multi-Step Constant-Pressure Injection Test

For detailed characterization of low-permeability caprocks, multi-level (multi-step) constant-pressure injection tests are commonly conducted. This test method was used to characterize the three Wallula pilot caprock test zones (Zone 9, 10A, and 10B). Results from these low-permeability tests were previously discussed in McGrail et al. (2009) and summarized in Section 2.0 of this report.

For a multi-step test, injection pressures are systematically increased with time, and the associated steady-state injection rates recorded during each injection pressure step. Injection rate declines during each injection step as a function of time, eventually reaching a pseudo steady-state flow rate. The early-time decline in injection rates can be analyzed using the transient straight-line solution presented by Jacob and Lohman (1952). Late-time pseudo steady-state injection rates can be analyzed using the equation relationship presented in Zeigler (1976).

A distinct advantage of conducting a multi-step injection tests over a single injection pressure test is the ability to assess dependence of permeability to injection pressure level. Permeability-pressure dependence may occur in fractured rock types (e.g., flow interiors) and clays. If no dependence is evident, a straight-line relationship between steady-state injection rate and injection pressure will be indicated. Examples of multi-step injection pressure tests and their analysis for Columbia River basalt flow interior/caprocks are provided in Spane and Thorne (1985).

Analysis of recovery pressures following termination of constant injection tests in low permeability intervals usually is not performed. This analysis is due to the excessive time required to reach radial-flow conditions. However, for intermediate and/or higher permeability caprock intervals, recovery analyses can be used. Unless steady-state injection rates are maintained for prolonged periods of time, constant-rate recovery methods cannot be used. In these instances, multi-rate analytical methods (to take into account the nonuniformity in injection rates) must be employed. A description of the various multi-rate analytical approaches is presented in Earlougher (1977), as well as the previous variable-rate discussion in this appendix section.

A.5 Property Conversions/Calculations/Assumptions

The test methods described above provide direct estimates for transmissivity, T, for the interval tested. Hydraulic conductivity, K, was calculated by dividing the value for T by the assumed contributing basalt interflow thickness, b. For analysis purposes, the contributing interflow thickness, L, was assumed to be equivalent to the observed flowtop thickness, which was determined based on wireline geophysical survey responses. As noted by Lohman (1979), both T and K are functions of fluid and formation properties, while intrinsic permeability, k, is only a property of the formation. The standard relationship between K and k is shown in Equation (A.5):

$$K = k\,(\gamma_{fw}/\mu_{fw}) \qquad (A.5)$$

where γ_{fw} is the formation fluid specific-weight density, and μ_{fw} is the formation fluid dynamic viscosity.

For analyses performed for Wallula tests zones, the γ_{fw} was calculated based on observed or projected, equilibrated downhole pressure measurements for the test interval, and for the measured downhole temperature and observed formation water salinity conditions. For these observed input values, the test zone average fluid-specific weight value was then calculated using a computer problem HEADCO (Spane and Mercer 1985), which can be used to calculate γ_{fw}, given formation fluid temperature, pressure, and salinity conditions. The μ_{fw} was calculated based on the relationships presented in Meehan (1980a), which also takes into account observed/assumed temperature, pressure, and salinity conditions.

At standard temperature and pressure conditions (STP: temperature = 60˚F; pressure = 14.696 lb/in^2), γ_{fw}, = 62.3664 lb/ft^3 and μ_{fw} = 1.1295 cp (2.359 × 10^{-5} lb-sec/ft^2), assuming fresh-water conditions (i.e., ρ = 0.999014 g/cm^3), a k value of 1 darcy (1.0624 × 10^{-11} ft^2) would be equivalent to a K value of 2.43 ft/d under STP conditions. For comparison purposes, for the Wallula well injection zone with an observed formation water salinity of 400 ppm, a temperature ~95˚F, and a pressure ~1,170 lb/in^2, the calculated formation specific-weight density and viscosity are γ_{fw} = 62.292 lb/ft^3, and μ_{fw} = 0.708 cp. Under these Wallula injection zone test conditions, a permeability (k) of 1 darcy would be equivalent to a K value of ~3.86 ft/d for these specified test conditions.

Depending on the particular hydrologic test method, storativity, S, is either determined directly from the test analysis results or assumed or calculated from independent physical relationships. As indicated below, S is equal to the product of the formation specific storage, S_s, and test thickness, b, as shown in Equation (A.6):

$$S = S_s\, b = b\, \gamma_{fw}\, (c_f + n\, c_{fw}) \qquad (A.6)$$

where c_f is the rock matrix compressibility, n is the formation porosity, and c_{fw} is the formation fluid compressibility.

For example purposes, for Grande Ronde basalt flow tops having a formational compressibility of ~1.5 × 10^{-7} psi^{-1}(Sublette 1986), an assumed porosity of 10%, and a c_{fw}, estimated from relationships presented in Earlougher (1977) and Meehan (1980b) for Wallula injection zone conditions (i.e., 95˚F, 1170 psi), yields an S_s estimate of 1.4 × 10^{-6} ft^{-1}. This estimate is within the range of S_s values listed for highly consolidated formations (e.g., sandstones), as reported in Shestakov (2002) and serves as the initial estimate for calculating S for test methods requiring this input for analysis (e.g., slug-injection tests) or for calculating combined wellbore storage/well-skin effects.

Wellbore storage, C_D, is an important parameter for recovery phases following injection tests conducted at the Wallula pilot well site. For open well tests, C_D is related to S and well test system parameters by the following relationship (Equation A.7) reported in Spane and Wurstner (1993):

$$C_D = r_c^2 / 2(r_w^2\, S) \qquad (A.7)$$

where r_c is the radius of the test tubing/casing where fluid change is occurring, and r_w is the radius of the well/borehole.

As noted, Equation (A.7) is strictly for situations where test recovery occurs in an open borehole condition. For cases where recovery occurs using a downhole shut-in tool (as during recovery phases following pumping tests during the Wallula borehole characterization phase), C_D must be modified to represent the closed-system response condition. As noted in Bredehoeft and Papadopulos (1980), for closed-in recovery response, r_c^2 is replaced by the following (Equation A.8):

$$r_c^2 = (V_{ts}\, c_{ts}\, \gamma_{fw})/\pi \qquad (A.8)$$

where V_{ts} is the volume of closed, in-well test system, and c_{ts} is the compressibility of the closed, in-well test system; commonly equal to c_w.

During the well drilling and completion process, formation damage can occur, which represents a zone around the well of altered formational permeability. This zone of altered formational permeability is referred to as a *skin effect* or "well skin" (Earlougher 1977; Ramey 1970, 1982). For cases where well skin, s_K, is present, Equation (A.7) can be re-written to account for the added wellbore storage effect caused by well skin as shown in Equation (A.9):

$$C_D e^{2sk} = r_c^2 / 2(r_w^2\, Se^{2sk}) \qquad (A.9)$$

Estimates for well skin in this report were determined by dividing the value derived for Se^{2sk} from test analysis by the calculated value for S (Equation A.6) as indicated in Equation (A.10):

$$s_K = -\ln (Se^{2sk}/S)/2 \qquad (A.10)$$

The *radius of investigation* of the hydrologic tests is variable and a function of the 1) duration and magnitude of the stress applied, 2) formation of hydraulic and storage properties, and 3) test system/formation fluid compressibility. Of these parameters, the presence of gas and its large influence on total fluid compressibility greatly limits the radius of investigation of the imposed hydrologic test. Radius of investigation relationships are commonly expressed in terms of *detecting* the pressure perturbation effects of an outside boundary. Horne (1990) provides the following area of investigation, A_i, relationship for detecting a closed (no-flow) circular reservoir boundary surrounding a test well, expressed in standard petroleum industry units (Equation A.11):

$$A_i > 2.64E\text{-}4(k\, t)/(\phi\, \mu\, c_t) \qquad (A.11)$$

And Equation (A.12):

$$r_i > (A_i/\pi)^{1/2} \qquad (A.12)$$

As emphasized by Horne (1990), this is the radius at which a boundary would begin to be manifest at the test well. If the *actual* detection of a boundary is used as a parameter criterion, therefore, the radius of investigation relationship expressed in Equations (A.11) and (A.12) represent maximum distance estimates. Note the pressure perturbation imposed by a hydrologic test affects a larger region (i.e., *area or radius of influence*), but the more restrictive radius of investigation is a more meaningful parameter for assessing actual characterization distances.

References

Agarwal RG. 1980. "A New Method to Account for Producing Time Effects When Drawdown Type Curves Are Used to Analyze Pressure Buildup and Other Test Data." SPE Paper 9289, Society of Petroleum Engineers, Dallas, Texas.

Barlow PM and AF Moench. 1999. "WTAQ – A Computer Program for Calculating Drawdowns and Estimating Hydraulic Properties for Confined and Water-Table Aquifers." Water-Resources Investigations Report 99-4225, U.S. Department of the Interior and U.S. Geological Survey, Northborough, Massachusetts.

Bourdet DJ, A Ayoub, and YM Pirard. 1989. "Use of Pressure Derivative in Well-Test Interpretation." *SPE Formation Evaluation* June:293–302.

Bredehoeft JD and SS Papadopulos. 1980. "A Method for Determining the Hydraulic Properties of Tight Formations." *Water Resources Research* 16(1):233–238.

Butler JJ, Jr. 1990. "The Role of Pumping Tests in Site Characterization: Some Theoretical Considerations." *Ground Water* 28(3):394–402.

Butler JJ, Jr. 1997. *The Design, Performance, and Analysis of Slug Tests*. Lewis Publishers, CRC Press, Boca Raton, Florida.

Butler, JJ, Jr. and WZ Liu. 1991. "Pumping Tests in Non-Uniform Aquifers - the Linear Strip Case." *Journal of Hydrology* 128:69-99.

Butler JJ, CD McElwee, and W Liu. 1996. "Improving the Quality of Parameter Estimates Obtained from Slug Tests." *Ground Water* 34(3):480–490.

Cinco-Ley H and F Samaniego-V. 1981. "Transient Pressure Analysis for Fractured Wells." SPE Paper 7490, *Journal of Petroleum Engineers*, September: 1749-1766.

Cinco-Ley H and F Samaniego-V. 1989. "Use and Misuse of the Superposition Time Function in Well Test Analysis." SPE Paper 19817, 64th Annual Technical Conference and Exhibition of the Society of Petroleum Engineers, October 8-11, 1989, San Antonio, Texas.

Cooper HH, Jr., and CE Jacob. 1946. "A Generalized Graphical Method for Evaluating Formation Constants and Summarizing Well-Field History." *American Geophysical Union, Transactions* 27(4):526–534.

Cooper HH, JD Bredehoeft, IS Papadopulos. 1967. "Response of a Finite-Diameter Well to an Instantaneous Charge of Water." *Water Resources Research* 3(1):263-269.

Correa AC and HJ Ramey, Jr. 1987. "A Method for Pressure Buildup Analysis of Drillstem Tests." SPE Paper 16802, Society of Petroleum Engineers, 62nd Annual Technical Conference and Exhibition of the Society of Petroleum Engineers, September 27–30, 1987, Dallas, Texas.

Duffield GM. 2007. *AQTESOLV for Windows Version 4.5 User's Guide*. HydroSOLVE, Inc., Reston, Virginia (http://www.aqtesolv.com).

Duffield GM. 2009. "Upgrading Aquifer Test Analysis, by William C. Walton." *Ground Water - Comment Discussion Paper* 47(6):756-757.

Earlougher RC, Jr. 1977. *Advances in Well Test Analysis*. Monograph Vol. 5, Society of Petroleum Engineers, Richardson, Texas.

Ehlig-Economides CA, P Hegeman, and S Vik. 1994. "Well Testing – 1: Guidelines Simplify Well Test Interpretation." *Oil and Gas Journal* July:33-40.

Enachescu C and LP Ostrowski. 1993. "Special Aspects of Applying Constant Rate Analysis Approach in Low-Permeability Formations." SPE Paper 25877, Society of Petroleum Engineers, SPE Rocky Mountain Regional/Low Permeability Reservoirs Symposium of the Society of Petroleum Engineers, April 12–14, 1993, Denver, Colorado.

Gringarten AC and Ramey HJ, Jr. 1974a. "Unsteady-State Pressure Distribution Created by a Well with a Single Horizontal Fracture, Partial Penetration, or Restricted Entry." *Society of Petroleum Engineers Transactions* 257:413-426.

Gringarten AC and Ramey HJ, Jr. 1974b. "Unsteady-State Pressure Distribution Created by a Well with a Single Infinite-Conductivity Vertical Fracture." SPE Paper 4051, Society of Petroleum Engineers, SPE-AIME 47 Annual Fall Meeting, October 8-11, 1972, San Antonio, Texas.

Hantush MS. 1964. "Hydraulics of Wells." *Advances in Hydroscience*, ed VT Chow, 1:282–433, Academic Press, New York.

Horner DR. 1951. "Pressure Build-Up in Wells." In *Proceedings of the Third World Petroleum Congress*, The Hague, Session II:503-523.

Horne RN. 1990. *Modern Well Test Analysis: A Computer-Aided Approach*. Petroway, Inc., Palo Alto, California.

Jacob CE. 1946. "Drawdown Test to Determine Effective Radius of an Artesian Well." In *Proceedings, ASCE*, Paper No. 2321.

Jacob CE, and SW Lohman. 1952. "Non-Steady Flow to a Well of Constant Drawdown in an Extensive Aquifer." *Transact American Geophysical Union* 33(4):559–569.

Jenkins DN and JK Prentice. 1982. "Theory of Aquifer Test Analysis in Fractured Rocks Under Linear (Nonradial) Flow Conditions." *Ground Water* 20(1):12-21.

Karasaki K. 1990. "A Systematized Drillstem Test." *Water Resources Research* 26(12):2913–2919.

Karasaki K, JCS Long, and PA Witherspoon. 1988. "Analytical Models of Slug Tests." *Water Resources Research* 24(1):115–126.

Liu WZ and JJ Butler, Jr. 1995. *The KGS Model for Slug Tests in Partially Penetrating Wells (Version 3.0)*. Kansas Geological Survey Computer Series Report 95-1, Lawrence, Kansas.

Meehan DN. 1980a. "Estimating Water Viscosity at Reservoir Conditions." *Petroleum Engineer* July:117–118.

Meehan DN. 1980b. "A Correlation for Water Compressibility." *Petroleum Engineer* July:125-126.

Moench AF. 1997. "Flow to a Well of Finite Diameter in a Homogeneous, Anisotropic Water-Table Aquifer." *Water Resources Research* 33(6):1397–1407.

Moench AF and PA Hsieh. 1985. *Analysis of Slug Test Data in a Well with Finite Thickness Skin*. In *Proceedings of the 17th International Conference of Assoc. of Hydrogeologists*, January 1985, Tucson, Arizona, pp. 17-27.

Neuzil CE. 1982. "On Conducting the Modified 'Slug Test' in Tight Formations." *Water Resources Research* 18 (2):pp. 439-441.

Neuman SP. 1975. "Analysis of Pumping Test Data from Anisotropic Unconfined Aquifers Considering Delayed Gravity Response." *Water Resources Research* 11(2):329–342.

Newman GH. 1973. "Pore-Volume Compressibility of Consolidated, Friable, and Unconsolidated Reservoir Rocks Under Hydrostatic Loading." *Journal of Petroleum Technology* February: 129–134.

Novakowski KS. 1989. "Analysis of Pulse Interference Tests." *Water Resources Research* 25(11):2377-2387.

Ostrowski LP and MB Kloska. 1989. "Use of Pressure Derivatives in Analysis of Slug Test or DST Flow Period Data." SPE Paper 18595, Society of Petroleum Engineers, SPE Production Operations Symposium, March 13–14, 1989, Oklahoma City, Oklahoma.

Peres AM, M Onur, and AC Reynolds. 1989. "A New Analysis Procedure for Determining Aquifer Properties from Slug Test Data." *Water Resources Research* 25(7):1591–1602.

Ramey HJ Jr. 1970. "Short-Time Well Test Data Interpretation in the Presence of Skin Effect and Wellbore Storage." *Journal of Petroleum Technology, AIME* 249:97-104.

Ramey HJ Jr. 1982. "Well-Loss Function and the Skin Effect: A Review." *Geological Society of America Special Paper 189*:265-271.

Ramey HJ Jr., RG Agarwal, and I. Martin. 1975. "Analysis of 'slug test' or DST flow period data." *Journal of Canadian Petroleum Technology* July–September:37–47.

Reidel SP, VG Johnson, and FA Spane. 2002. *Natural Gas Storage in Basalt Aquifers of the Columbia Basin, Pacific Northwest USA: A Guide to Site Characterization*. PNNL-13962, Pacific Northwest National Laboratory, Richland, Washington.

Reilly TE, OL Franke, and GD Bennett. 1987. "The Principle of Superposition and its Application in Ground-Water Hydraulic." In *Techniques of Water-Resources Investigations, Book 3.* Applications of Hydraulics, Chapter B6, Reston, Virginia: U.S. Geological Survey, 28.

Renard P, D Glenz, and M Mejias. 2009. "Understanding Diagnostic Plots for Well-Test Interpretation." *Hydrogeology Journal* 17(3):589-600.

Rorabaugh MI. 1953. "Graphical and Theoretical Analysis of Step Drawdown Tests of Artesian Wells." Proceedings, *ASCE* 79, Paper No. 362.

Roscoe Moss Company. 1990. "Handbook of Ground Water Development." Wiley-Interscience Publication, John Wiley & Sons, New York, New York, p. 512.

Shestakov VM. 2002. "Development of Relationship Between Specific Storage and Depth of Sandy and Clay Formations." *Environmental Geology* 42:127-129.

Spane FA, Jr. 1993. *Selected Hydraulic Test Analysis Techniques for Constant-Rate Discharge Tests*. PNL-8539, Pacific Northwest Laboratory, Richland, Washington.

Spane FA, Jr. 1996. "Applicability of Slug Interference Tests for Hydraulic Characterization of Unconfined Aquifer: (1) Analytical Assessment." *Ground Water* 34(1):66-74.

Spane FA. 2008. *Results of Detailed Hydrologic Characterization Tests Conducted Within Ohio Geological Survey CO_2 No. 1 Well*. PNWD-4000, Pacific Northwest National Laboratory, Richland, Washington.

Spane FA, Jr. and RB Mercer. 1985. *HEADCO: A Program for Converting Observed Water Levels and Pressure Measurements to Formation Pressure and Standard Hydraulic Head*. RHO-BW-ST-71 P, Rockwell Hanford Operations, Richland, Washington.

Spane FA and DR Newcomer. 2009. *Field Test Report: Preliminary Aquifer Characterization Results for Well 299-W15-225: Supporting Phase 1 of the 200-ZP-1 Groundwater Operable Unit Remedial Design*. PNNL-18732, Pacific Northwest National Laboratory, Richland, Washington.

Spane FA, Jr. and PD Thorne. 1985. "The Effects of Drilling Fluid Invasion on Hydraulic Characterization of Low-Permeability Basalt Horizons: A Field Evaluation." *Environmental Geology and Water Sciences* 7(4):227-236.

Spane FA, Jr. and SK Wurstner. 1993. "DERIV: A Program for Calculating Pressure Derivatives for Use in Hydraulic Test Analysis." *Ground Water* 31(5):814-822.

Spane, FA Jr., PD Thorne, and LC Swanson. 1996. "Applicability of Slug Interference Tests for Hydraulic Characterization of Unconfined Aquifers: (2) Field Test Examples." *Ground Water* 34(5):925-933.

Sublette WR. *Rock Mechanics Data Package.* RHO-BWI-DP-41, Rev. 1, Rockwell Hanford Operations, Richland, Washington.

Theis CV. 1935. "The Relationship Between the Lowering of the Piezometric Surface and the Rate and Duration of Discharge of a Well Using Ground-Water Storage." *American Geophysical Union, Transactions*, 2:519-524. Reprinted in *Society of Petroleum Engineers*, "Pressure Transient Testing Methods," SPE Reprint Series (14):27-32, Dallas, Texas; also reprinted in *Benchmark Papers in Geology*, "Physical Hydrogeology," 72:141-146, RA Freeze and W Back (eds.), Hutchinson Ross Publishing Company, Stroudsburg, Pennsylvania.

Thorne PD and FA Spane, Jr. 1985. "A Comparison of Under-Pressure and Over-Pressure Pulse Tests Conducted in Low-Permeability Basalt Horizons at the Hanford Site, Washington State." In *Proceedings of the 17th International Congress, International Association of Hydrogeologists*, January 7-12, 1985, Tucson, Arizona.

Zeigler TW. 1976. *Determination of Rock Mass Permeability*. U.S. Army Engineers Waterways Experimental Station, Technical Report S-76-2.

Appendix B

Selected Hydrologic Test Analysis Figures

Appendix B

Selected Hydrologic Test Analysis Figures

B.1. Wallula Well and McNary Dam Reservoir Elevation Spectral Frequency Comparison

B.2. Wallula Well and McNary Dam Tail-Water Elevation Spectral Frequency Comparison

B.3. Fluid Temperature vs. Depth Profile Comparison

B.4. Pneumatic Slug Test SW-3 Analysis Plot: Homogeneous Formation Solution

B.5. Pneumatic Slug Test SW-4 Analysis Plot: Homogeneous Formation Solution

B.6. Pneumatic Slug Test SW-5 Analysis Plot: Homogeneous Formation Solution

B.7. Constant-Rate Pumping Test: Pumping Rate History

B.8 Constant-Rate Pumping Test: Pumped Volume History

B.9. Specific Electrical Conductance vs. Total Groundwater Pumped

B.10 pH vs. Total Groundwater Pumped

B.11 Constant-Rate Pumping Test: General Linear-Fracture Recovery Analysis

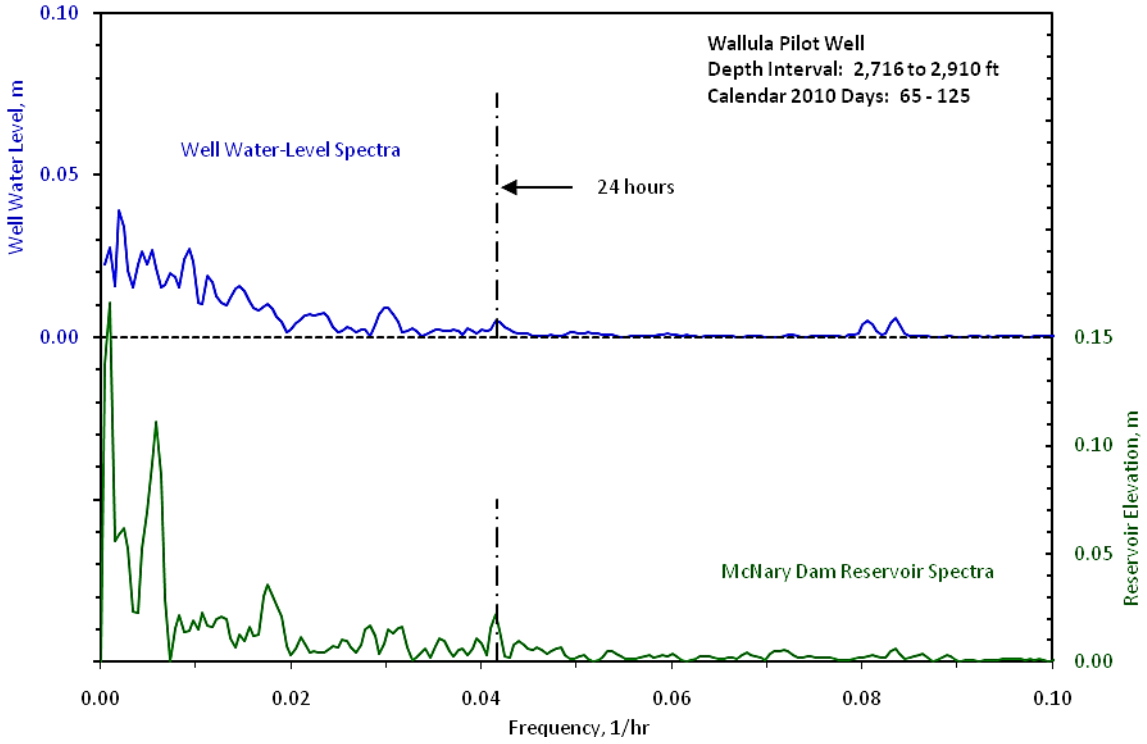

Figure B.1. Wallula Well and McNary Dam Reservoir Elevation Spectral Frequency Comparison

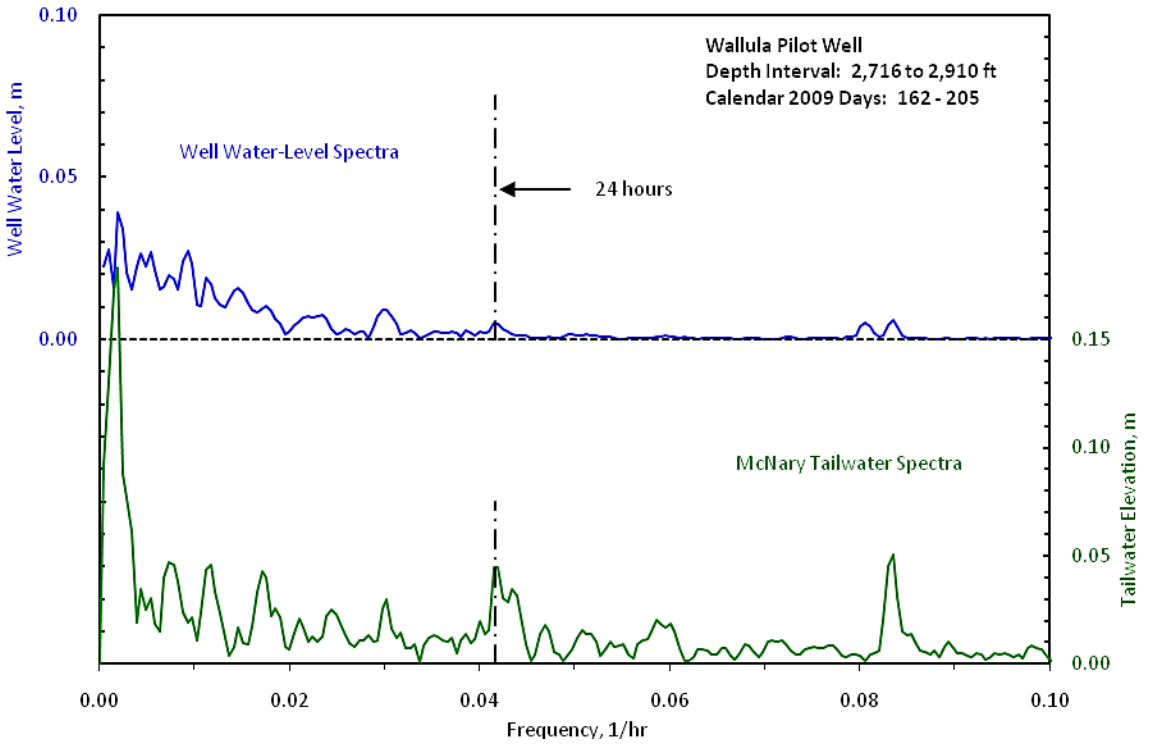

Figure B.2. Wallula Well and McNary Dam Tail-Water Elevation Spectral Frequency Comparison

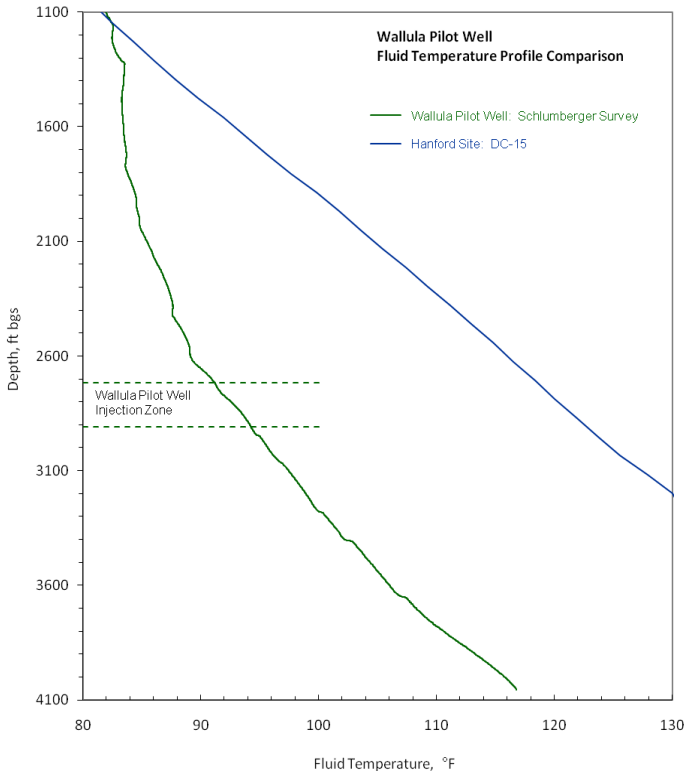

Figure B.3. Fluid Temperature vs. Depth Profile Comparison

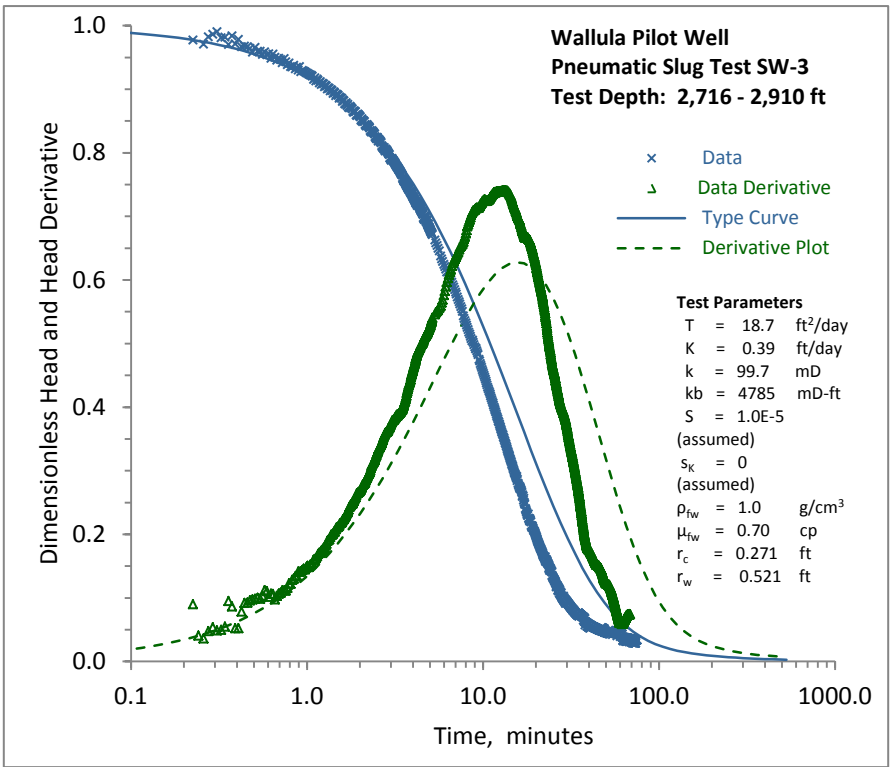

Figure B.4. Pneumatic Slug Test SW-3 Analysis Plot: Homogeneous Formation Solution

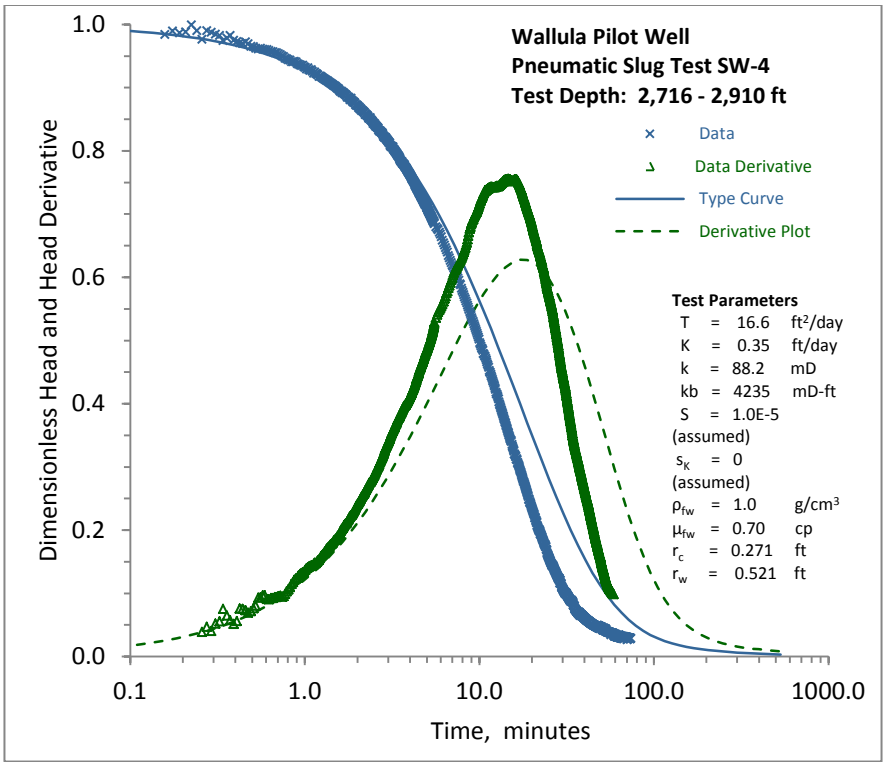

Figure B.5. Pneumatic Slug Test SW-4 Analysis Plot: Homogeneous Formation Solution

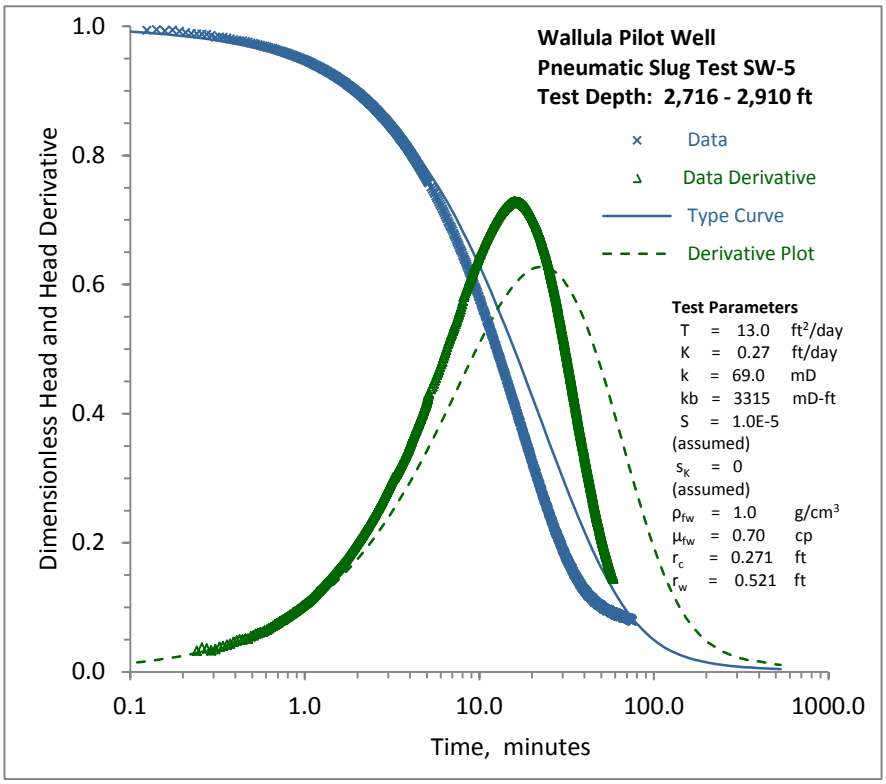

Figure B.6. Pneumatic Slug Test SW-5 Analysis Plot: Homogeneous Formation Solution

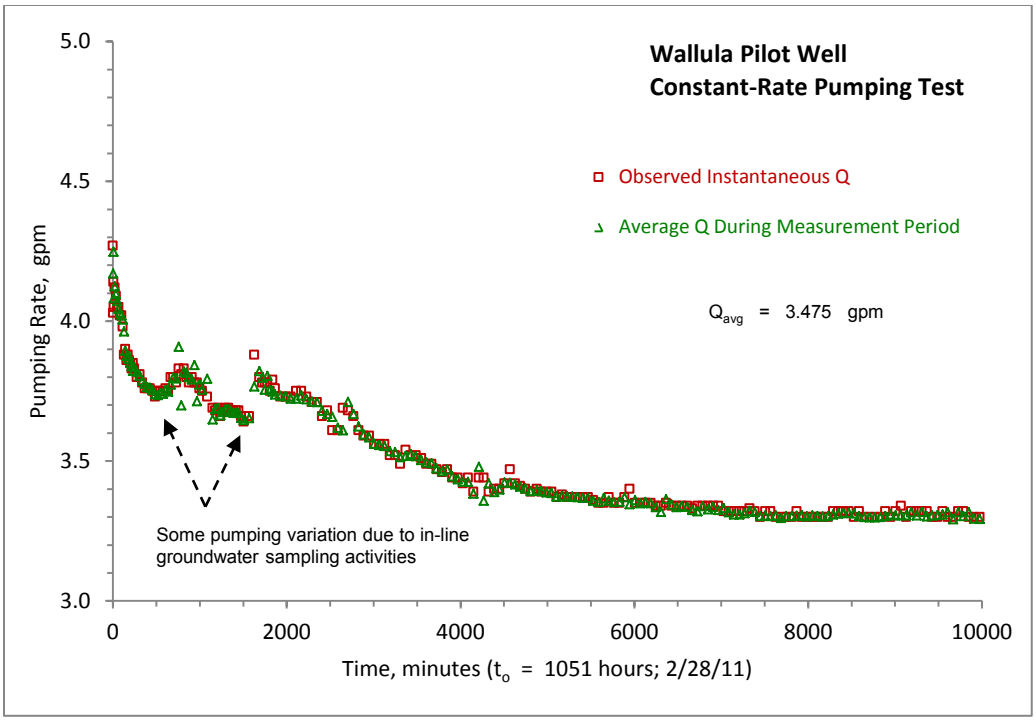

Figure B.7. Constant-Rate Pumping Test: Pumping Rate History

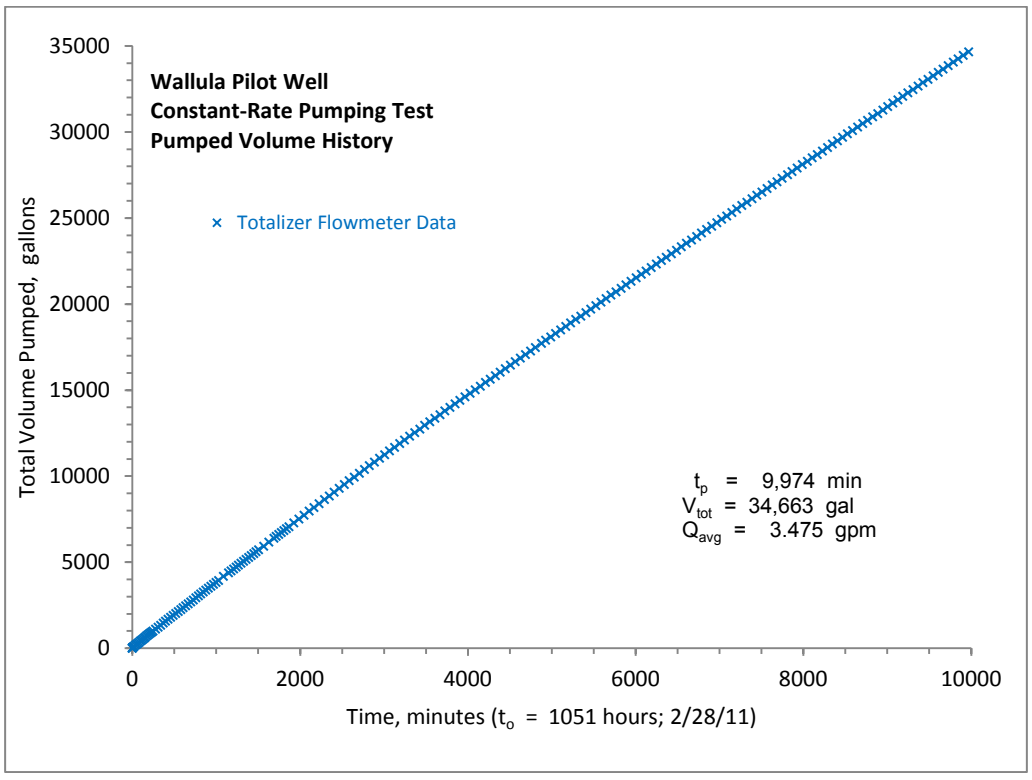

Figure B.8. Constant-Rate Pumping Test: Pumped Volume History

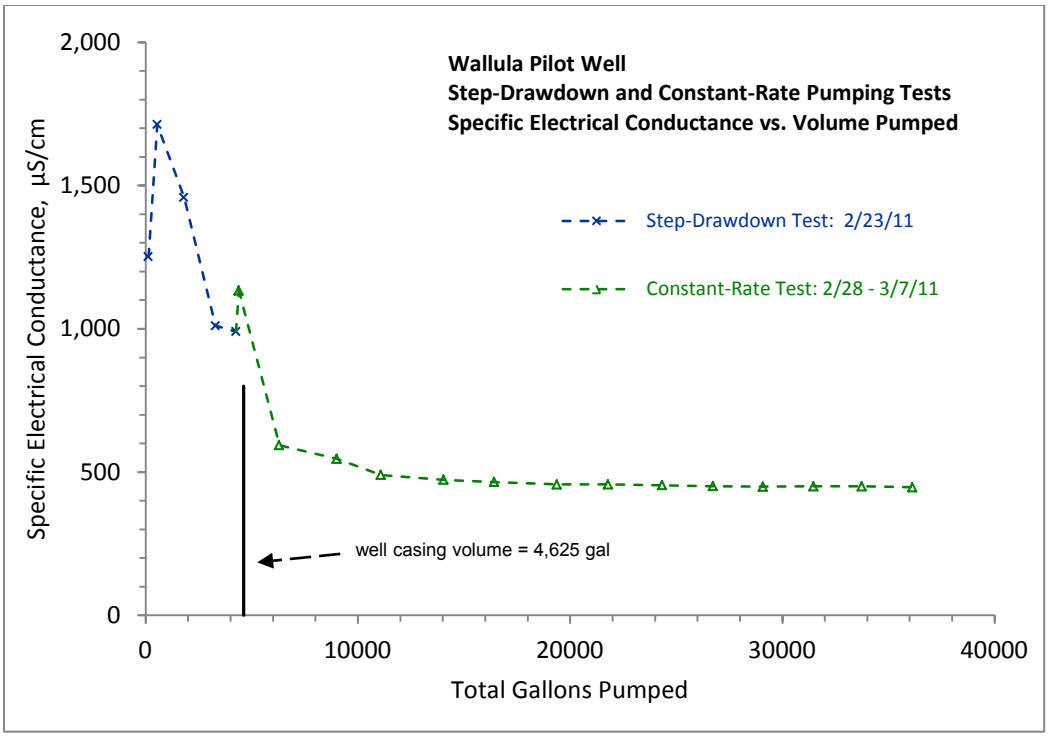

Figure B.9. Specific Electrical Conductance vs. Total Groundwater Pumped

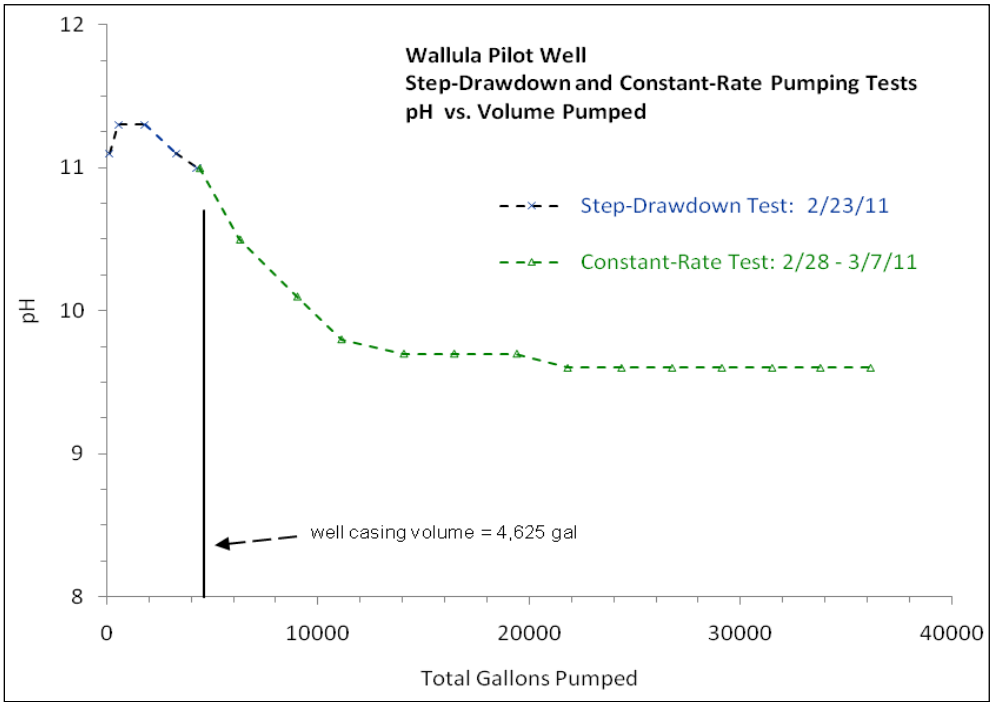

Figure B.10. pH vs. Total Groundwater Pumped

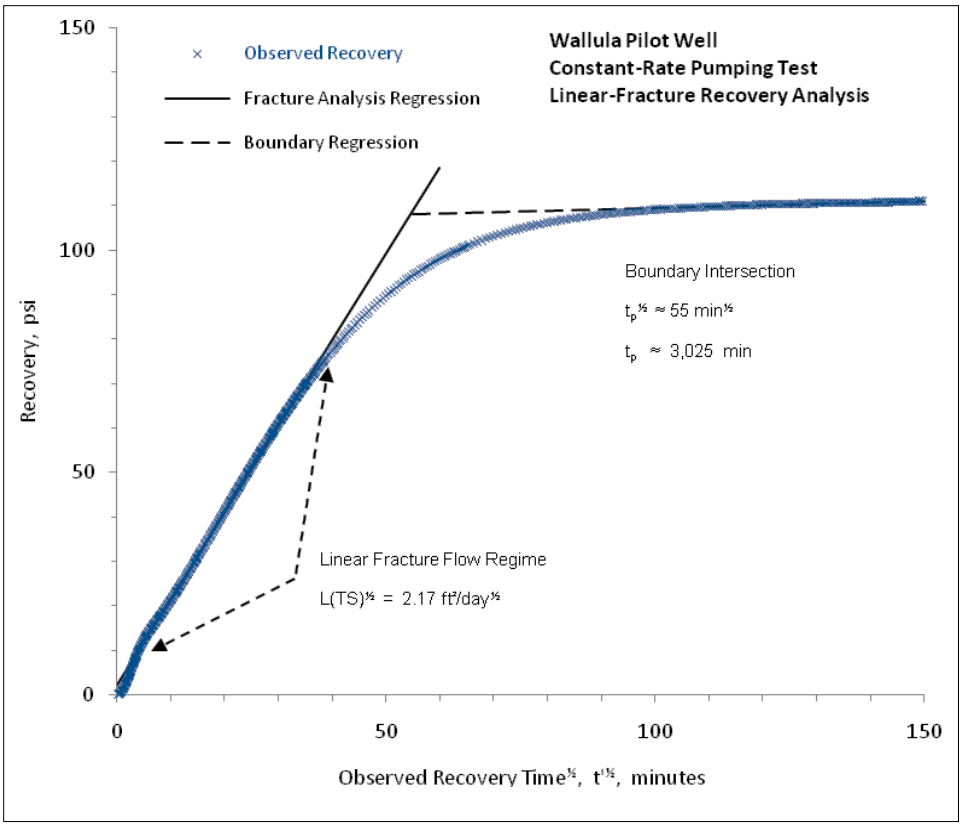

Figure B.11. Constant-Rate Pumping Test: General Linear-Fracture Recovery Analysis

Appendix C

Miscellaneous Wallula Well Test Equipment Pictures

Appendix C

Miscellaneous Wallula Well Test Equipment Pictures

C.1. Pneumatic Slug Test Wellhead Assembly

C.2. Components of Surface Discharge Line and Conveyance System

C.3. In-Line Surface Sampling Manifold

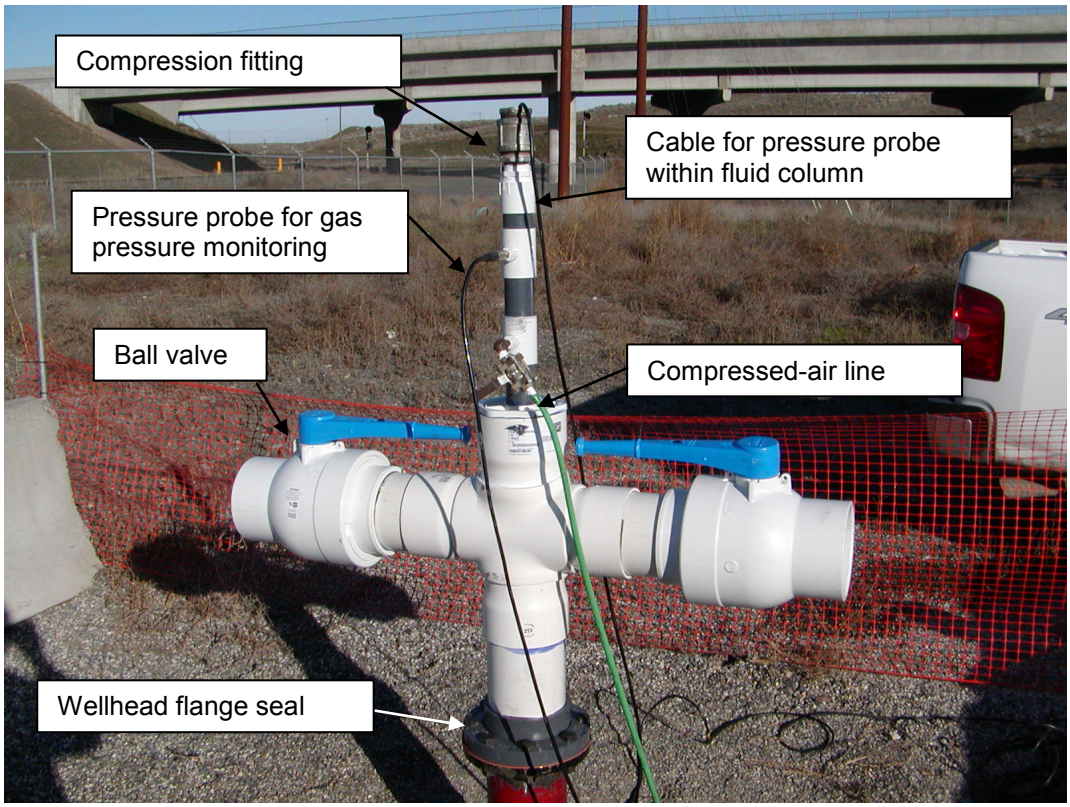

Figure C.1. Pneumatic Slug Test Wellhead Assembly

Figure C.2. Components of Surface Discharge Line and Conveyance System

Figure C.3. In-Line Surface Sampling Manifold

Distribution

No. of Copies

3

William W. Aljoe
General Engineer/Project Manager
U.S. Department of Energy
National Energy Technology Laboratory
626 Cochrans Mill Road
P.O. Box 10940
Pittsburgh, PA 15236-0940

Lee H. Spangler
Associate VP of Research
VP of Research Office
207 Montana Hall
Montana State University
Bozeman, MT 59717

Lindsey Tollefson
Outreach & Communications Manager
Big Sky Carbon Sequestration Partnership-MSU
P.O. Box 173905
Bozeman, MT 59717-3905

No. of Copies

7 **Local Distribution**
Pacific Northwest National Laboratory
P.O. Box 999
Richland, WA. 99352

Alain Bonneville	K6-84
Christopher Brown	K6-81
Thomas Brouns	K9-69
Pete McGrail	K6-90
Frank Spane	K6-96
Paul Thorne	K6-96
Walter Weimer	K2-06